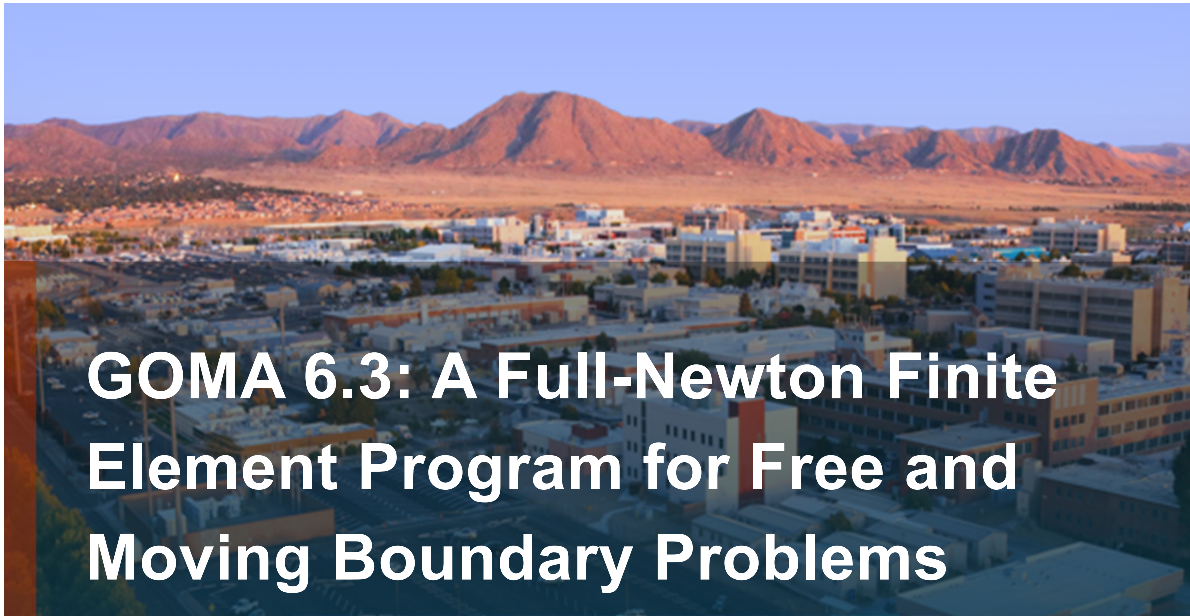

GOMA 6.3: A Full-Newton Finite Element Program for Free and Moving Boundary Problems

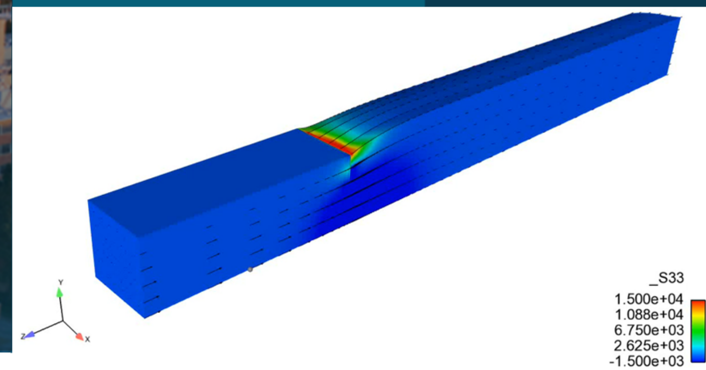

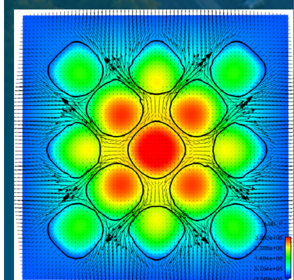

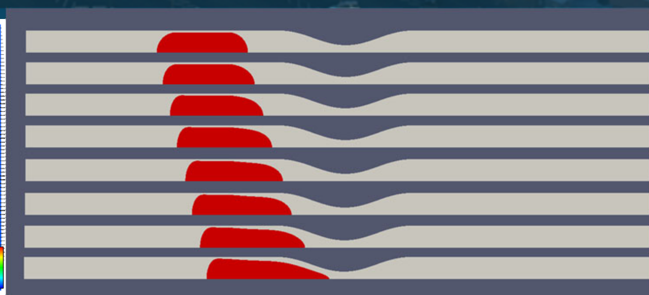

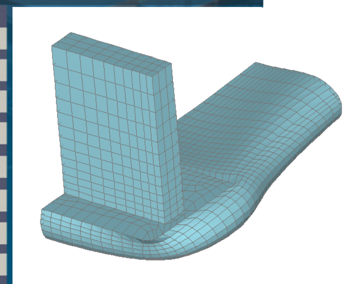

PRESENTED BY

Rekha Rao

For: P.R. Schunk, S.A. Roberts (SNL)

Kristianto Tjiptowidjojo, Weston Ortiz, Richard Martin, Andrew Cochrane, Robert Malakhov (UNM)

Josh McConnell (U of Utah)

Robert Secor (Hirdeal & Associates)

SAND2020-8554 PE

Sandia National Laboratories is a multimission laboratory managed and operated by National Technology & Engineering Solutions of Sandia, LLC, a wholly owned subsidiary of Honeywell International Inc., for the U.S. Department of Energy's National Nuclear Security Administration under contract DE-NA0003525.

COMPUTER SIMULATIONS IN MANUFACTURING

GOMA, A Multiphysics Finite Element Code

MOLD FILLING
-POLYMERS
-METALS
-FLUID FLOW, HEAT
PHASE CHANGE,
FREE SURFACES

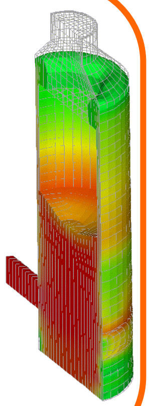

DP

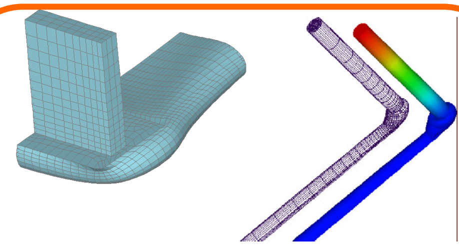

EXTRUSION AND COATING
3D FLUID FLOW, FREE SURF

SOLDERING
-HEAT, MOMENTUM,
FREE SURFACE,
SOLIDIFCATION

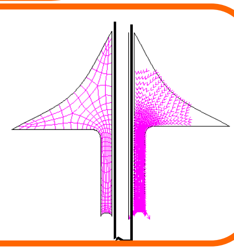

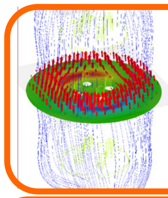

BRAZING, FURNACE
MODELING

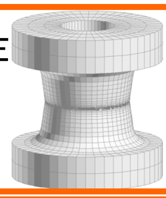

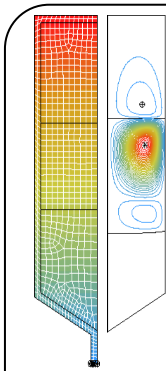

ALLOY
PROCESSING

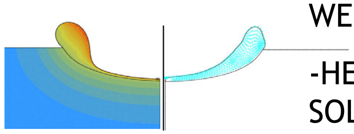

WELDING
-HEAT, MOMENTUM,
SOLIDIFICATION,

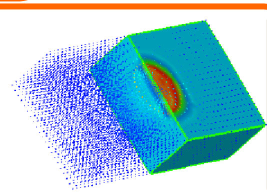

- Coupled or separate heat, n-species, momentum (solid and fluid) transport
- Fully-coupled free and moving boundary parameterization
- Solidification, phase-change, consolidation, reaction of pure and blended materials
- Host of material models for complex rheological fluids and solids

UNIQUE FEATURES
•FREE SURFACES ARE UBIQUITOUS
•COUPLED FLUID-SOLID MECHANICS
•COMPLEX MATERIAL RHEOLOGY/LOW SPEED

COATING/ENCAPSULATION

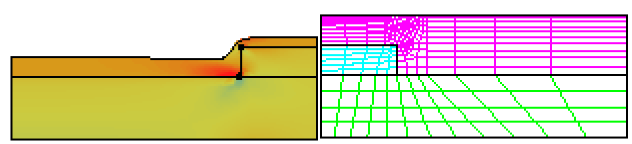

GOMA: HISTORICAL PERSPECTIVE

TIME

- 1993 – **Goma development begins, ALE mesh motion**
- 1995 – Coating Consortia
- 1996 – *JCP* Paper on ALE Distinguishing Conditions
- 1997 – *3D ALE*, Contact line motion, joining, encapsulation
- 1998 – Novel fluid-structural algorithms, 8-mode viscoelasticity
- 1998 – **Explosion of customers at Sandia and Industry**
- 2000 – *IJNMF* 3D ALE papers
- 2001 – MPI port, Level-set Eulerian front tracking
- 2003 – Shells equations, sharper interfaces
- 2005 – **Sierra Aria adopts Goma’s algorithms/customers (Ouch!)**
- 2009 – UNM Goma Schunk Group founded
- 2012 – NSF NASCENT Center – UNM, UT, 3M etc
- 2013 – Goma 6.0 Open source license
- 2014 – **R&D 100 award, 3M Umbrella CRADA**
- 2018 – 2 DOE/HPC4Mfg Funding for GOMA – 3M and Dow
- 2019 – 2 DOE/EERE Fuel-cell Technology & Drying/Coating (ORNL, NREL, ..)
- 2020 – Follow-on HPC4Mfg DOE funding for Electromagnetics with 3M

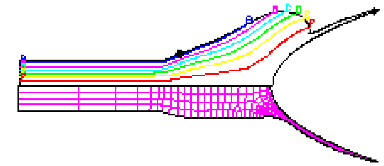

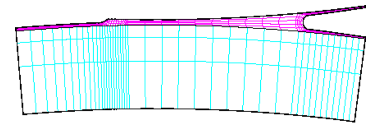

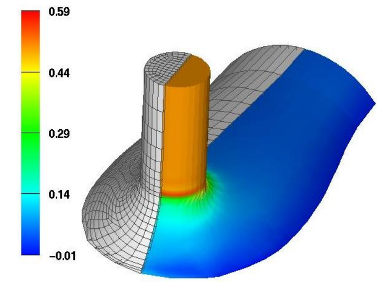

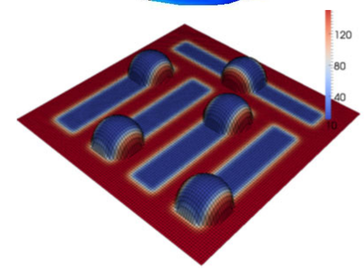

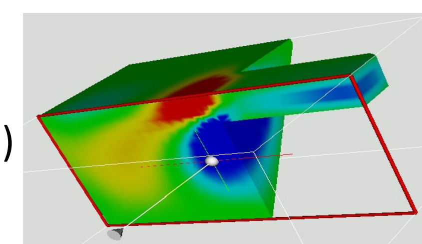

GOMA'S CAPABILITIES: MECHANICS

- MECHANICS
  - Includes all major branches of mechanics with conjugate capability
- MATERIALS MODELS
  - Generalized Newtonian: Bingham, Carreau, suspensions, foams, etc
  - Viscoelastic Fluids: PTT, Giesekus, Oldroyd-B, FENE-P, Saramito
  - Hookean and elasto-viscoplastic for solids
  - Pixel/voxel to mesh
- MOVING BOUNDARY METHODS
  - Moving mesh with ALE
  - Level set with XFEM and subgrid integration
- FLUID-STRUCTURAL INTERACTIONS
  - Computational Lagrangian solids
  - ALE in both solids and fluids (TALE)
  - Coupled ALE and level set
  - Dual mesh with overset grid
- DEFORMABLE POROUS MEDIA
  - Saturated and unsaturated
  - Poro-elastic/poro-plastic

1. **ALE SOLID**
2. **ALE FLUID**
3. **ALE SOLID & FLUID (TALE)**
4. **LAGRANGIAN SOLID (DYNAMIC)**
5. **ALE FLUID/LAGRANGIAN SOLID**
6. ***EULERIAN SOLID***
7. **EULERIAN FLUID(LEVEL SET)**
8. ***EULERIAN SOLID/FLUID***
9. ***EULERIAN FLUID/LAGRANGIAN SOLID (OVERSET GRID)***

GOMA'S CAPABILITIES: INFRASTRUCTURE

PARALLEL OR SERIAL EXECUTION

- Trilinos matrix solvers
- Iterative solvers, direct solvers, and parallel direct solvers
- Access to advanced preconditioners: IFPACK and ML through Stratimikos

MULTIDIMENSIONAL

- 2D, Axisymmetric, 2.5D (Swirling) and fully 3D
- Shell capability

ELEMENT TYPES

- quadrilateral/hexahedral (P1 or P2)
- triangle/tetrahedra (P1 only)

ADVANCED CAPABILITIES

- Full-Newton coupled algorithms
- Segregated solvers
- Automated continuation and augmenting conditions,
- Stability analysis
- Advanced post processing features

USER-PRESCRIBED/USER-DEFINED CAPABILITY

GOMA's – Advanced Analysis Capabilities

- ❑ Augmenting conditions
  - Volume and mesh constraints
  - Sensitivity and optimization
- ❑ Bordered algorithm
  - Numerical and analytical Jacobian
- ❑ Automated zeroth, first, arclength and multiparameter continuation
- ❑ Nonlinear parameter operating space prediction for manufacturing
- ❑ Linear stability analysis using ARPACK
  - 2D/3D linear stability of dynamic systems
  - 3D stability of 2D base flow.

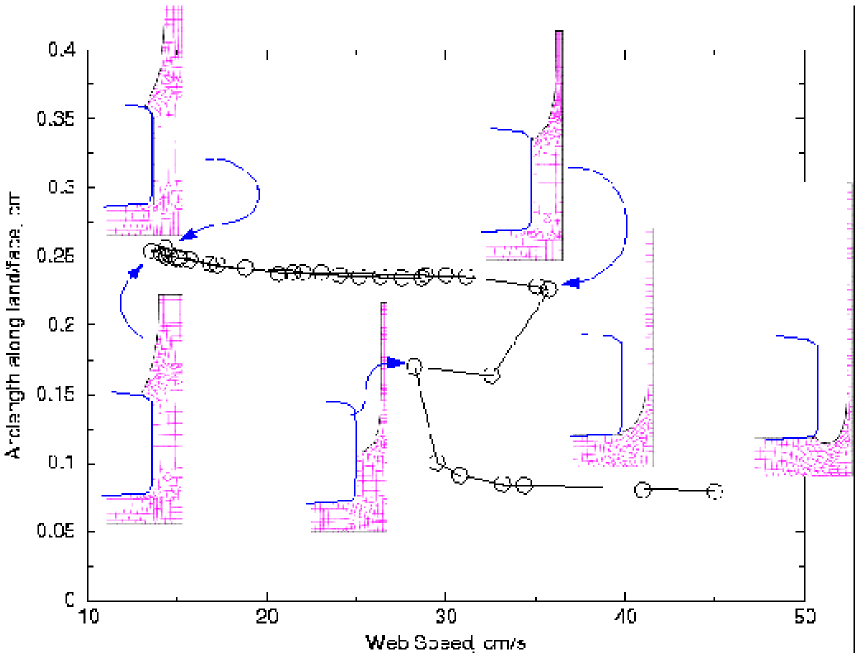

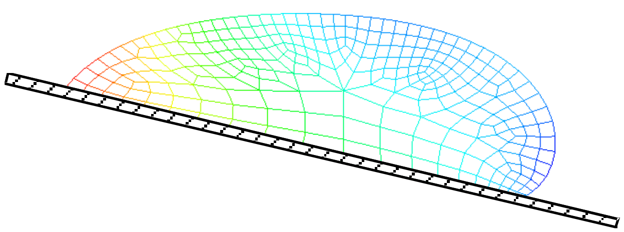

SUPPORT OF THESE IS "HIGH MAINTENANCE" AND REQUIRES GOOD INTERFACE FOR USER TO DEFINE CONDITIONS

GOMA'S CAPABILITIES: INFRASTRUCTURE

- Post Processing
  - PARAVIEW (available freely on web)
  - ENSIGHT
  - SEACAS
- Pre-Processing Meshing/Domain Decomposition
  - ANSYS Workbench, MSC Software-PATRAN (PATEXO)
  - CUBIT/Trelis
  - Auto brk/fix for running parallel Goma
- Integrated Adaptive Remeshing and Refinement (Goma 7.0)
  - Omega_h library (https://github.com/SNLComputation/omega_h)
  - brk/fix included in Goma, SEACAS epu supplants fix
- Platforms
  - LINUX/UNIX (RedHat, CentOS, or Ubuntu)
  - Automated build scripts of Goma and its TPLs
- Documentation
  - All Manuals available on github
  - Open source format – Sphinx

Basic Foundation for Coupled Mechanics ALE/Lagrangian

- *TREAT MESH EVERYWHERE AS A DEFORMABLE SOLID BODY*
- *INVOKE LAGRANGIAN AND/OR ALE FORMULATIONS AS REQUIRED BY REGION*
- *APPLY IMPLICIT DISTINGUISHING CONDITIONS FOR USER-PRESCRIBED, KINEMATIC, OR DYNAMIC BOUNDARY MOTION*

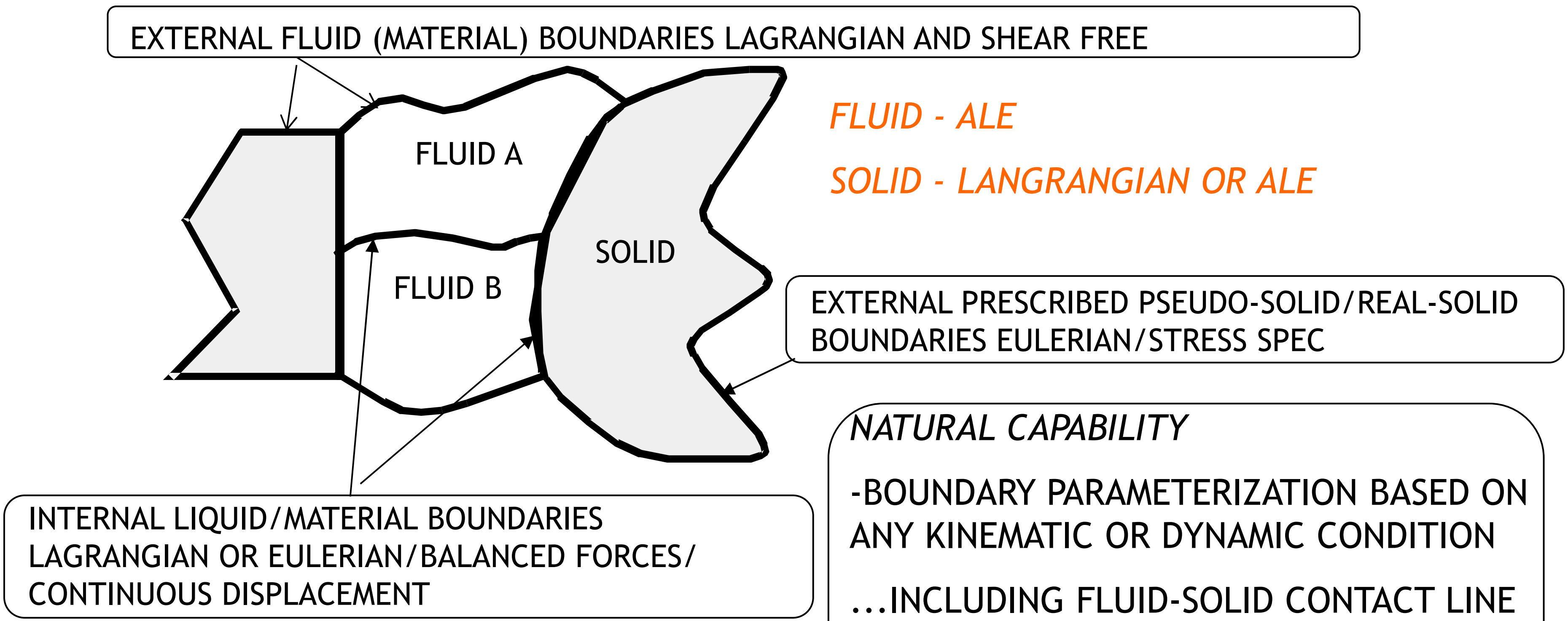

FLUID - ALE

SOLID - LANGRANGIAN OR ALE

NATURAL CAPABILITY

-BOUNDARY PARAMETERIZATION BASED ON ANY KINEMATIC OR DYNAMIC CONDITION

...INCLUDING FLUID-SOLID CONTACT LINE MOTION

Comprehensive Mechanics Coupling

NEWTON'S METHOD

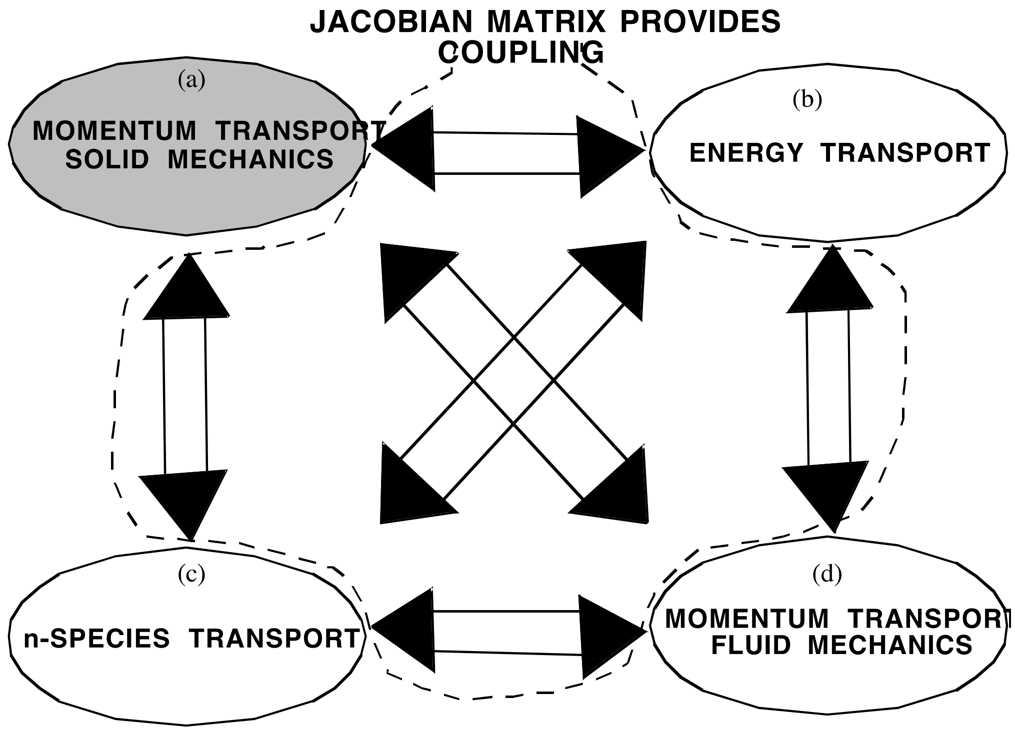

EVERY MAJOR BRANCH OF MECHANICS CLOSELY COUPLED!

- MINIMAL TUNING REQUIRED OF ALGORITHMS
- FASTER, QUADRATIC CONVERGENCE
- OPTIMAL ALGORITHM FOR VISCOUS AND CAPILLARY-DOMINATED PROBLEMS
- MACHINERY FOR INCORPORATING ADVANCED ALGORITHMS, E.G., AUGMENTING CONDITION CAPABILITY, LINEAR STABILITY, AUTOMATED, HIGHER-ORDER CONTINUATION…

Fluid Material Models

- GENERALIZED NEWTONIAN
  - Concentration, temperature and shear-rate dependence
  - Carreau, Carreau-WLF, molten glass, epoxy cure, Bingham-plastic
- SUSPENSION MODELS
  - Phillips model for particle concentration, Krieger for viscosity
  - Suspension Balance Model for blood rheology
- MULTIMODE VISCOELASTICITY
  - EVSS Split stress, discontinuous Galerkin, and log conformation tensor methods
  - Phan-Thien Tanner, Giesekus, Oldroyd-B, FENE-P
  - Level set or ALE

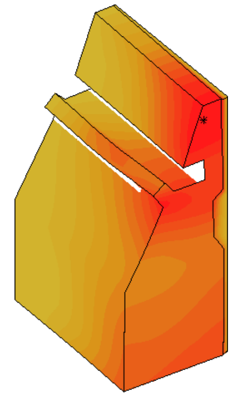

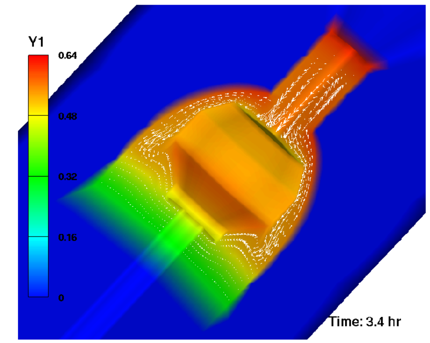

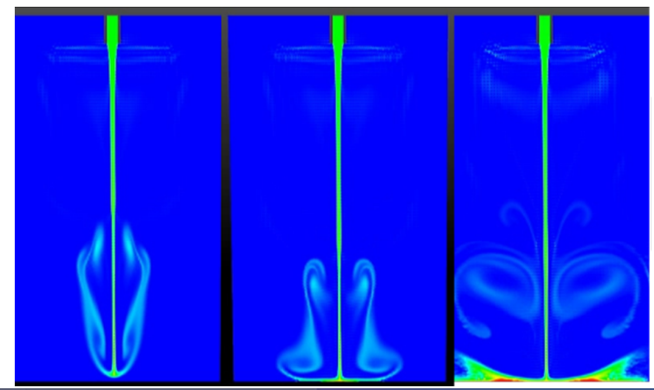

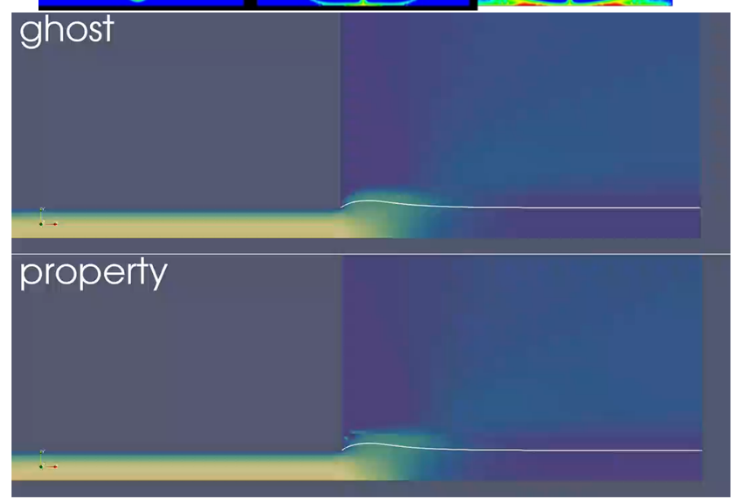

Thermo-physical Property/Phase Change Models

- Vapor/liquid equilibrium - Ideal and Flory-Huggins
- Discontinuous variables approach for interphase mass-momentum transport
- Vapor-pressure vs (T, c) models, viz. Kelvin equation, Riedel, Antoine, etc.
- Liquid/solid equilibrium
  - Scheil or solute dependent solidification
  - Latent heat release with enthalpy or interfacial Stephan condition
- Liquid/solid macro-segregation with Flemings-Mehrabian model
- Polymer thermoset and condensation chemistry for curing and viscosity
- Fickian and Non-Fickian diffusion with n-species

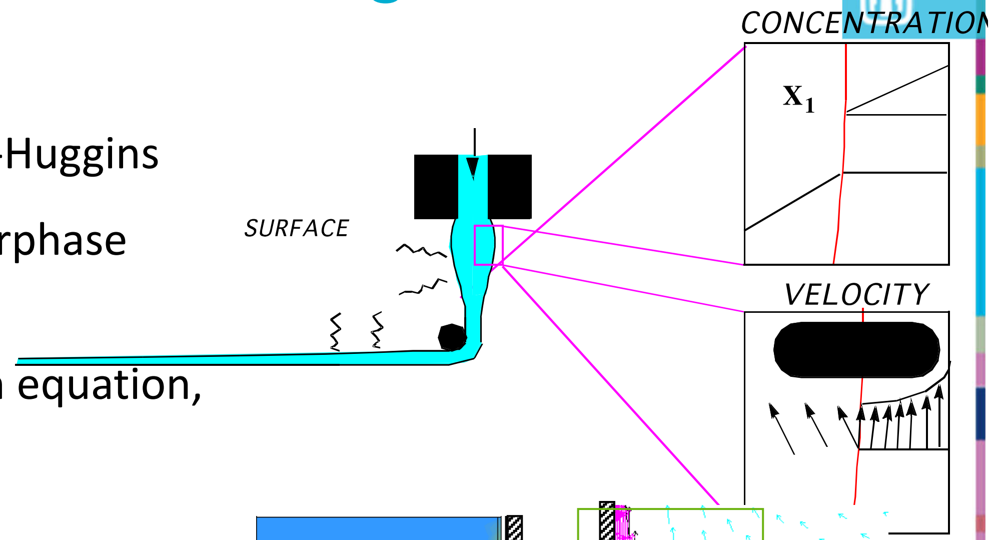

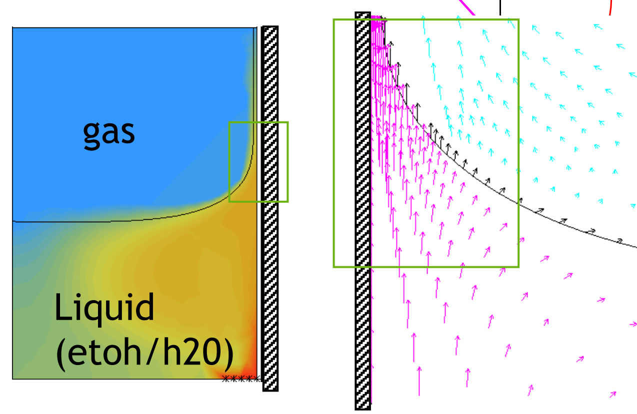

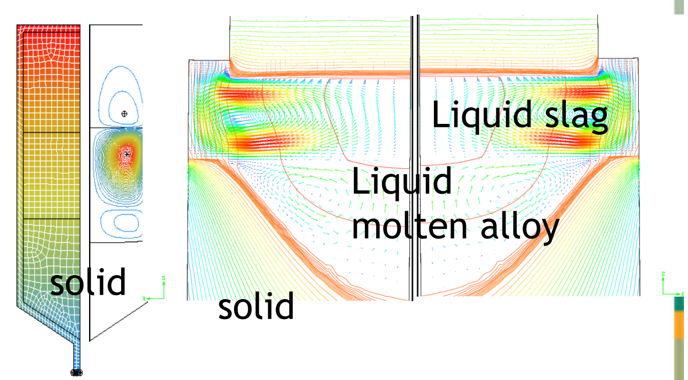

3D Mesh Motion: Rectangular Die Extrusion

Rotations and nonlinear elastic model for mesh motion allow large deformation from initial conditions

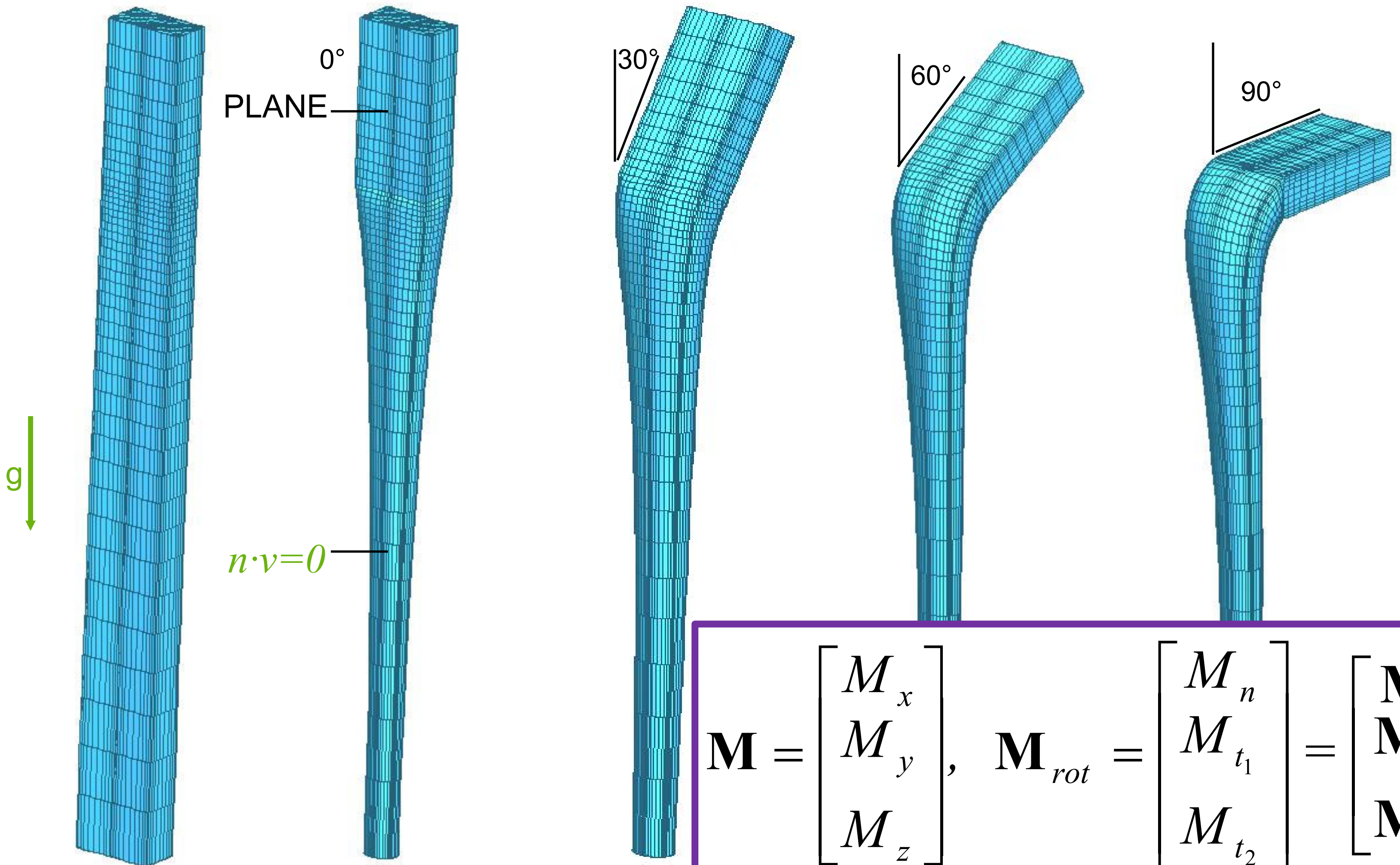

$$\mathbf{M} = \begin{bmatrix} M_x \\ M_y \\ M_z \end{bmatrix}, \quad \mathbf{M}_{rot} = \begin{bmatrix} M_n \\ M_{t_1} \\ M_{t_2} \end{bmatrix} = \begin{bmatrix} \mathbf{M}\cdot n \\ \mathbf{M}\cdot t_1 \\ \mathbf{M}\cdot t_2 \end{bmatrix}$$

Current Project to Simplify 3D Free Surface Flows – no more ROT Conditions!

Capabilities for Flow in Porous Media

Formulation and Capabilities

- Darcy formulation
  - Fully saturated, partially saturated, two-phase (pressure gradient in receding fluid)
  - Solid-source models (swelling fibers)
  - Saturation-capillary pressure formulation – hysteresis
  - Permeability and relative permeability models
  - Poro-elastic coupling
  - Thin sheet/shell capability
  - Continuum flow, free surface coupling
  - Verification and validation available

- Brinkman formulation
  - Add a permeability term to Navier-Stokes equation
  - Easy to couple porous and Navier-Stokes regions

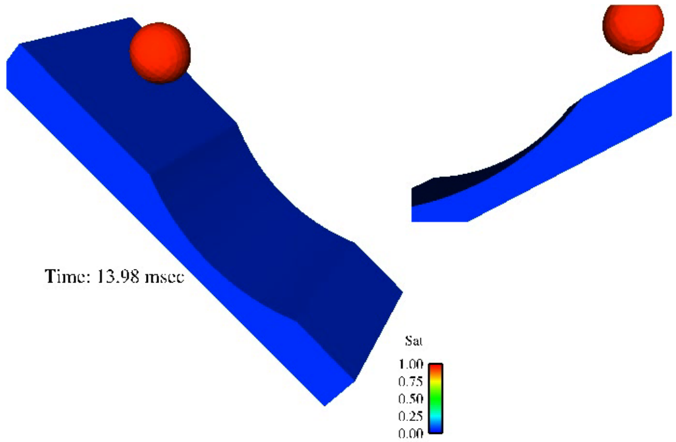

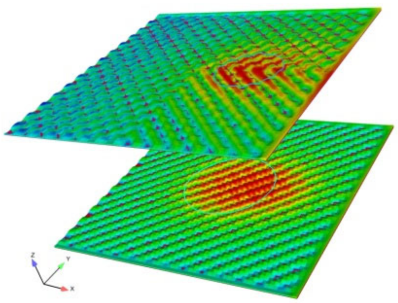

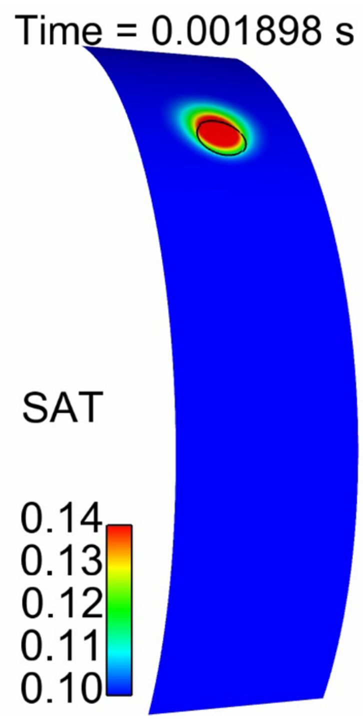

Fluid Filling with a Porous Insert: Pressure Driven vs. Gravity Flow

μ_0 = 100 Poise - GMB Content 20%

Q = 2 cm²/s **Q = 10 cm²/s**

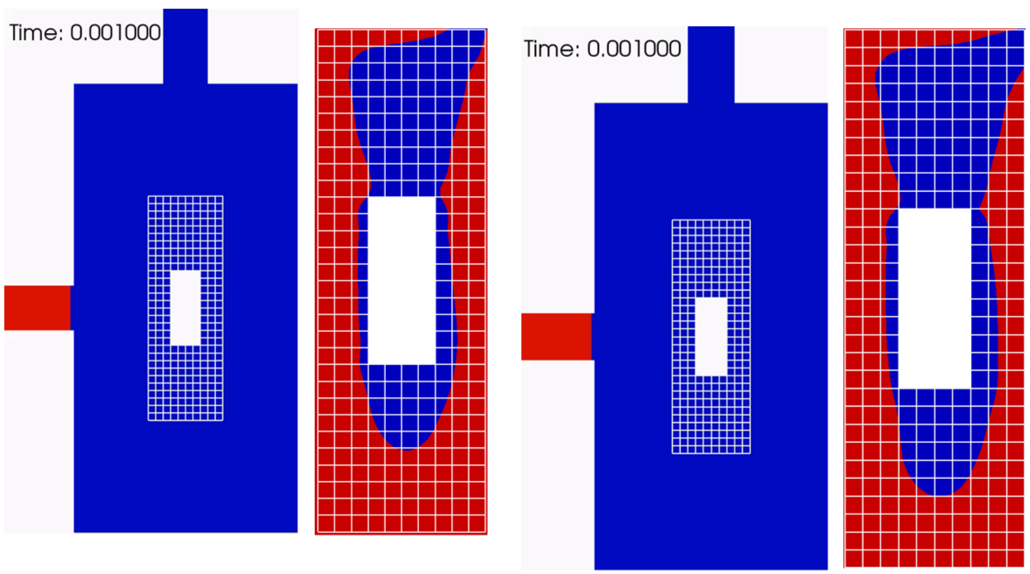

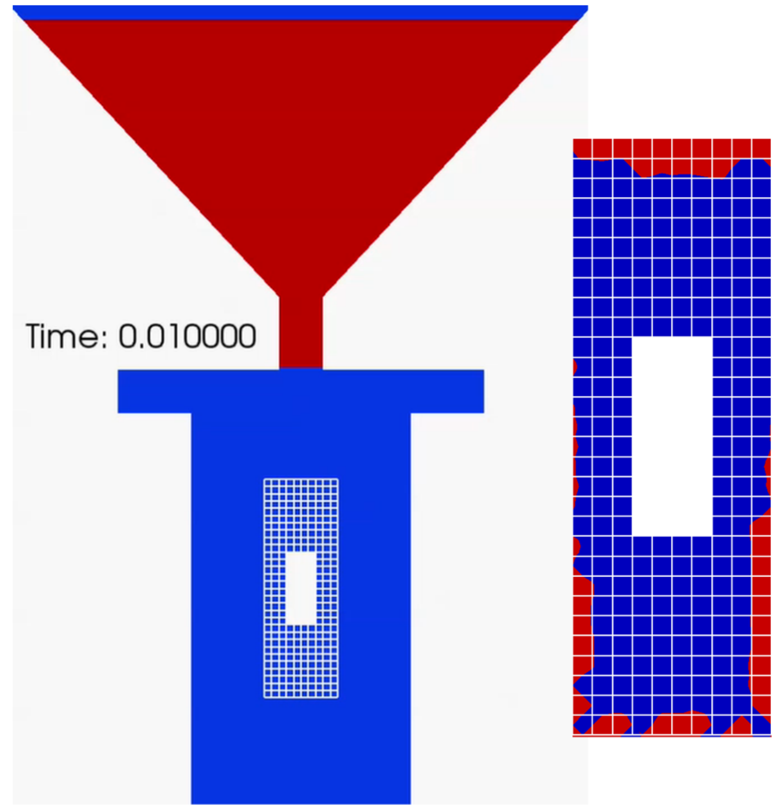

- Higher flow rate fills up the container faster but needs more time to allow imbibition in the medium – bottleneck is in the porous medium
- Extent of porous infiltration is about the same

- Flow rate depends on the viscosity and pressure head – $q \sim 1/\mu$ → less control
- Resistance from winding leads to buckling instability of the liquid jet
- Trapped air is a big problem

Thin-Continuous Liquid Film Coatings and Structures

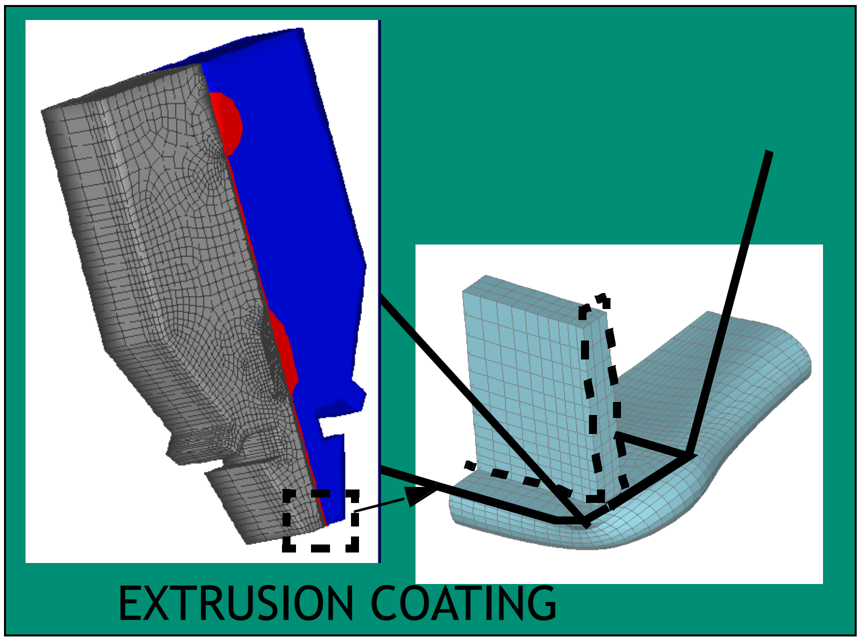

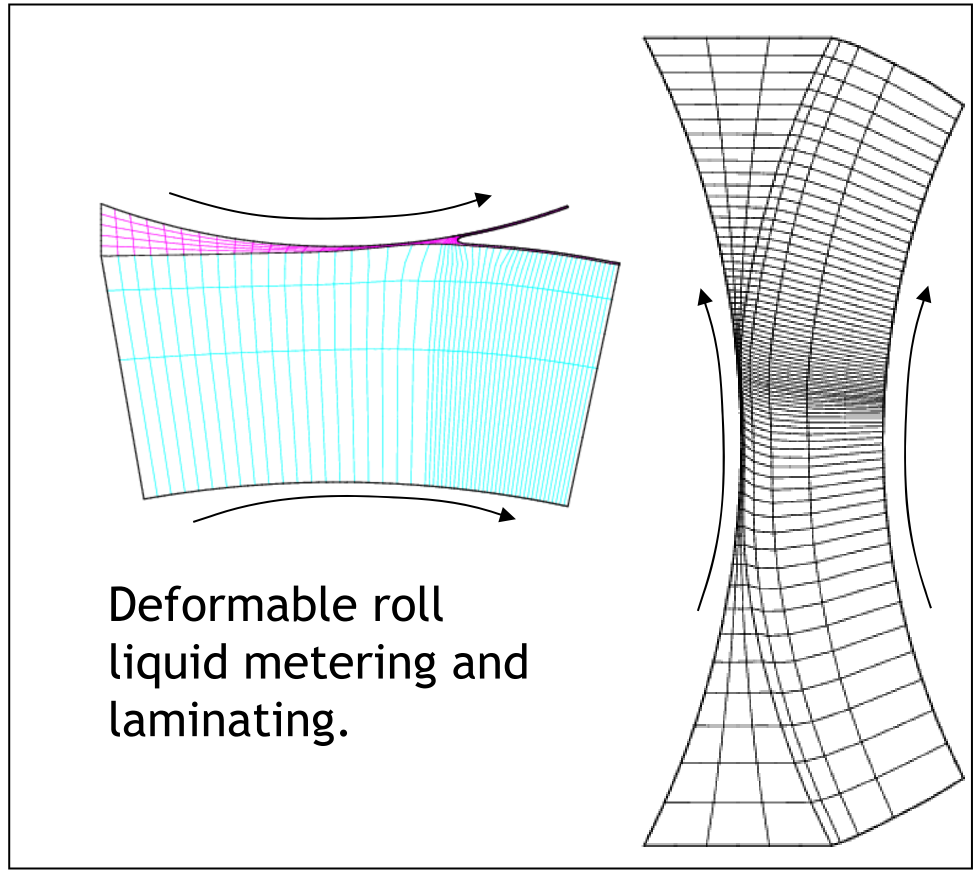

Gravure Roll Coating (Overlap Grid Method)

Viscosity – 10 P
Roll Speed – 100 cm/s (ID)
Density – 1 gm/cm^3

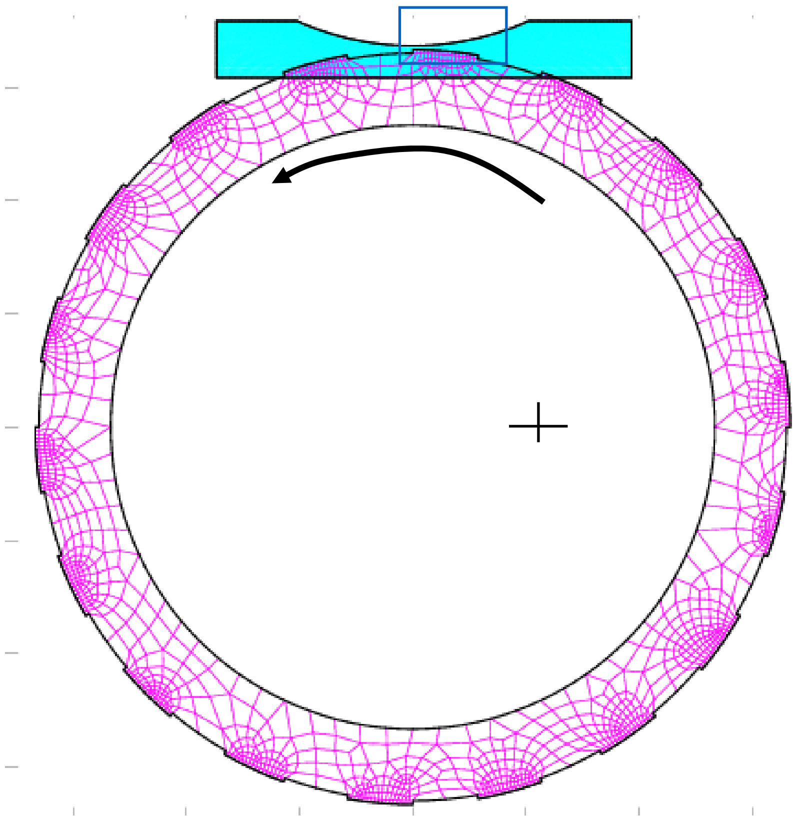

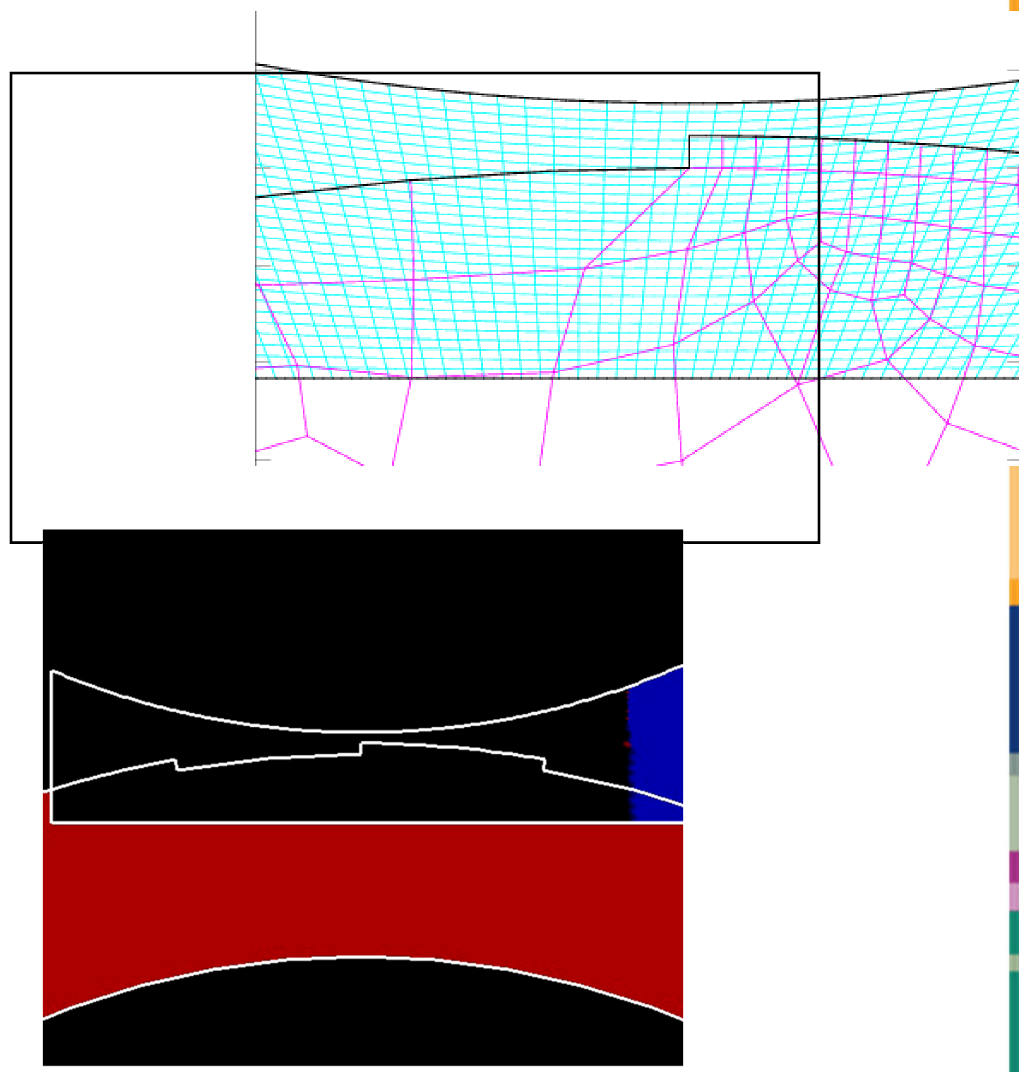

Drying and Curing of Thin Films

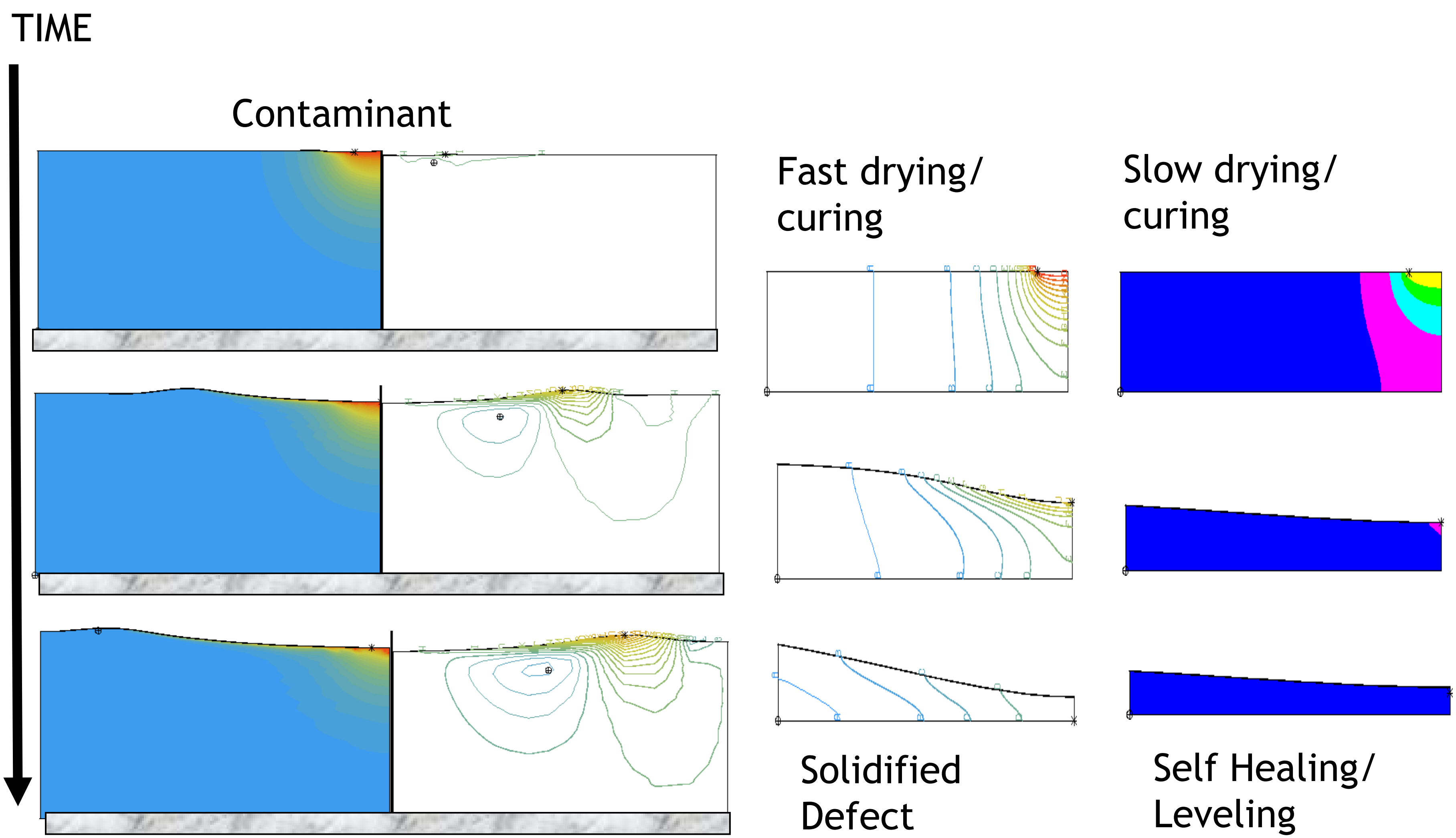

Solidification Physics/Thermodynamics Beam Bending Experiments

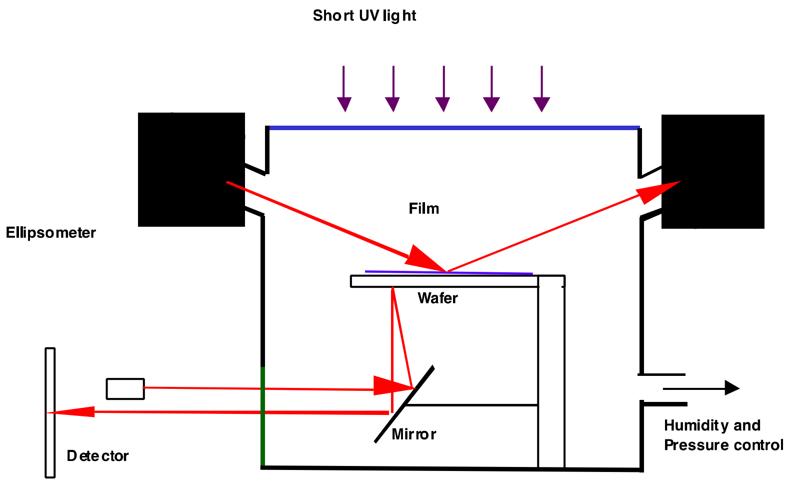

Wafer props

Lame Mu = 35245 MPa

Lame Lambda=62712 Mpa

Length=5 cm

Thickness=0.15 cm

Gelled Gelatin Props

Lame Lambda = 100 Mpa

Yield stress = 32-300 Mpa

Plastic Viscosity = 8 P

All constant for now

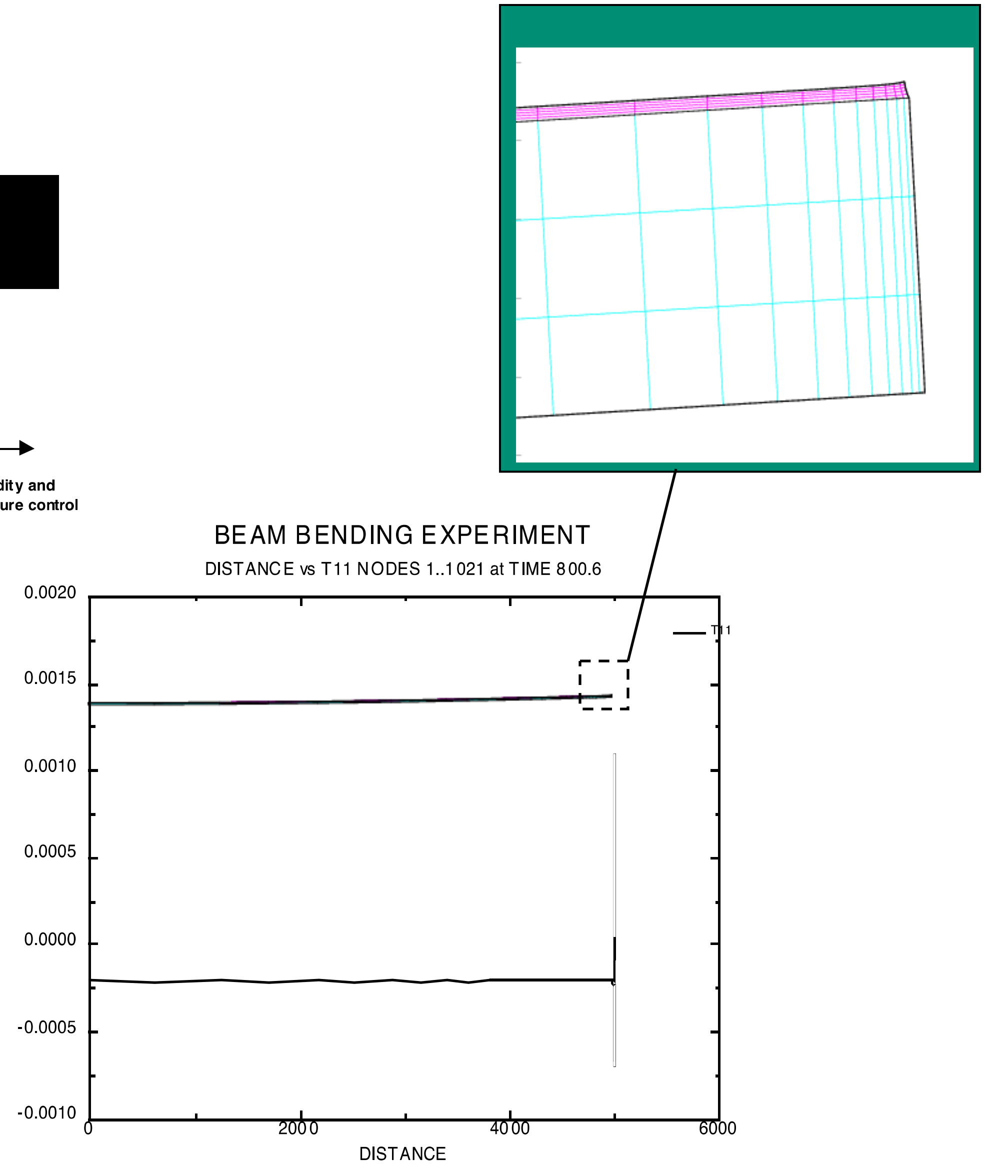

Analysis of Heat Transfer in a Geometry with Internal Heat Source

- Heat source from 29 to 2900 W
- ¼ inch stainless steel, ¾ inch plywood case or a ¾ inch plastic case
- Looked at temperature during two days

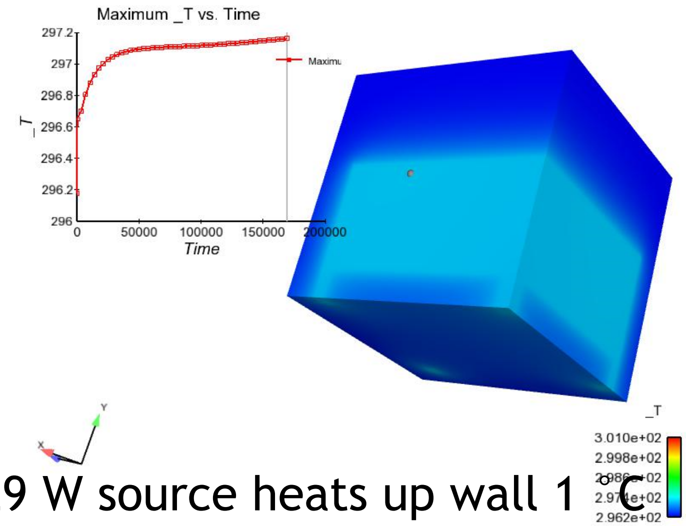

29 W source heats up wall 1 °C

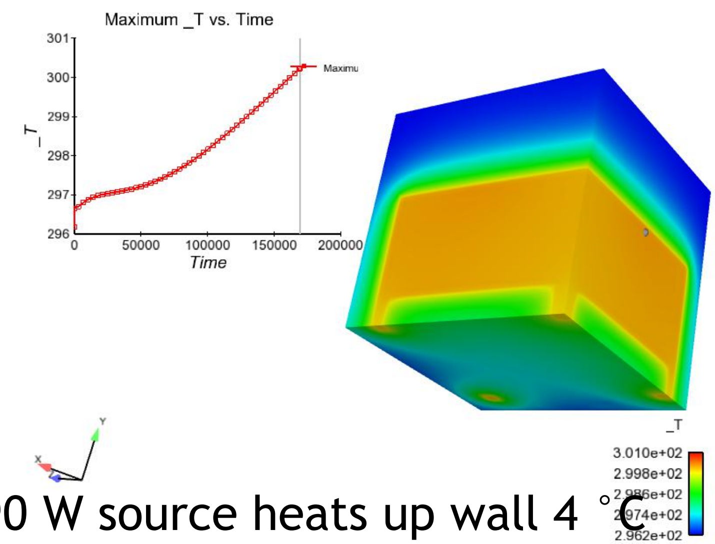

290 W source heats up wall 4 °C

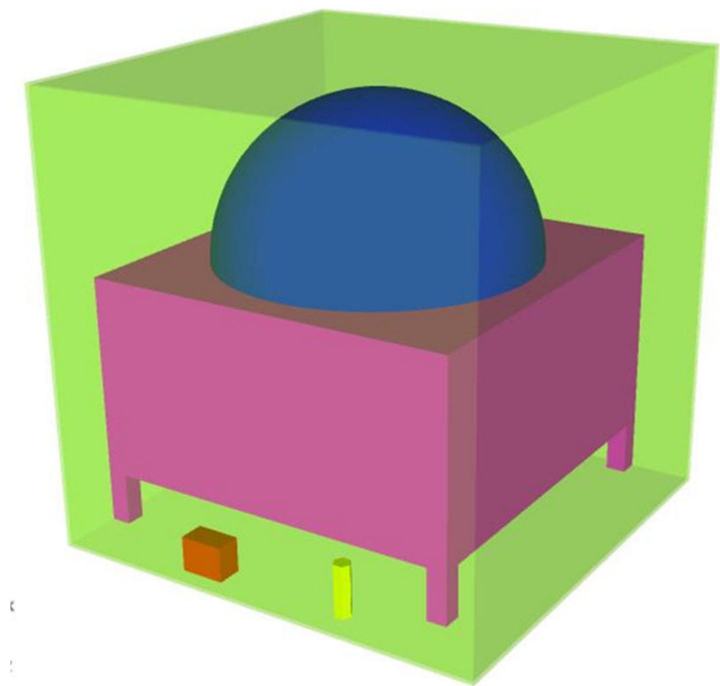

GOMA Shell "Machinery"

•Wall Kinematics: Straight sliding, slanted sliding/plowing, roll-on, roll-to-roll, melting, coupled 3D Structural

•Wall structure functions: Slanted/sliding, roll-on, superimposed pixel pattern

•Continuum element coupling: FSI with nonlinear elastic solids, mass/fluid exchange, etc.

•Pattern to mesh Capability:

ORIGINAL PATTERN IMAGE (pixel/voxel)

IMAGE PROCESSING + LEAST SQUARES FIT TO MESH

$$A^TAx=A^Tb$$

PATTERN OVERLAID MESH FIELD

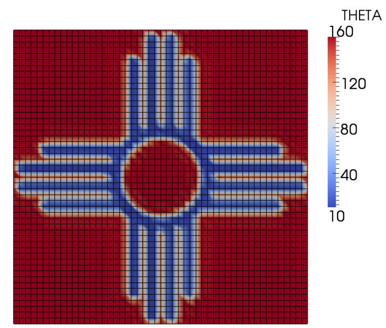

➢ ***NO NEED TO GRID THE PATTERN INTO THE MESH → REDUCE NUMBER OF GRIDS REQUIRED TO RESOLVE THE PATTERN***

GOMA Shell Pattern-to-Mesh Tool

Rolling tire hydroplaning, Microstructure/property calculation

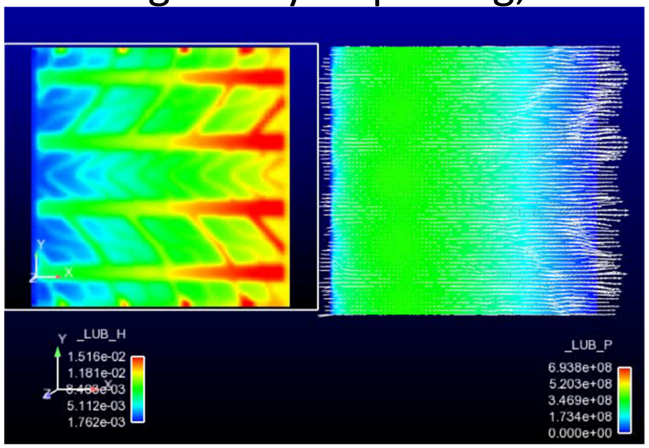

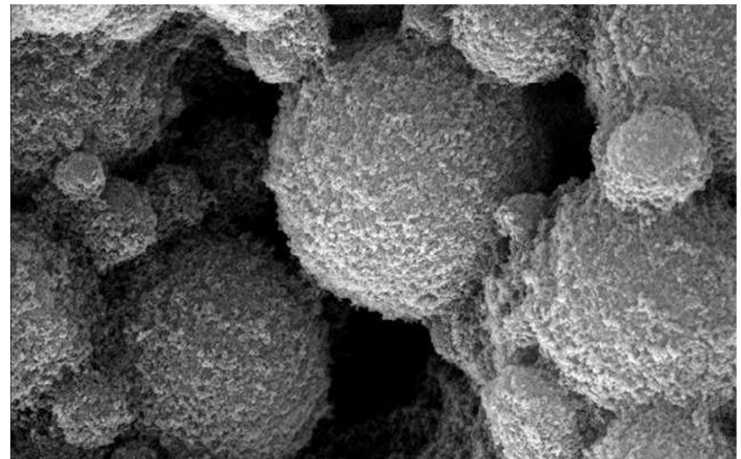

DEM-To Background Structured Mesh

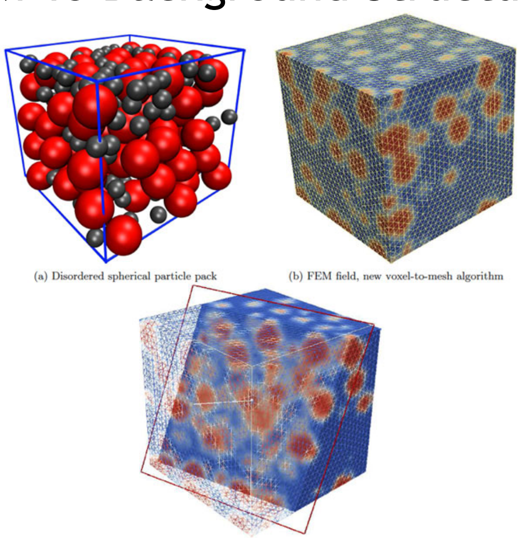

(a) Disordered spherical particle pack

(b) FEM field, new voxel-to-mesh algorithm

(c) FEM field, new voxel-to-mesh algorithm, view showing internal structure

Figure 2: 3-D pixel-to-mesh capability
BB

Tomographic Data-To-Mesh

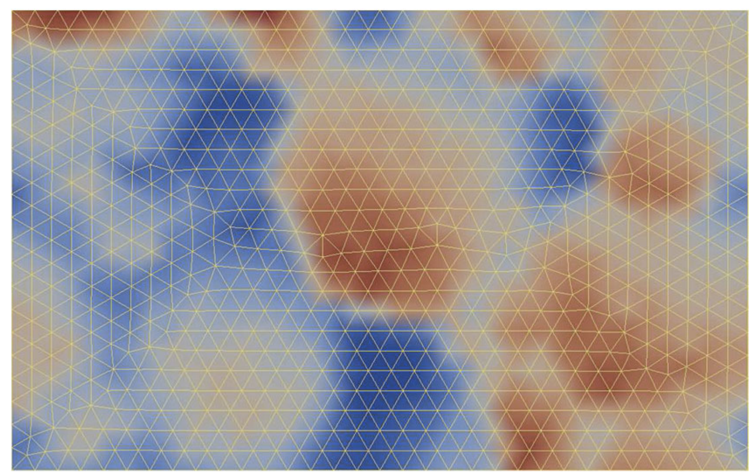

Thin Regions Call for Shell Elements

- **Shell Element Technology Ideal when large-aspect-ratio regions (structures) prevail.**
  - Shell-Element: reduced-order continuum element (integrated with presumed mechanical response in one direction – membrane, inextensible shell, lubrication, porous) – *Three dimensional coordinates but only two integration coordinates*
  - We have developed and integrated true curvilinear shell capability for *lubrication* (first of its kind to our knowledge integrated with continuum codes), *porous penetration*, and *integrated structure*.

Lubricated Slider Bearing, Melt Lubrication

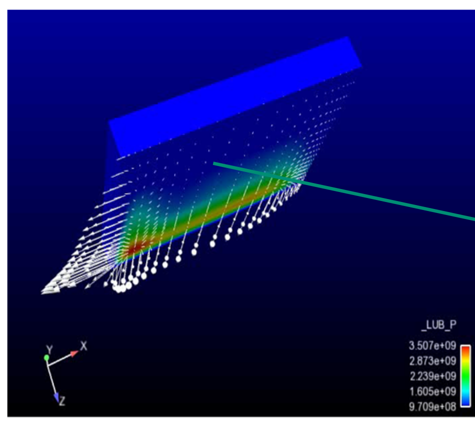

Layer thickness < 5 microns, slider dimension ~10 cm

"Shell elements are also thought of as a way (data-structure, mechanism) to apply overloaded, fancy BCs"

Motivation is Application Driven

Top-down nano-manufacturing: fluid distribution, printing, mold filling in large-aspect ratio regions

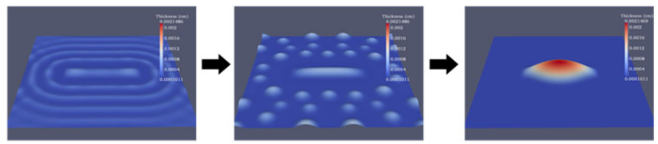

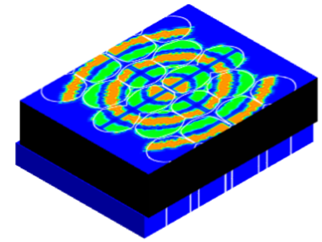

Thin-liquid film coating: film flow, metering flows, thin metering structures

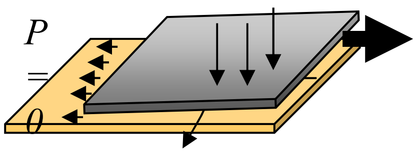

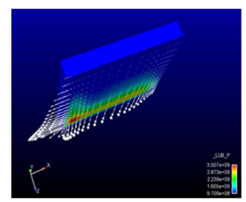

Tensioned web Slot

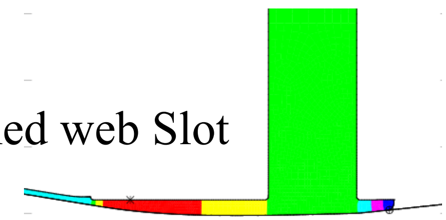

Sliding Contacts: electrical brush

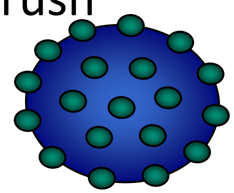

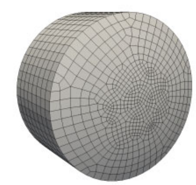

Capillary surface microstructure, surface rheology: emulsions, surface rheometry, oil recovery

Goma Shell Capability

-Reynolds lubrication equation (highly accessorized):

$$\frac{\partial(\rho h)}{\partial t}+\nabla_{II}\bullet\left(\frac{\rho h}{2}(\underset{\sim}{U}_A+\underset{\sim}{U}_B)-\frac{\rho h^3}{K\mu}[\nabla_{II}p-\boxed{\sigma\kappa\delta(\phi)\underline{n}}-\rho(\phi)\underline{g}+\underline{f}]\right)+\boxed{(j_A+j_B)}=0$$

Moving Control Vol (squeezing) *Moving Walls* *Pressure Driven* *Capillary interfaces (multiphase)* *Body forces* *Exchange Fluxes*

-Shell energy equation (highly accessorized):

$$h\rho C_p\frac{\partial T}{\partial t}+h\rho C_p\underset{\sim}{u}_{II}\cdot\nabla_{II}T-hK_{eff}\nabla_{II}\cdot\nabla_{II}T+Q_{surf}+Q_{VD}+Q_{Joule}=0$$

Ohmic Heating *Viscous heating* *lateral fluxes*

-Film Equations:

$$\frac{\partial h}{\partial t}+\nabla_{II}\cdot[\frac{h^3}{3\mu}(-\nabla_{II}p)+\underset{\sim}{U}_B h]+\dot{E}=0$$

$$p=-\sigma\nabla_{II}\bullet h-\Pi$$

Other interoperable models:
- -Turbulence models
- -Electrostatic energy
- -Lorentz forces

-Structural shells (2D only, and inextensible):

Goma Shell Capability

-Porous shells

$$\frac{dS}{dt} = -\frac{1}{\phi}\frac{\kappa_{zz}}{H\mu}\frac{dP}{dz}$$

Closed pore

$$\frac{dS}{dt} = -\frac{1}{\phi}\frac{\kappa_{zz}}{H\mu}\frac{dP}{dz} + \frac{\kappa}{\mu}\nabla_{II}P$$

Open pore

$$-\phi\frac{\partial S}{\partial t} = \boldsymbol{\nabla}\cdot\boldsymbol{v}.$$

-Particle diffusion shells

$$\frac{\partial(\varphi h)}{\partial t} + \nabla_{II}\bullet\left[\frac{h^3}{3\mu}(-\nabla_{II}p)\varphi + \underset{\sim}{U}_B h\varphi\right] - \nabla_{II}\bullet\left[D\nabla_{II}(h\varphi)\right] = 0$$

-Evolution shells (melting, growth, etc.):

$$\rho E_0\frac{d\delta h}{dt} = H_{trans}(T - T_0)$$

Phase Change

$$\boldsymbol{v} = (\mathbb{I} - \boldsymbol{nn})\cdot\boldsymbol{v} + \boldsymbol{nn}\cdot\boldsymbol{v} = \boldsymbol{v}_{\mathrm{II}} + \boldsymbol{v}_{\mathrm{n}}.$$

-Geometry Shells $-h_{\mathrm{por}}\phi\frac{\partial S}{\partial t} = -\frac{h_{\mathrm{por}}}{\mu}\boldsymbol{\nabla}_{\mathrm{II}}\cdot(\boxed{\mathbb{K}_{\mathrm{II}}}\cdot\boldsymbol{\nabla}_{\mathrm{II}}p_{\mathrm{por}}) + \frac{1}{\mu}\mathbb{K}_{\mathrm{n}}\boldsymbol{\nabla}_{\mathrm{n}}p_{\mathrm{por}}\Big|_{z=h_1},$

$$\kappa = -\nabla\cdot n = -\nabla\cdot\frac{\nabla F}{|\nabla F|}$$

Nanoimprint Background
(Inkjet Based Jet and Flash Imprint)

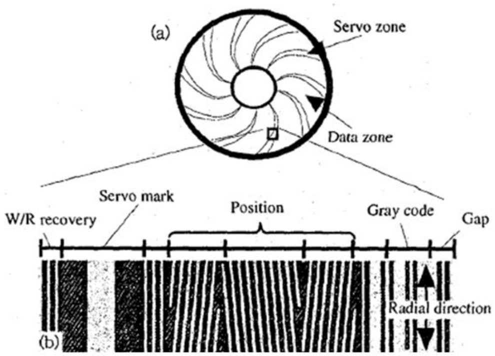

Macro-Scale Pattern Density Variations

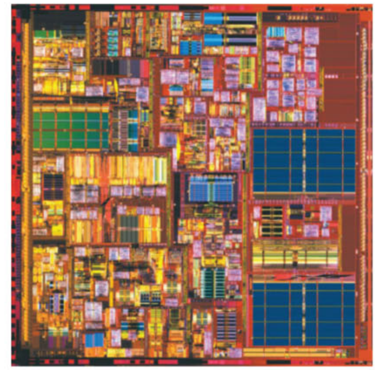

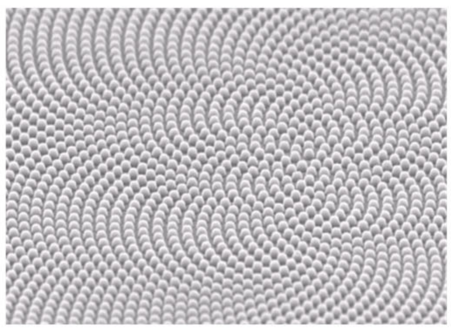

Micro-Scale Pattern Complexity

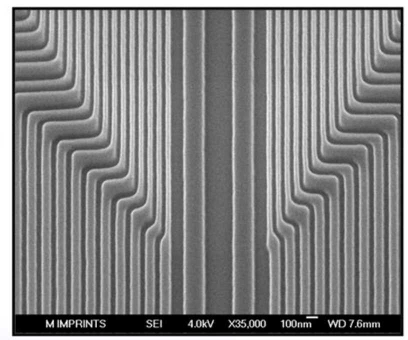

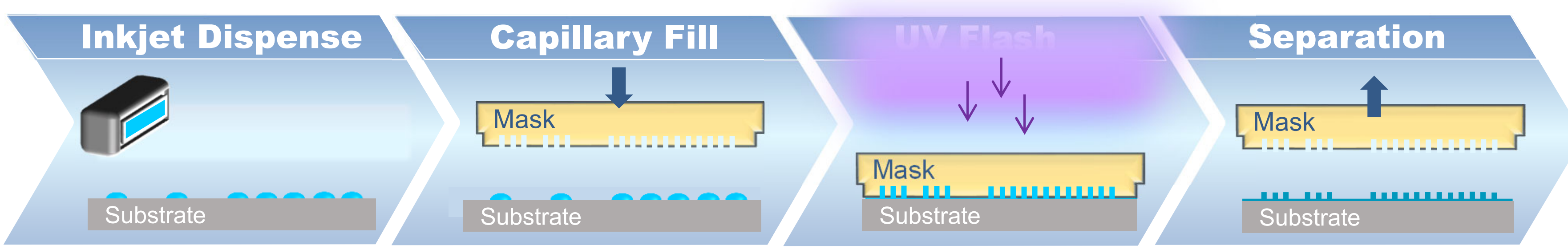

Jet and Flash Imprint Lithography (J-FIL)

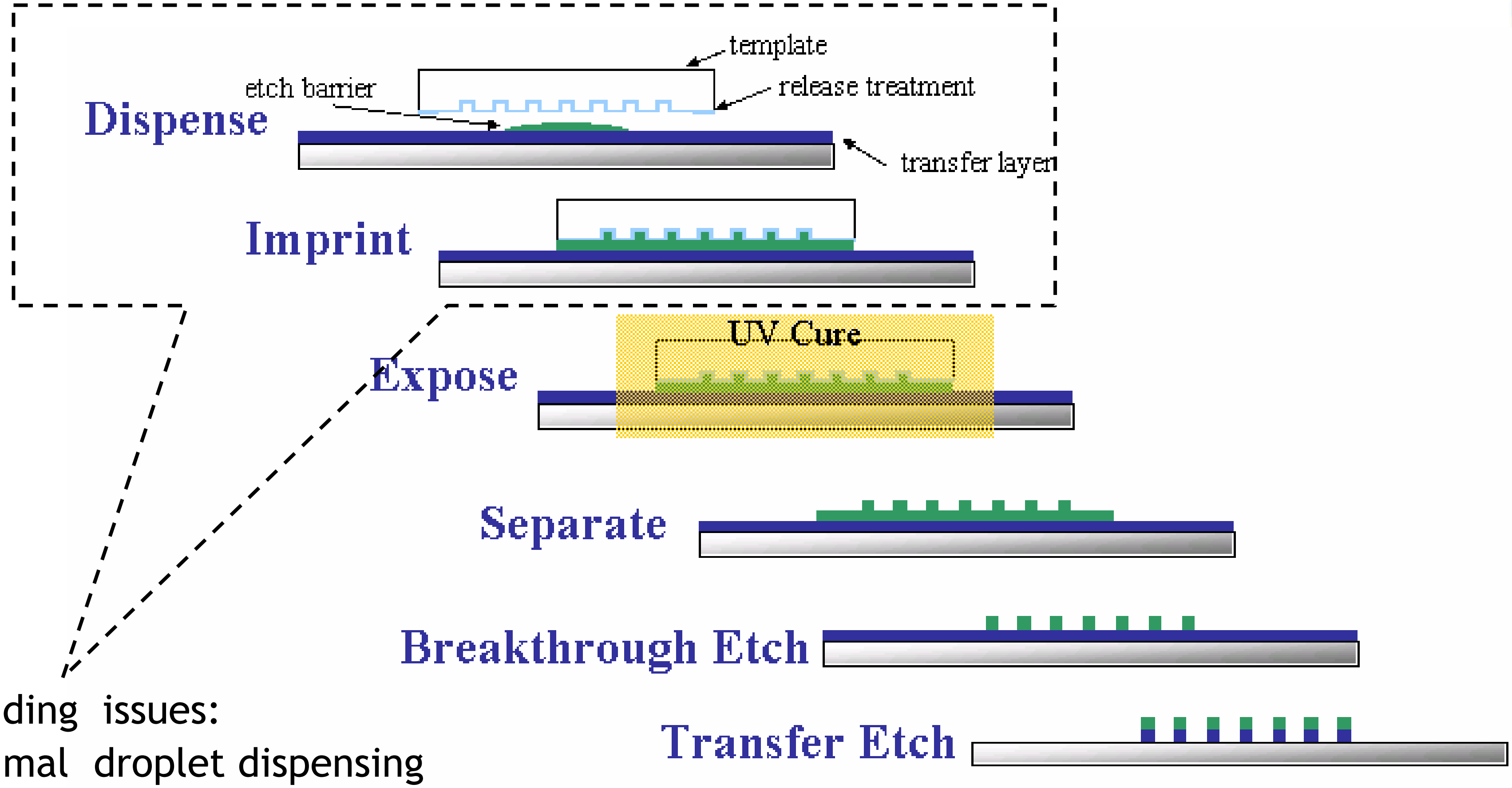

Outstanding issues:

- Optimal droplet dispensing
- Minimizing residual layer thickness (RLT), ideally < 15 nm
- Effect of nano-topography (nanometer variations over centimeter length scales)

Applicable to MEMS devices and chip fabrication

POC: Scott Roberts, Randy Schunk

JFIL: Bridging Multiple Scales

Important features:

- Six orders of magnitude difference in length scales
- Different physics at each scale

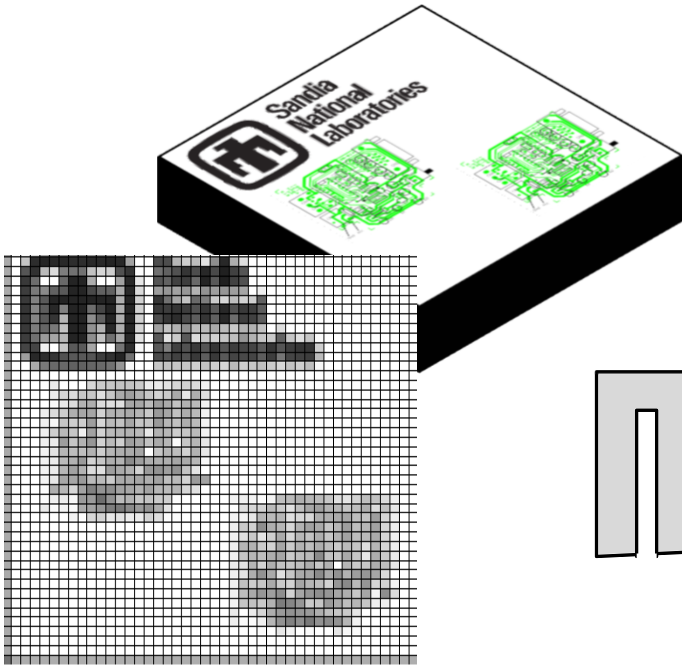

Machine-scale model

- 3-D Shell FEM
- Coarse-grained models
- Highly-parallel simulations
- 10 cm

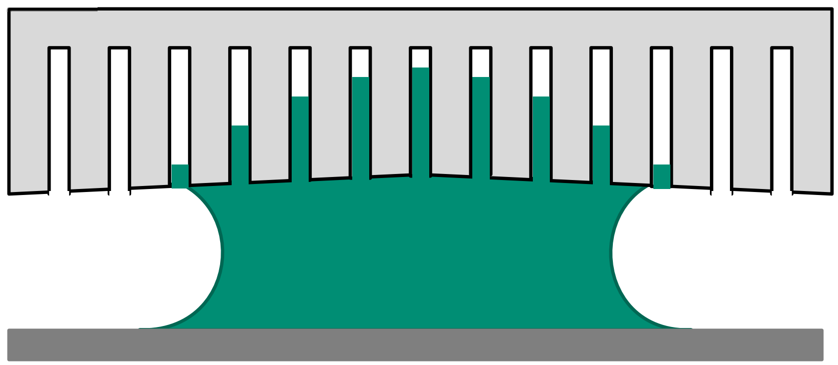

Meso-scale model

- 3-D FEM
- Analytical model development
- Effective medium approach
- 1 μm

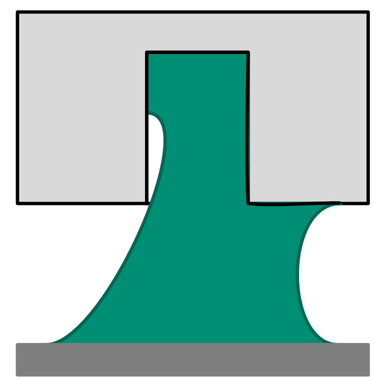

Feature Scale

- 3-D FEM
- Atomistics
- 10 nm

POC: Scott Roberts, Randy Schunk

Squeezing of Multiple Drops Under Template

Multiple drops do not spread symmetrically

Dynamics of the gas phase become much more important
- Gas must get out of the way
- Gas can become trapped

Template deforms over the scale of device

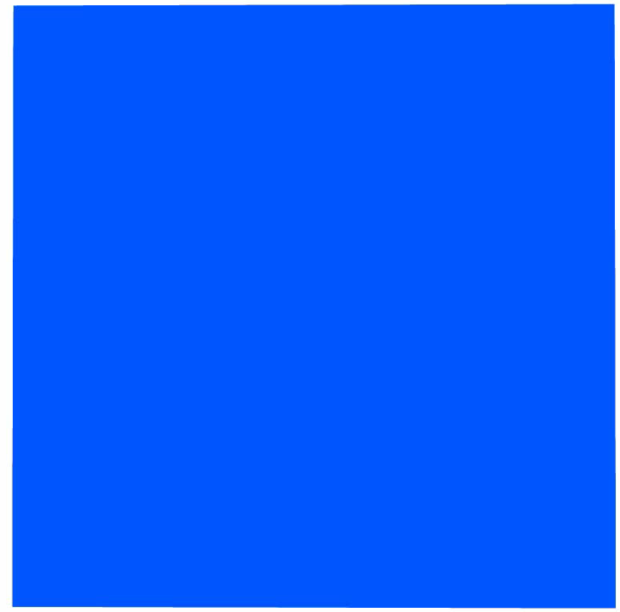

Pressure

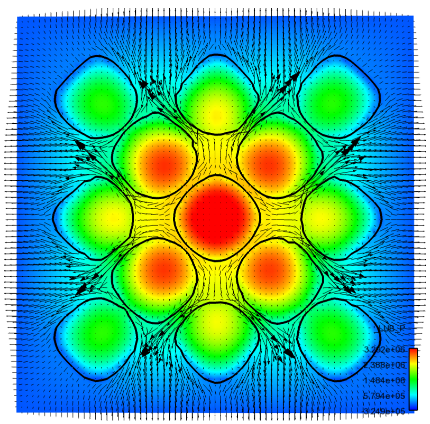

Velocity vectors

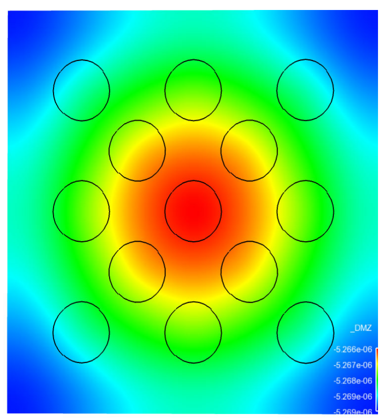

Template defle

Model Validation

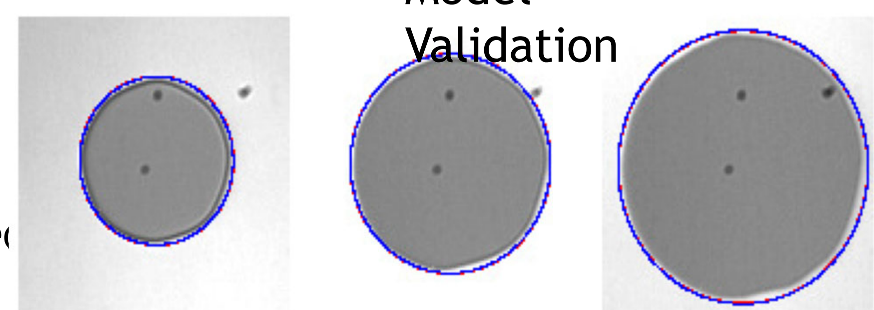

(a) $t = 0.06$ s (b) $t = 0.12$ s (c) $t = 0.18$ s

POC: Scott Roberts, Randy Schunk

Squeezing Under a Patterned Template

Real templates aren't uniform, but have regions of features and regions without

Presence of patterns have many effects:

- Pressure profile
- Template deflection
- Residual layer thickness / droplet distribution

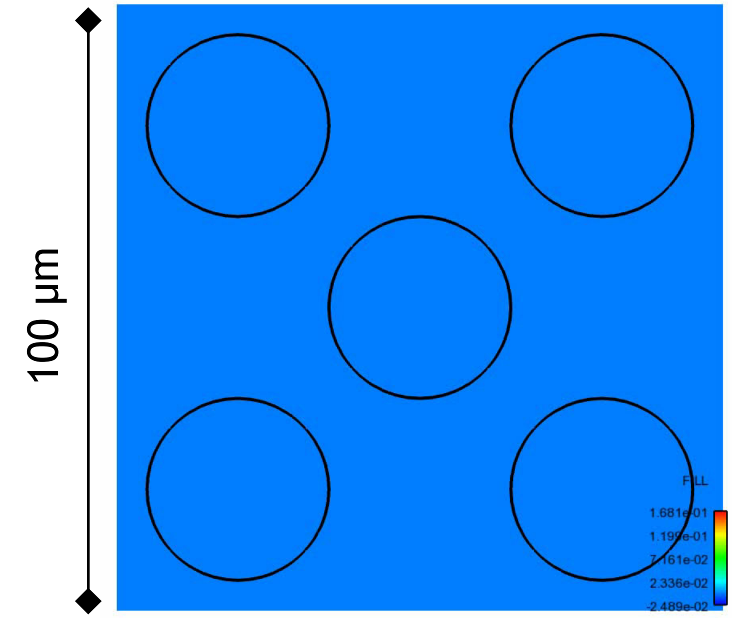

Saturation

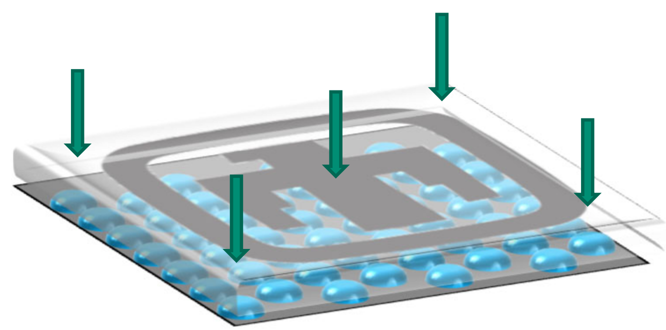

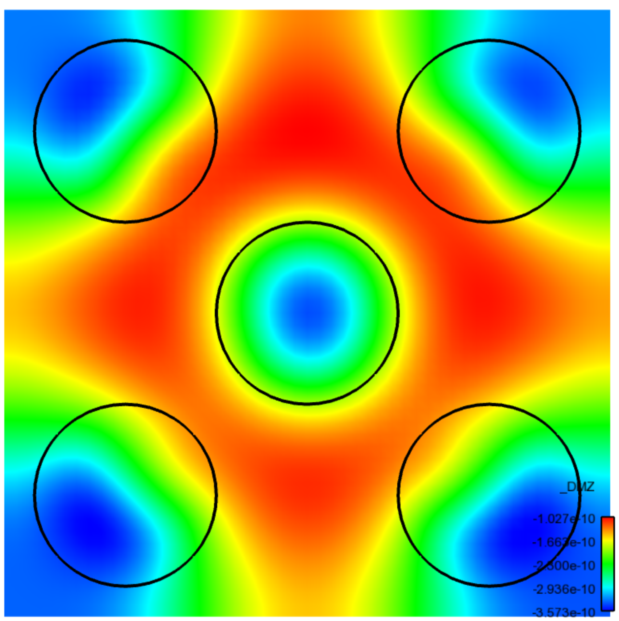

Template deflection

Structural Membrane-Lubrication Coupling

Drops merging on tensioned web for R2R nanoimprint lithography

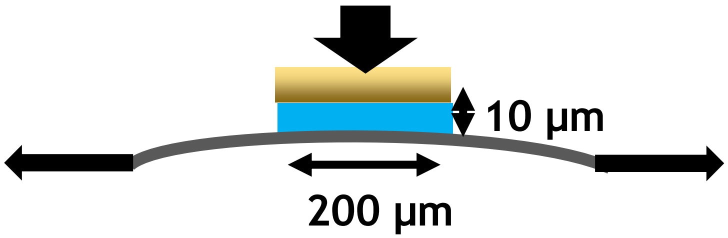

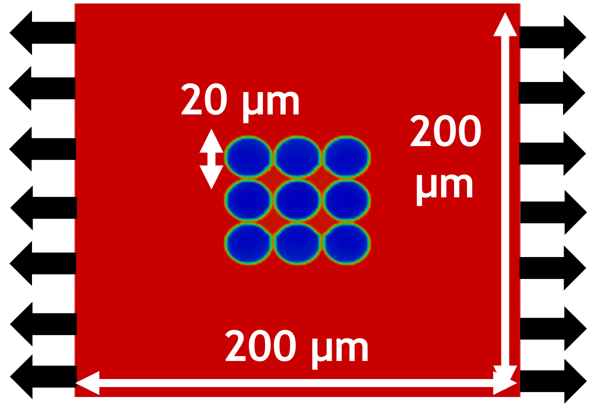

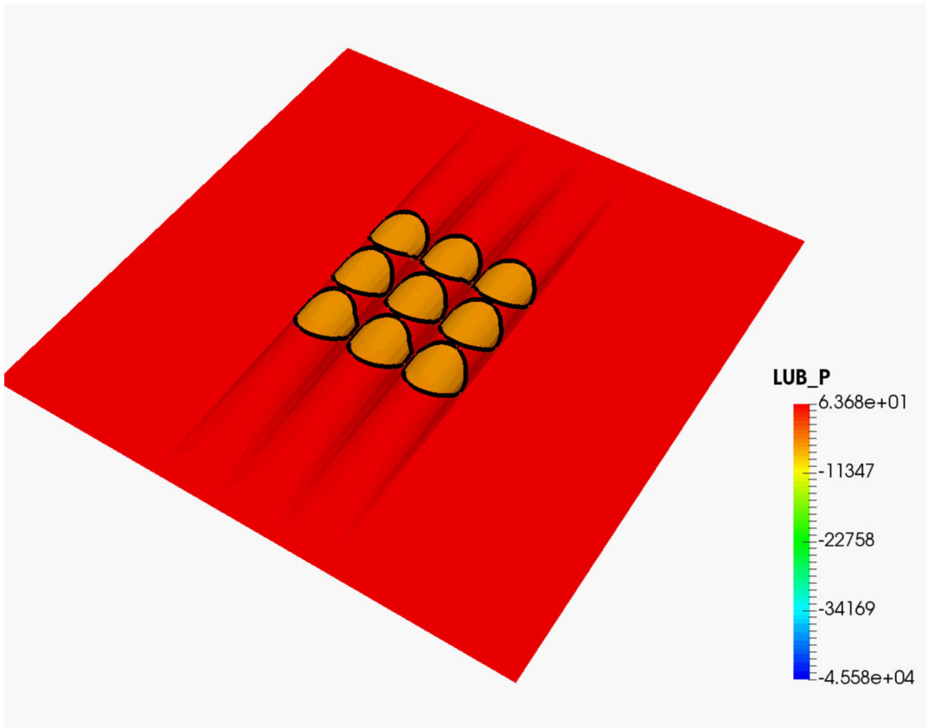

Flexible web: Membrane equation

$$\nabla_{II} \cdot \mathbf{T} + \boldsymbol{\tau}_{II} = \mathbf{0}$$

$$T_{11}\kappa_1 + T_{22}\kappa_2 + P = 0$$

Fluid phase: Reynolds lubrication with level set interface tracking.

$$\frac{\partial h}{dt} + \nabla_{II} \cdot \left\{ \frac{h^3}{12\mu} \left[\nabla_{II} P + F_{CSF}(\phi) \right] \right\} = 0$$

$$\frac{\partial \phi}{dt} + \mathbf{v}_{II} \cdot \nabla_{II} \phi = 0$$

Disperse Type Flow Model for Drop-on-Demand Imprinting

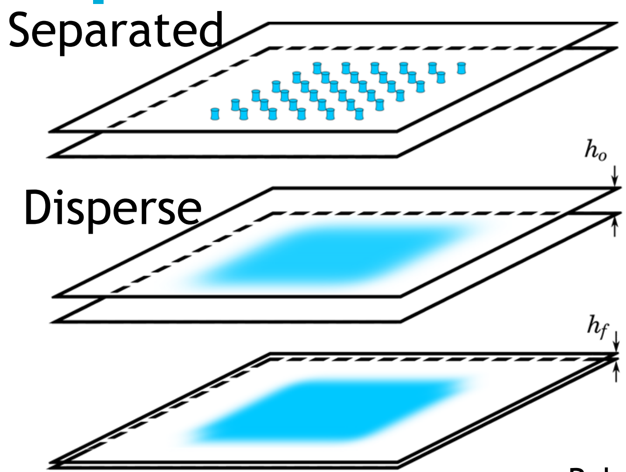

$$\boldsymbol{v}_\alpha = -\frac{h^2}{12\mu}\boxed{k_{r\alpha}}\boldsymbol{\nabla}_{\mathrm{II}}P$$

Relative Permeability: a measure of restriction of flow of one phase in the presence of another

Thin film transistor

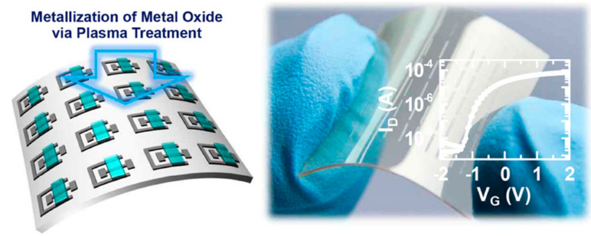

Choi, Y., W.-Y. Park, M. S. Kang, G.-R. Yi, J.-Y. Lee, Y.-H. Kim, and J. H. Cho, 2015, Monolithic metal oxide transistors, ACS Nano, p. 4288-4295.

Mask for conductive layer

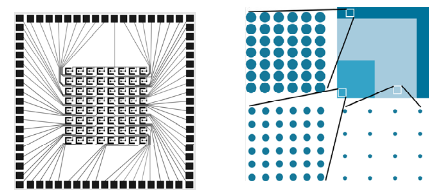

Regional drop density

Liquid bridge formation

Fluid from center overflows into wire region

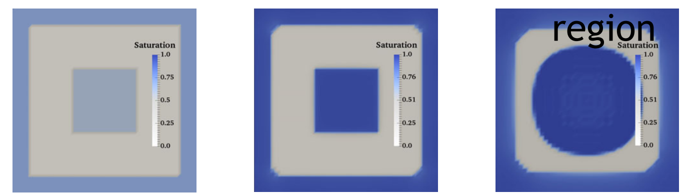

Gap thins, device region fills

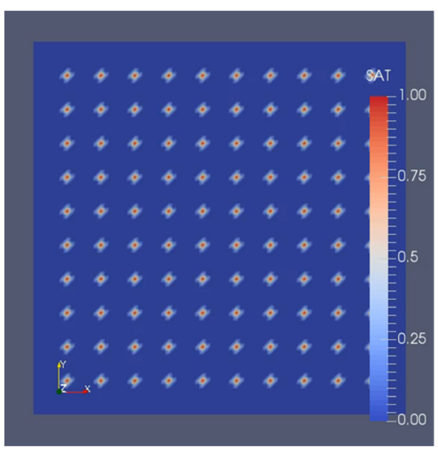

Separated

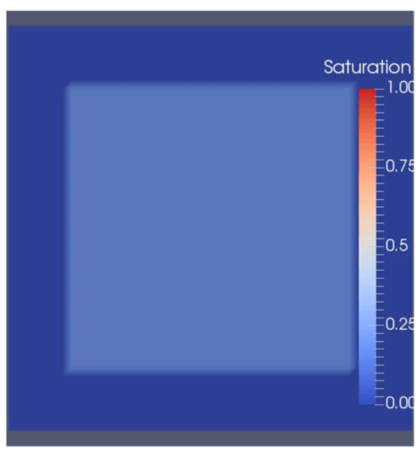

Disperse

- No template-filling model yet!
- Drop density is varied by saturation field initialization
- Model enables simulations with either separated or disperse type flow
- Gas trapping and dissolution is captured with analytical approximation
- Disperse representation enables large area simulations with coarse discretization

Cochrane, A., Tjiptowidjojo, K., Bonnecaze, R. T., Schunk, P. R. 2018 *Multiphase model for nanoimprint lithography*. International Journal of Multiphase Flow.

Reduced-Order Models for Thin Gap Multiphase Fluid Flow

$$h \ll L$$

$$Re\frac{h}{L} \ll 1$$

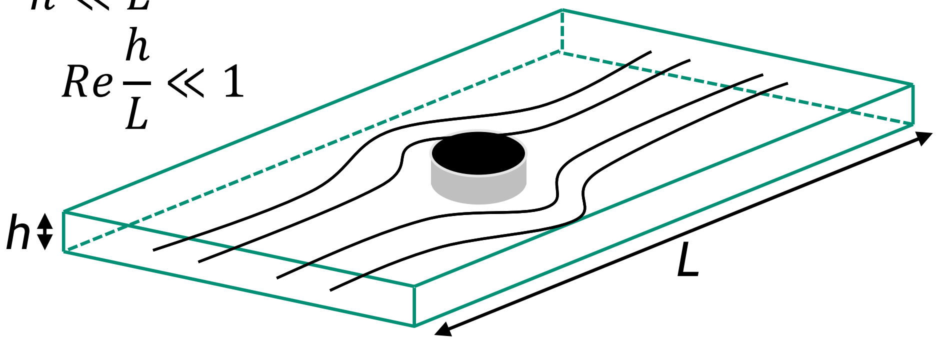

Reynolds, O., 1886, On the Theory of Lubrication and Its Application to Mr. Beauchamp Tower's Experiments, Including an Experimental Determination of the Viscosity of Olive Oil: Philosophical Transactions of the Royal Society of London, v. 177, p. 157-234.

In thin gaps momentum equations reduce to
2-D expression

$$\boldsymbol{v}_{\mathrm{II}} = -\frac{h^2}{12\mu}\boldsymbol{\nabla}_{\mathrm{II}}P$$

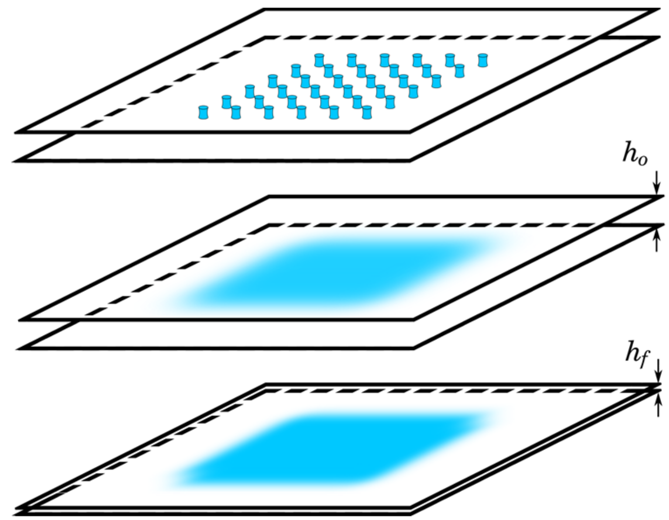

Relative Permeability

$$\boldsymbol{v}_{\alpha} = -\frac{h^2}{12\mu}\boxed{k_{r\alpha}}\boldsymbol{\nabla}_{\mathrm{II}}P$$

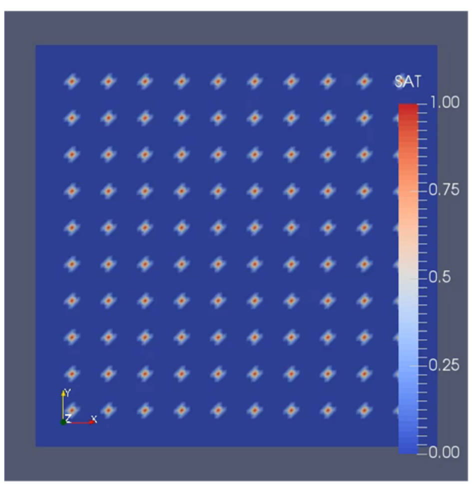

Separated

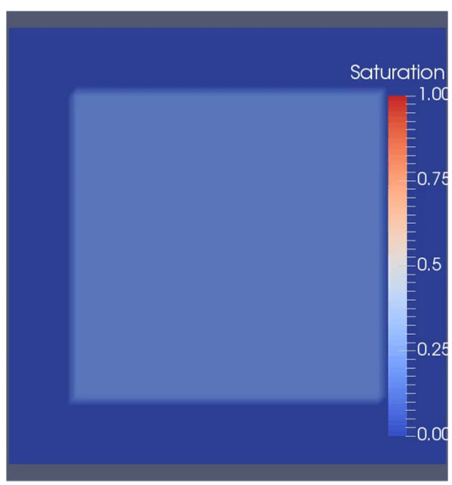

Disperse

Disperse representation enables large area simulations with coarse discretization

Gas Dissolution

Regular/known drop pattern

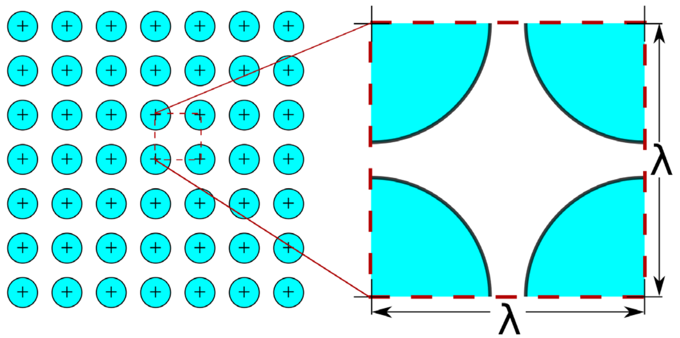

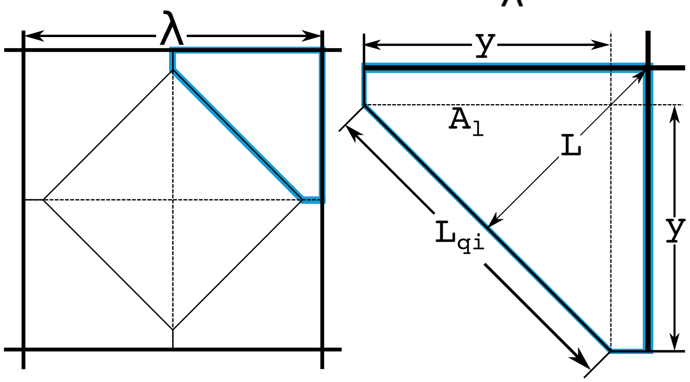

Analytic dissolution model

Gas Mass Balance

$$\frac{\partial((1-S)h\rho_g)}{\partial t} + \boldsymbol{\nabla}_{\mathrm{II}} \cdot (h\rho_g \boldsymbol{v}_g) + J = 0$$

Ideal Gas Law

$$\rho_g = \frac{M_g P}{RT}$$

Lumped Parameter Dissolution Model

$$J = h\frac{A_i}{V_G}\frac{D}{L}H(P - P_{\mathrm{atm}})$$

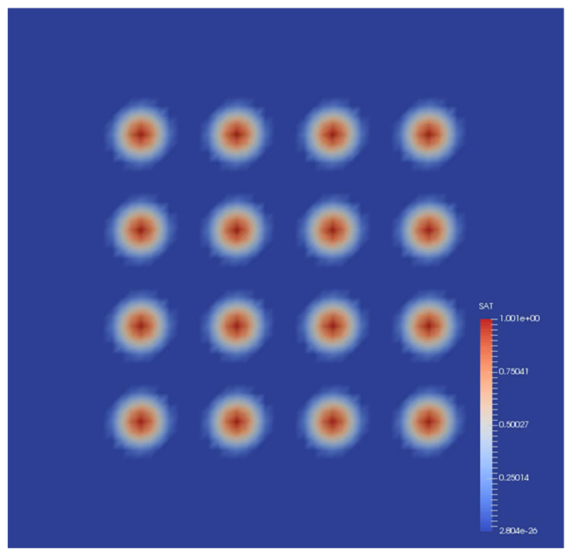

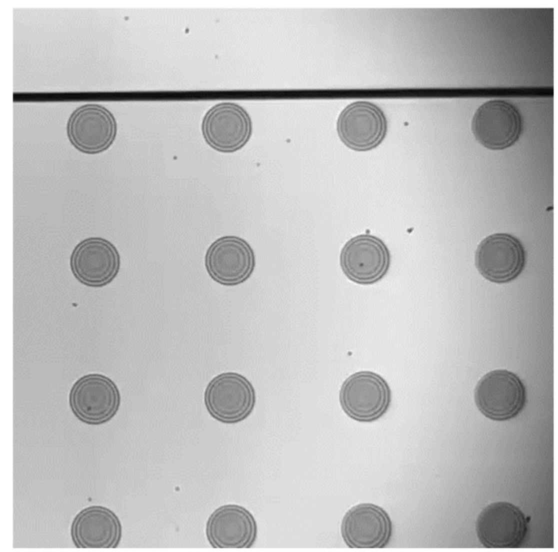

Reduced order models for two-phase, thin-gap, gas dissolving flow

Cochrane, A., Tjiptowidjojo, K., Bonnecaze, R. T., Schunk, P. R. 2018 *Multiphase model for nanoimprint lithography*. International Journal of Multiphase Flow.

Exemplar Device

Thin film transistor

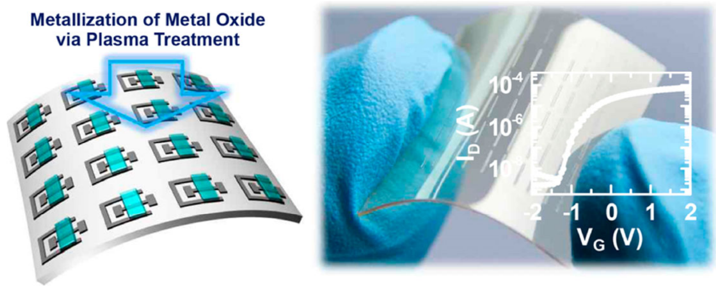

Choi, Y., W.-Y. Park, M. S. Kang, G.-R. Yi, J.-Y. Lee, Y.-H. Kim, and J. H. Cho, 2015, Monolithic metal oxide transistors, ACS Nano, p. 4288-4295.

NIL processing model

Disperse flow formulation

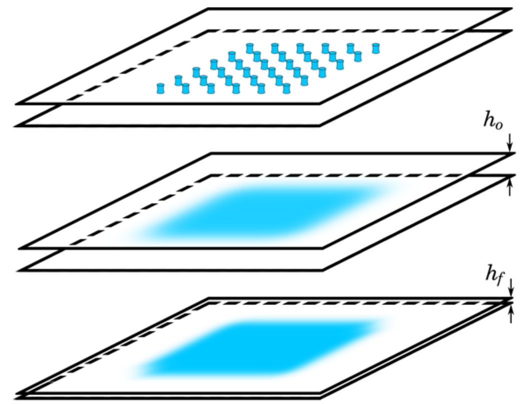

Pattern mask

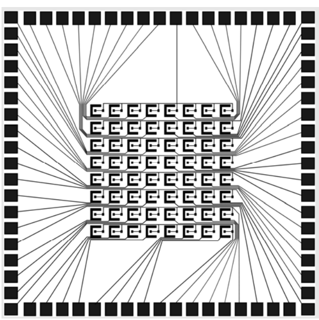

Regional drop density

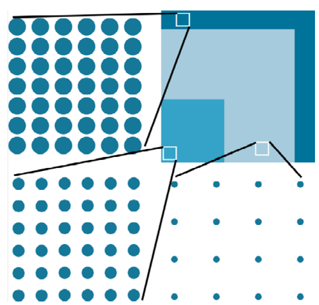

Liquid bridge formation

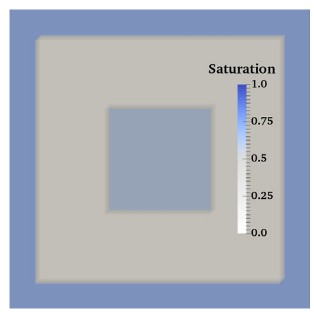

Full gap

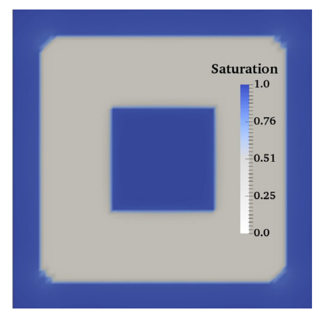

Overfull gap

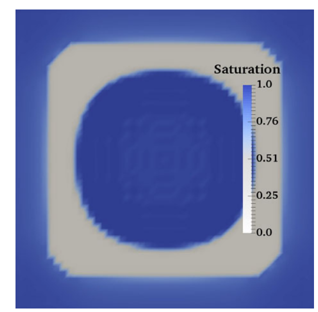

Initial saturation field is varied to represent

From Foil Bearing Theory to R2R Nano-Manufacturing

Magnetic Tape Drive

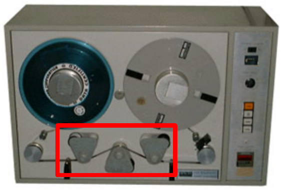

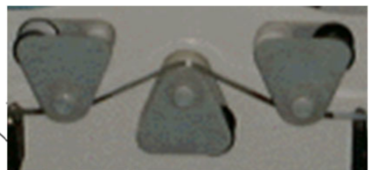

Foil-Air Journal Bearing

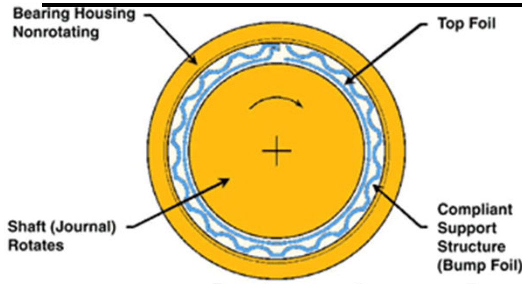

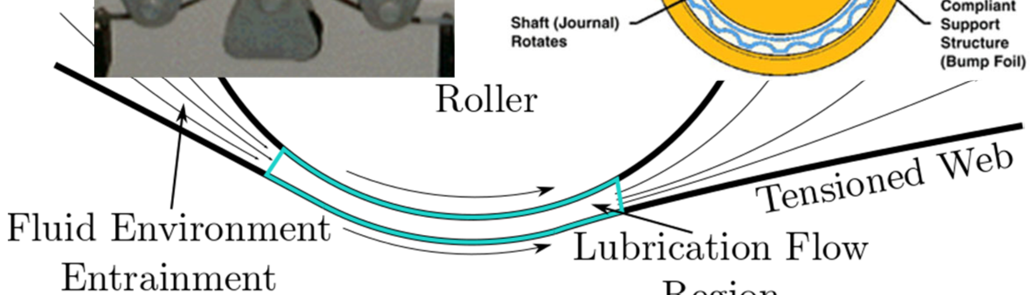

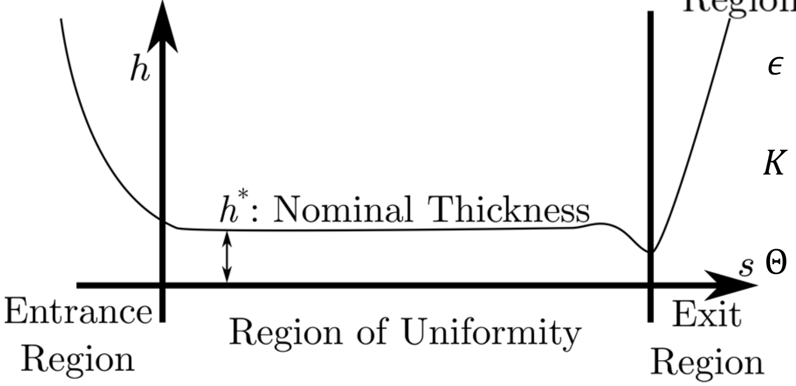

$$\epsilon = \frac{12\mu v_a}{T}$$ Viscous Forces / Tension Forces

$$K = \frac{h^*}{r\epsilon^{2/3}}$$ Dimensionless Gap Thickness

$$\Theta = \frac{\theta}{\epsilon^{1/3}}$$ Wrap Length / Transition Length

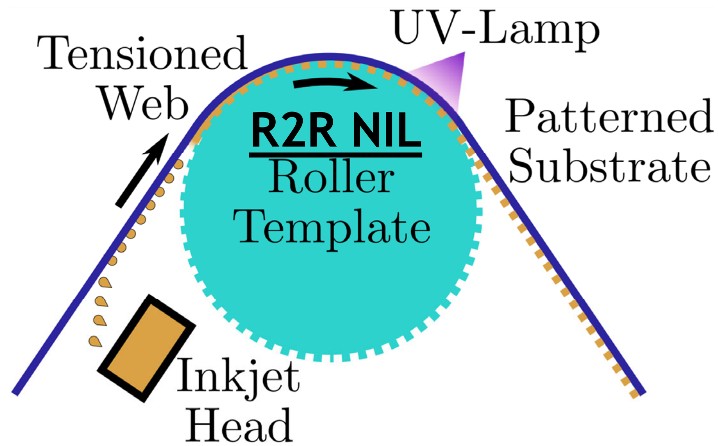

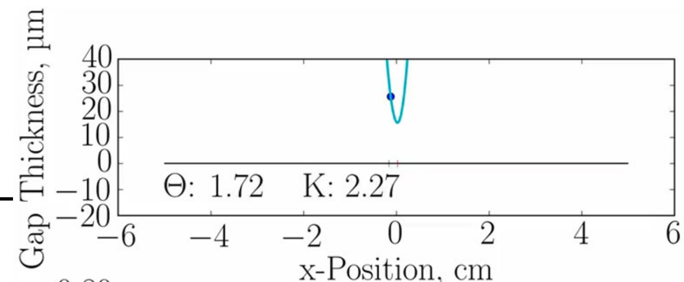

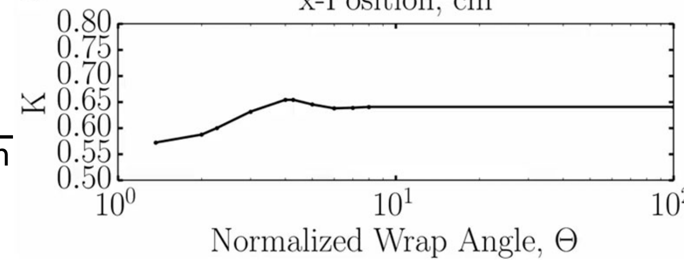

Steady-state models for foil-bearing lubrication film

Blok, H. and vanRossom, J. J. (1953) *The foil bearing – A new departure in hydrodynamic lubrication*. Lubrication Engineering (9)

Gross, W. A. et al . (1980) *Fluid Film Lubrication. John Wiley & Sons, Inc.,* United States

Cochrane, A. et al. (2019) *Elastohydrodynamics of roll-to-roll UV-cure imprint lithography*. Industrial & Engineering Chemistry Research 58(37)

Multiple – Feature Scale Study

DROPLET VOLUMES = 2 pL EACH

t = 0

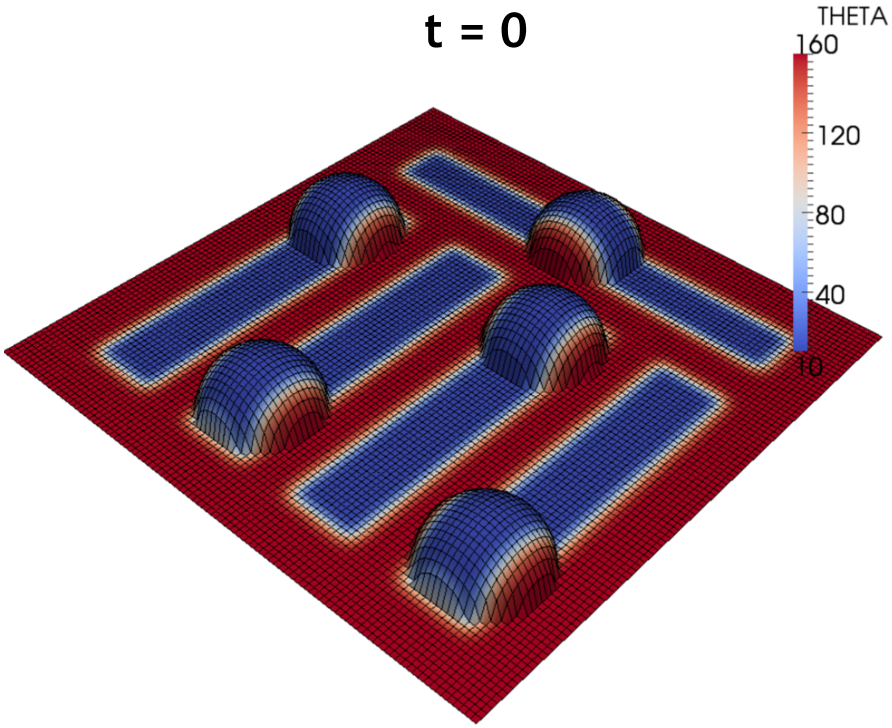

t = 492 μs

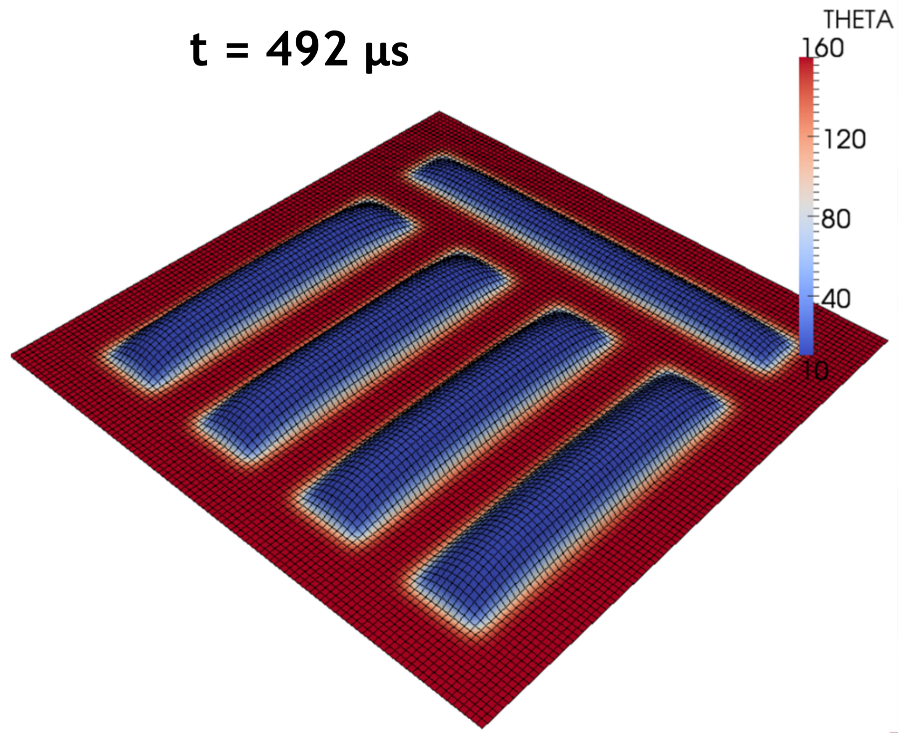

NO PARTICLES – INITIALIZED WITH DROPLETS

THE DROPLETS SPREAD AND COVER THE PATTERN

Free Surface Flow in Thin Geometry

Computation domain - 2.5D (Shell)

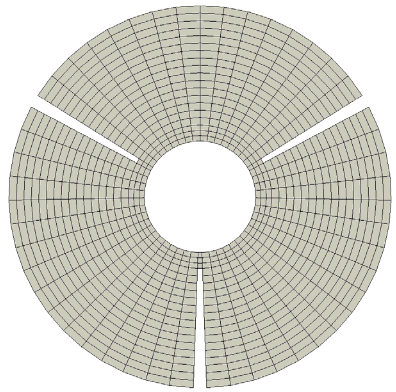

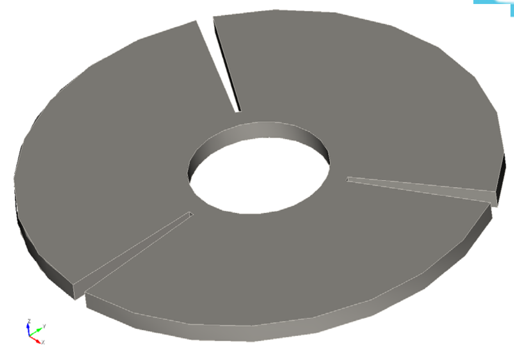

Flow domain - oblique view

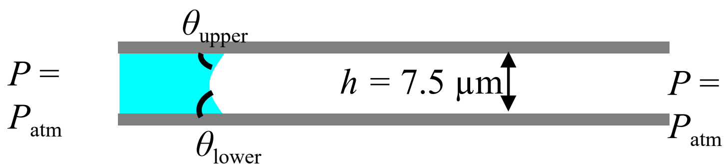

h/L << 1 ➔ lubrication approximation applies

$$\nabla_{II}\cdot\left\{\frac{h^3}{12\mu}\left[\nabla_{II}P+\underbrace{\sigma\kappa\delta(\phi)\mathbf{n}}_{\textit{capillary pressure jump}}\right]\right\}=0$$

Reynolds lubrication equation

$$\kappa=\frac{\cos\theta_{\text{upper}}+\cos\theta_{\text{lower}}}{h}$$

Meniscus curvature - Arc of circle

$$\frac{\partial\phi}{\partial t}+\mathbf{v}_{\text{lub}}\cdot\nabla_{II}\phi=0$$

Level set advection equation

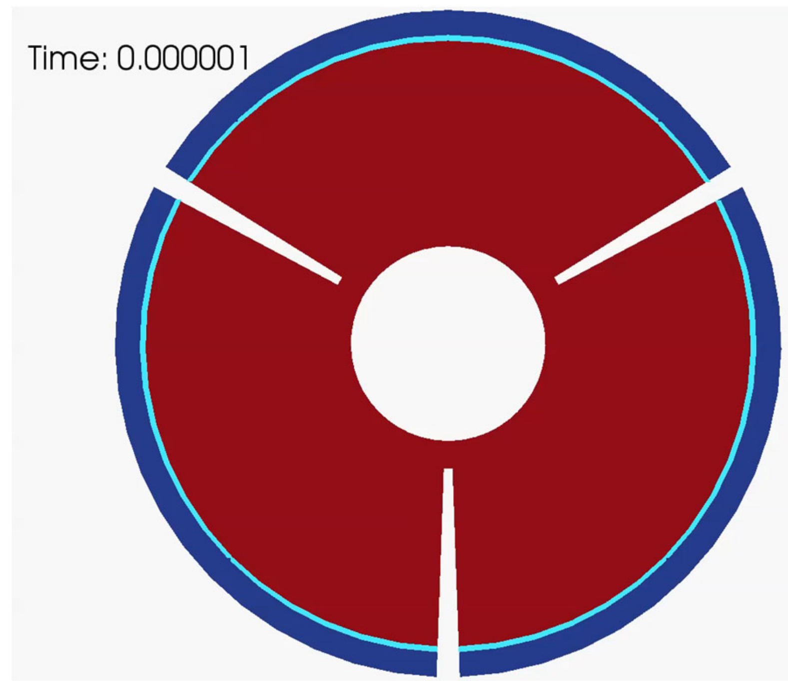

Roberts, et al. (2013). *Computers & Fluids*, *87*, 12-25.

Design Rules for Polymer Nanomanufacturing

We have developed computational tools that provide comprehensive understanding of polymer flow during nano-embossing.

EXPERIMENT

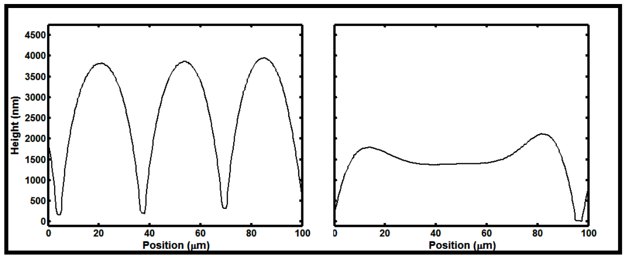

SIMULATION

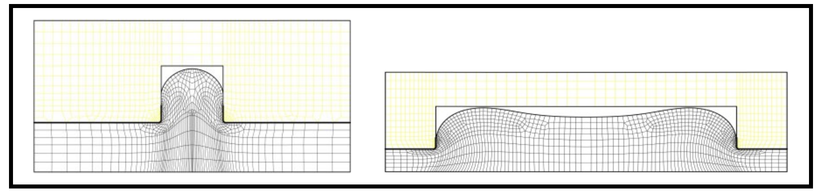

Simulation matches single or dual polymer peak deformation dependent on cavity geometry

<u>*Outer → Inner Fill*</u>

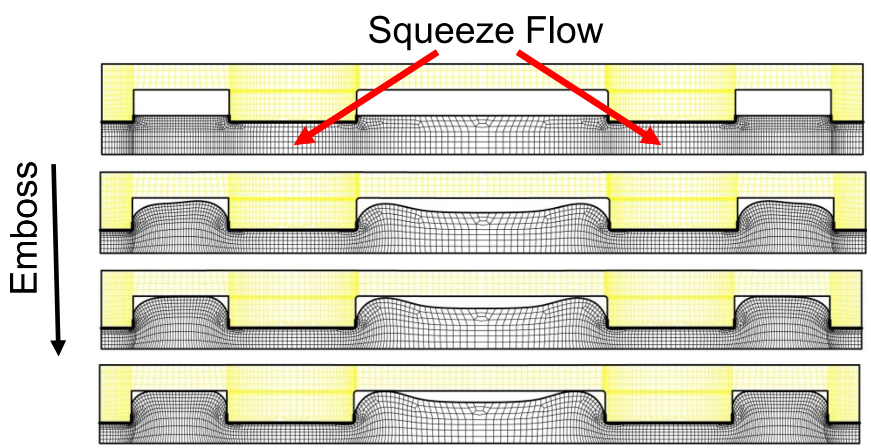

<u>*Inner → Outer Fill*</u>

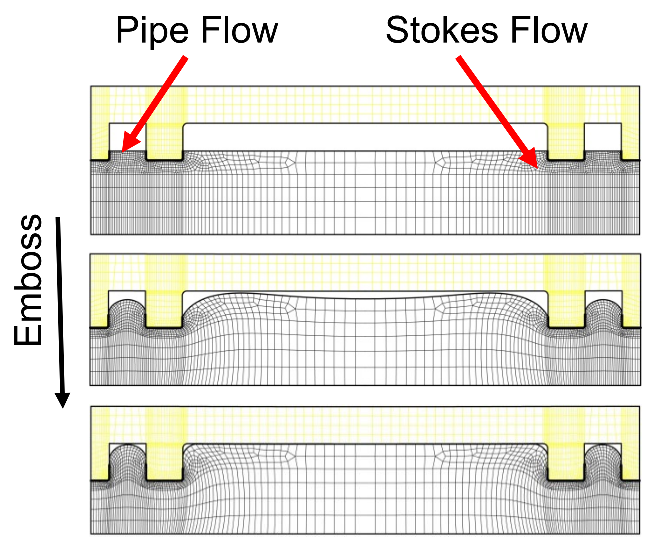

Filling order depends on flow mechanism

Slot-Die Coating Model

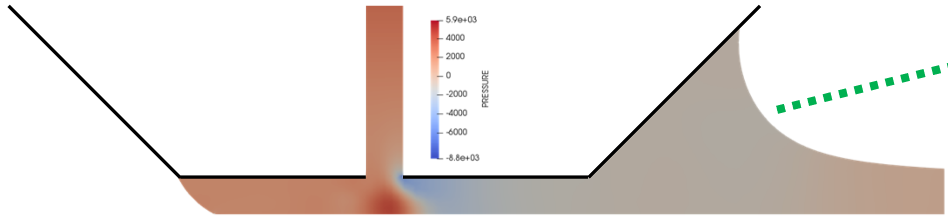

Low Viscosity fluid above Low-Flow Limit

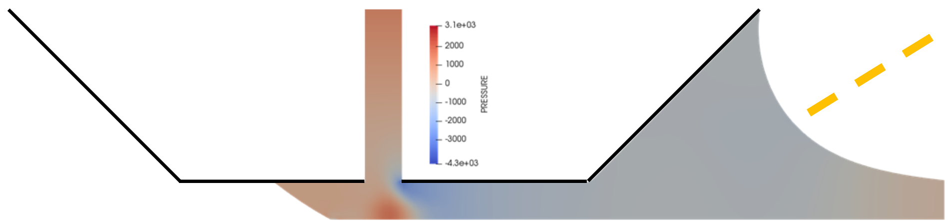

Low Viscosity fluid at Low-Flow Limit

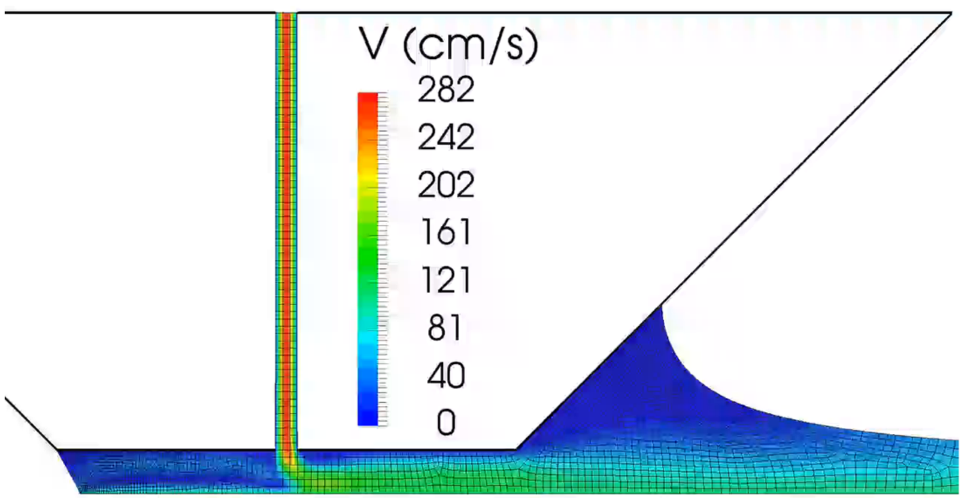

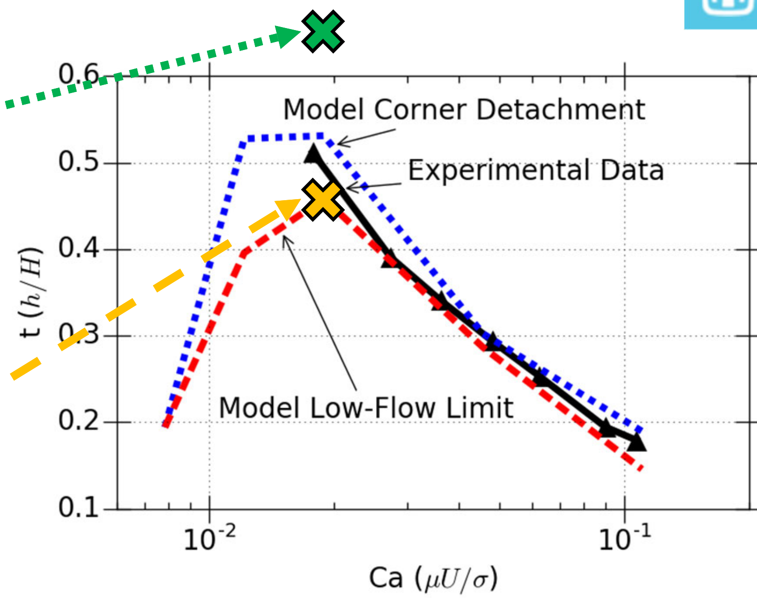

Low-Flow Limit for Low Viscosity
(1.2 mPas, static $\theta_{1,2} = 38^o$, dynamic $\theta_3 = f(Ca)$)

- Developed model with unpinned menisci that addresses all possible 2D changes in coating bead shape
- Validated via experimental low-flow limit data and flow visualizations from literature
- Investigated and determined mechanisms of the low-flow limit as a function of capillary number

3M Coating Flow with Tensioned Web

BASE CASE

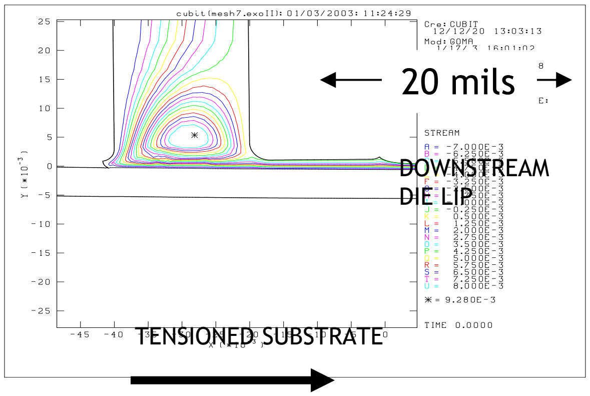

SHORTER LIP LENGTH

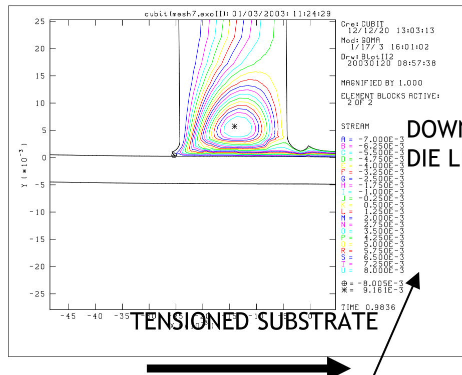

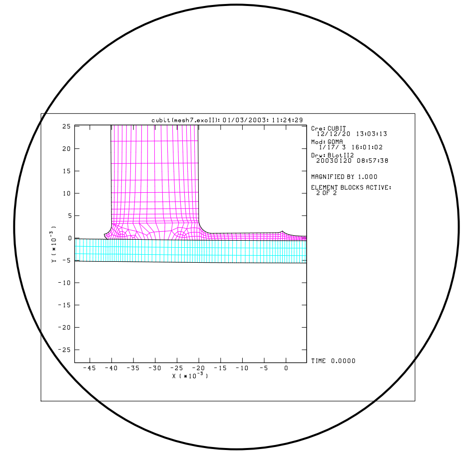

LARGER LIP RADIUS

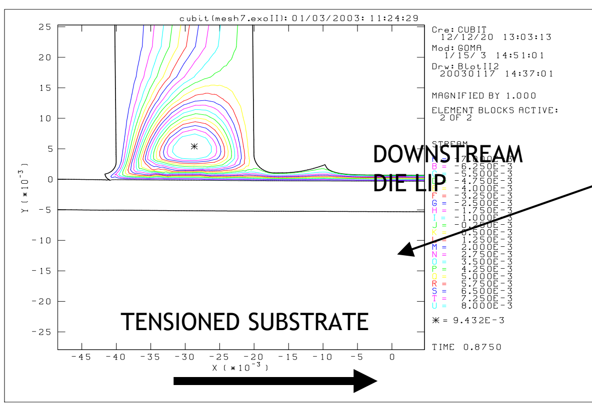

Custom Lip Shapes
In 3M Goma

Results:
- ESTC, Pioneer Verification of Streak Reduction
- Transfer to Menomonie

3M Two-Layer Knife Coater

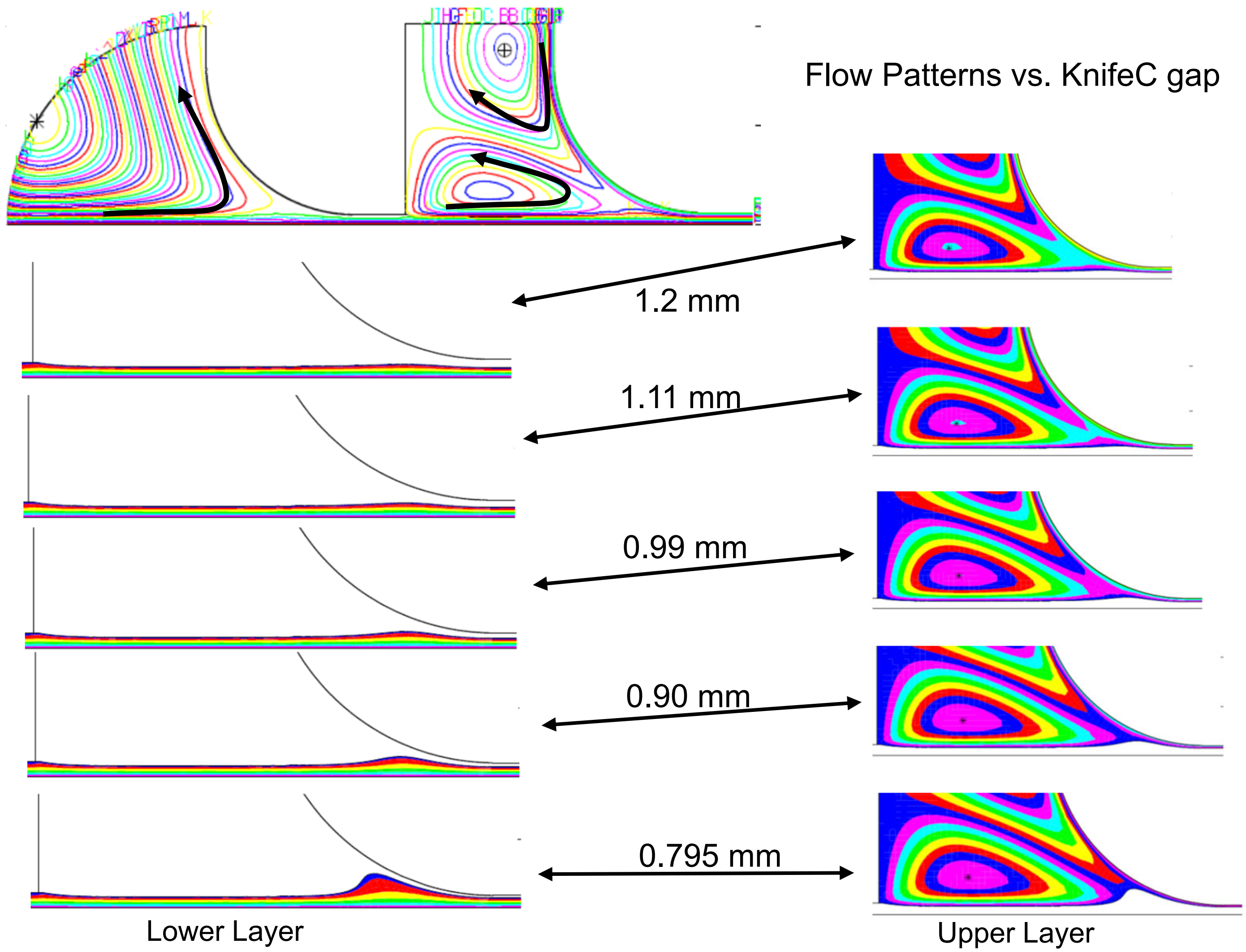

Linear Stability Analysis of Slide Coating

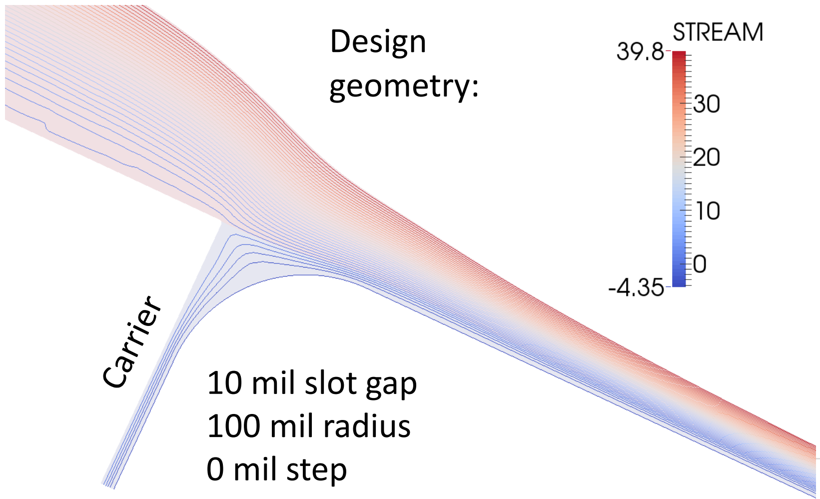

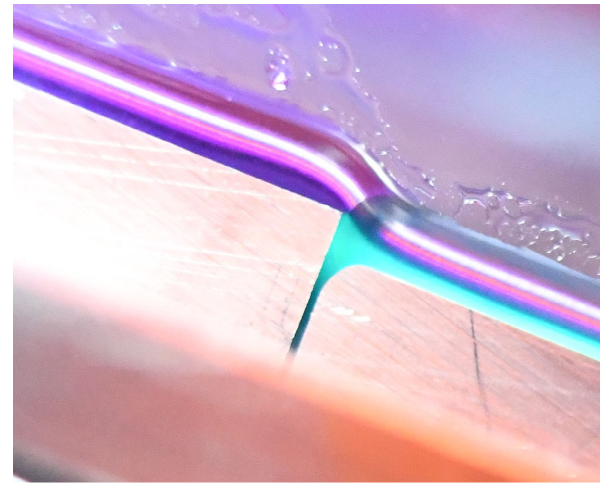

Layer stability of slide layer confluence:

$$\boldsymbol{u}(t) = \boldsymbol{u}^{\mathbf{0}} + \boldsymbol{\varepsilon}\, exp[(\lambda_{real} + i\omega)t]$$

Generalized Eigenvalue Problem:

$$\boldsymbol{J}\hat{\boldsymbol{u}} = \lambda \boldsymbol{M}\hat{\boldsymbol{u}}$$

$$disturbance \sim e^{\lambda t} = e^{(\lambda_{real} + i\omega)t}$$

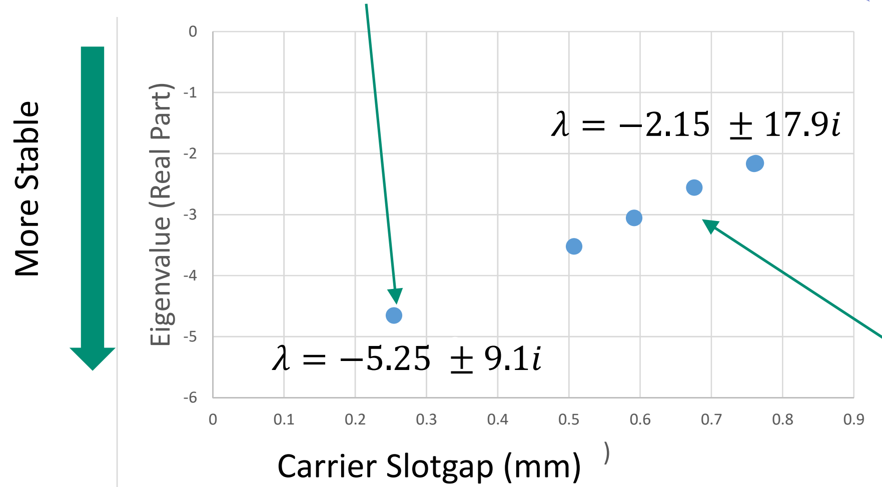

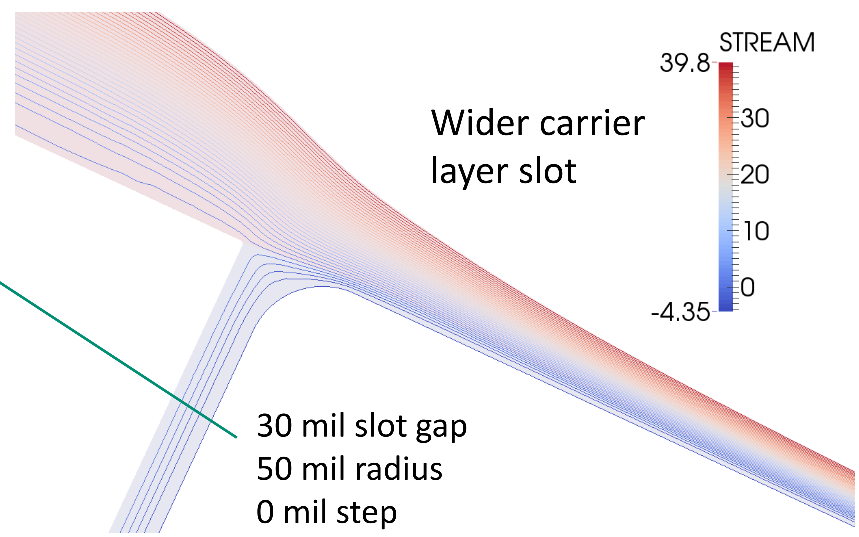

Notch Bar Coater with a Rolling Bank

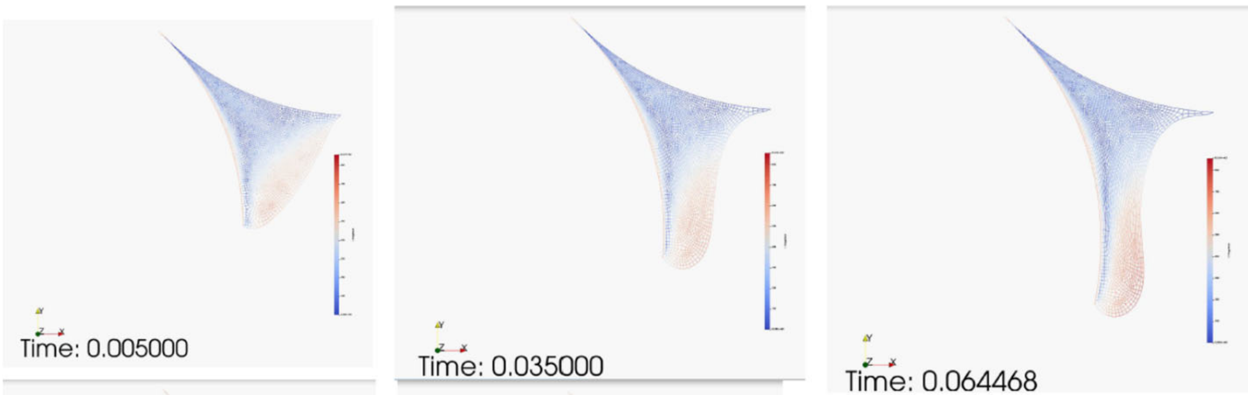

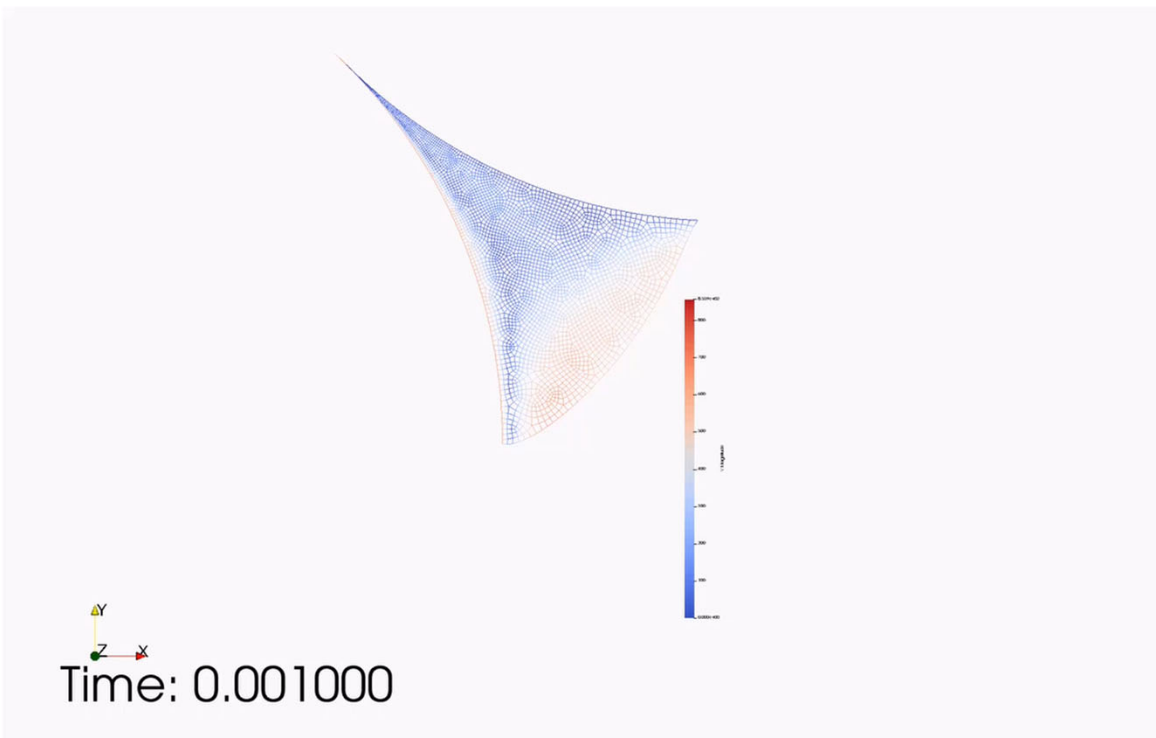

- Moving mesh algorithm can handle large deformation
- Remeshing in Cubit can improve mesh quality
- Dr. Secor's Perl script automates the process including remeshing, remapping solution to new mesh, and restarting Goma
- Approach can handle pinch off and beyond

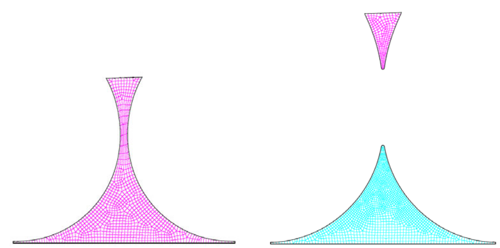

Micro-flexo-printing

Continuation & Stability –Coating Flow

Continuation and stability analysis of coating flow allow us to track turning points in the solution and stable and unstable regions

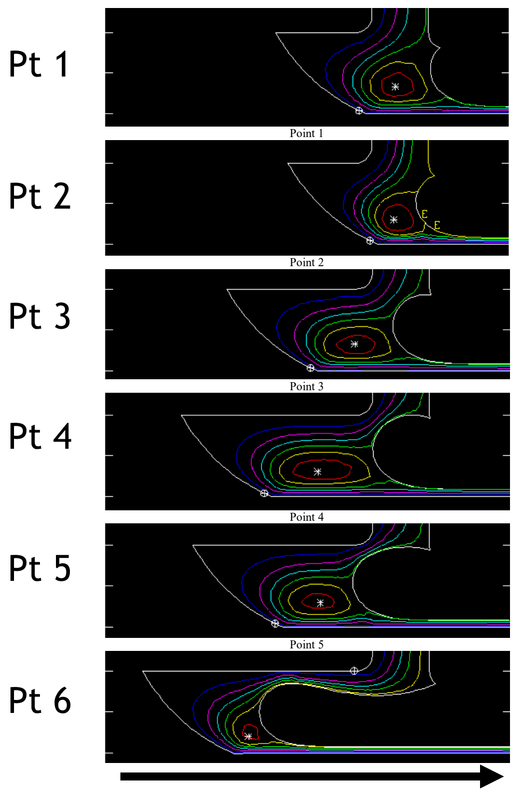

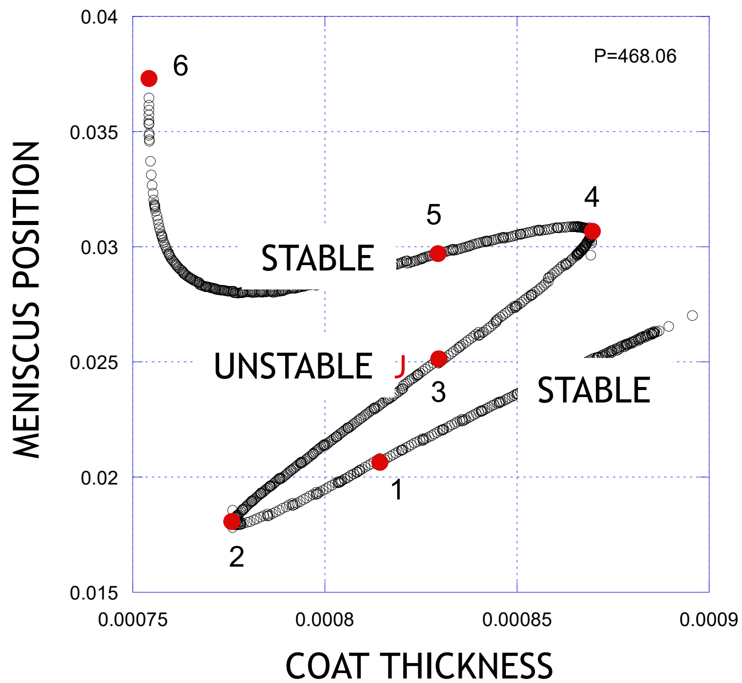

Benefits: Lip design, material characteristics for robust process windows (thinner, faster, higher quality).

Predict Operability Windows of Slot and Slide Coating

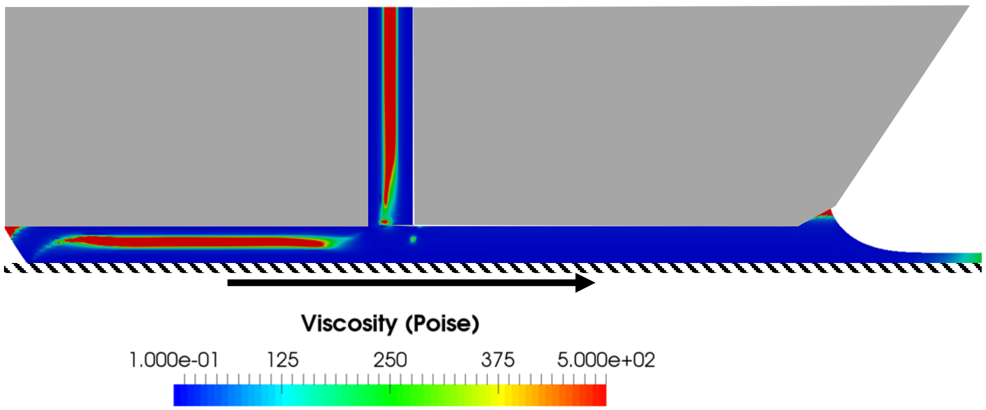

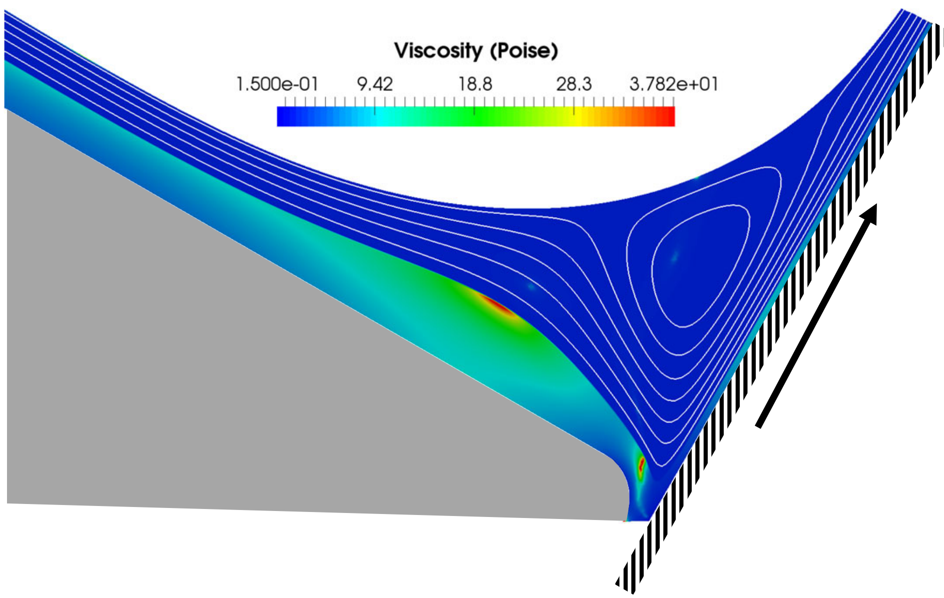

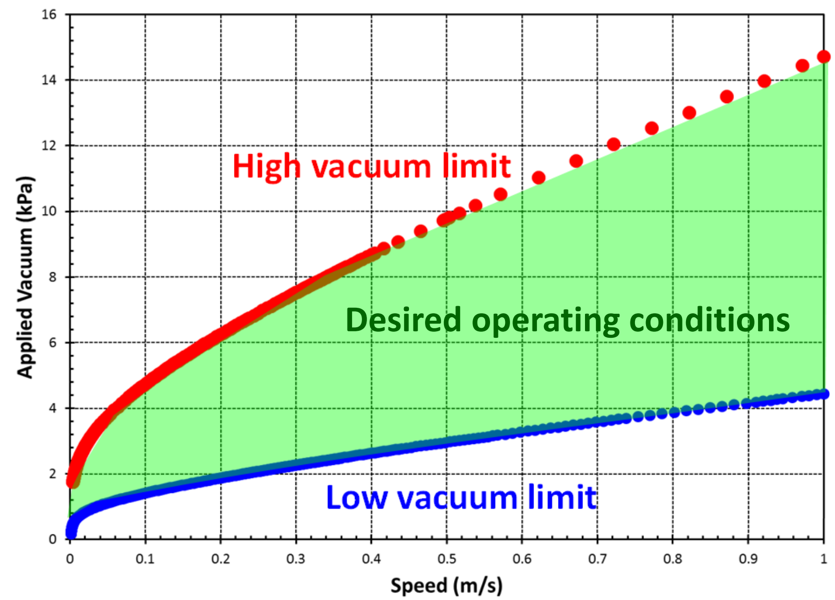

- Goal: ***Map operability window*** of slot and slide coating.
- Fluid: Particles-laden ink – ***shear thinning*** with power law index $n \sim 0.2 - 0.5$
- Steady state model + ***augmenting condition*** to solve for low and high vacuum limits

Funded by the U.S. Department of Energy, Office of Energy Efficiency and Renewable Energy, Advanced Manufacturing Office

Controlling Etch Depth in C-Si with Confinement

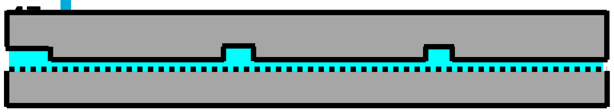

Tjiptowidjojo, Kristianto, et al. *ECS Journal of Solid State Science and Technology* 9.3 (2020): 034013.

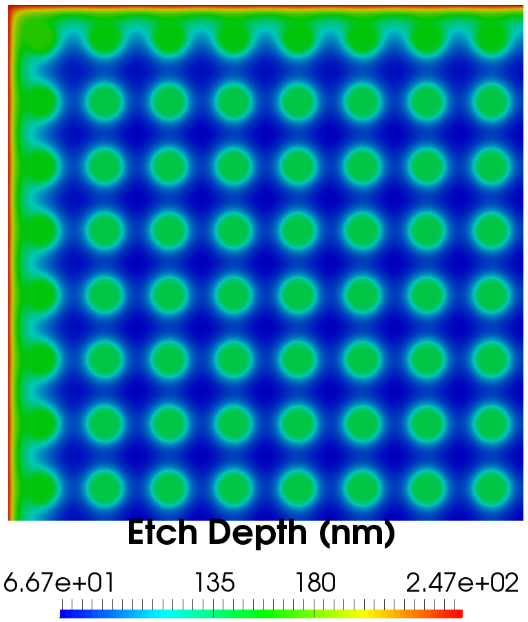

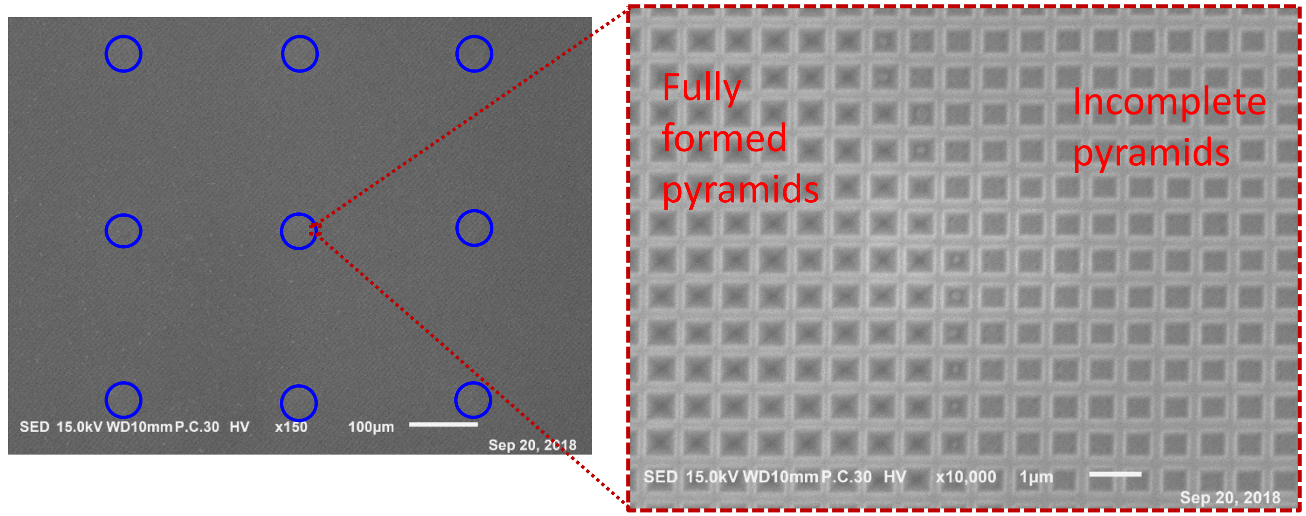

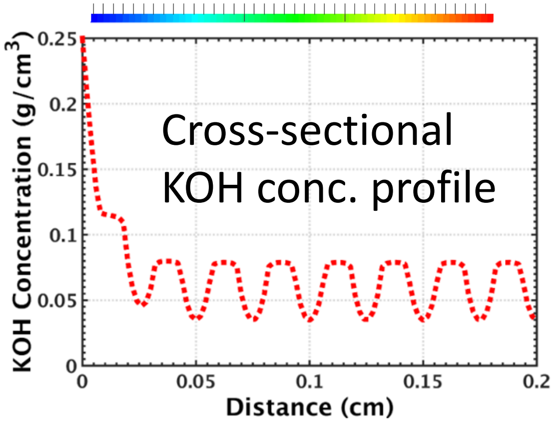

- Goal: ***Increase light trapping*** in thin c-Si for solar cell
- Create ***local mass transfer barrier*** for KOH transport to etching surface → controlling etch depth variation
- Thin region → use ***shell approach*** to model species transport and reaction
- Predictions agree with experimental results

Funded by the National Science Foundation under Cooperative Agreement No. SNM-1635334

3-D Elastic Solid-Lubrication Coupling

Doctoring excess liquid film in μ-gravure printing

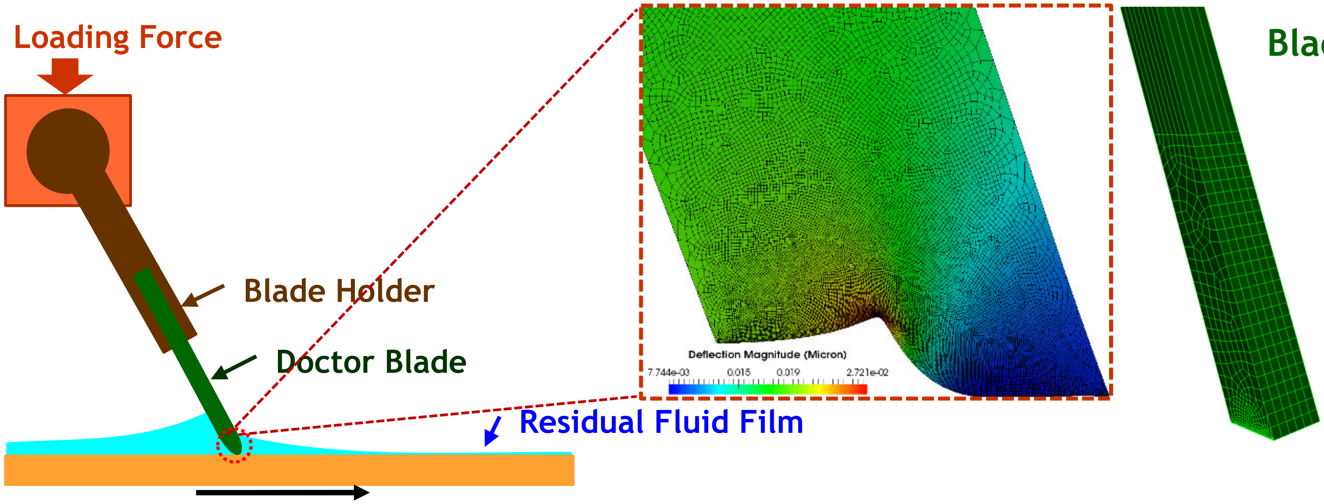

Blade - 3-D elasticity

$$\nabla \cdot \boldsymbol{\sigma}_s = \rho \frac{\partial^2 \mathbf{u}}{\partial t^2}$$

$$\boldsymbol{\sigma}_s = G\left(\nabla \mathbf{u} + \nabla \mathbf{u}^T\right) + \lambda\left(\nabla \cdot \mathbf{u}\right)\mathbf{I}$$

Gap - Reynolds Lubrication

$$\frac{\partial h}{\partial t} = \nabla_{II} \cdot \left(\frac{h^3}{12\mu} \nabla_{II} p - \frac{h}{2} \mathbf{t} V_W\right)$$

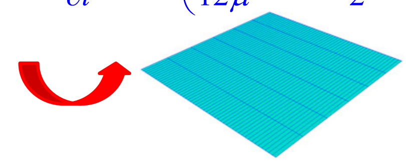

Model Validation

Hariprasad et al. (2016). *Journal of Applied Physics*, *119*(13), 135303.

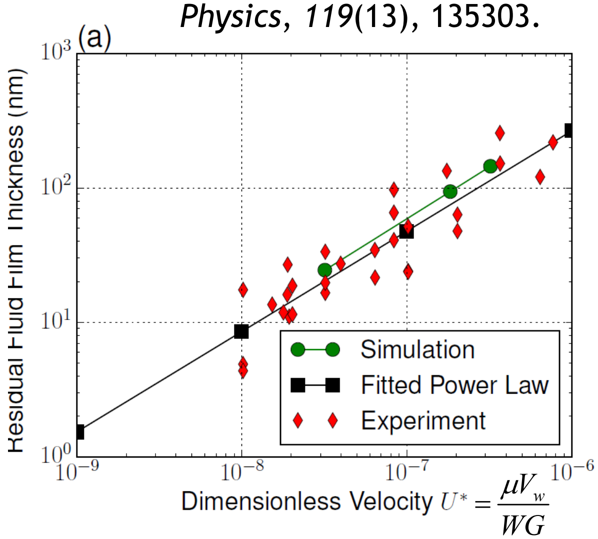

Effect of Blade Tip Shapes

Tjiptowidjojo et al. (2018). *Journal of Coating Technology and Research*, *15*(5), 983-992.

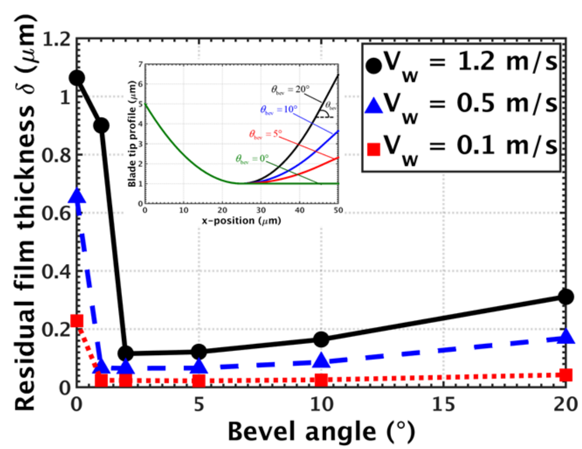

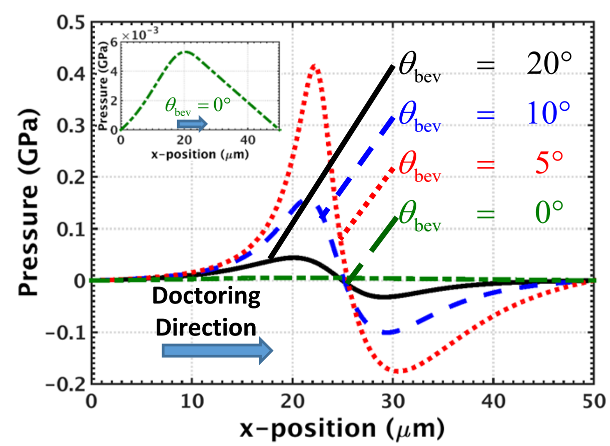

Weld Process-Modeling

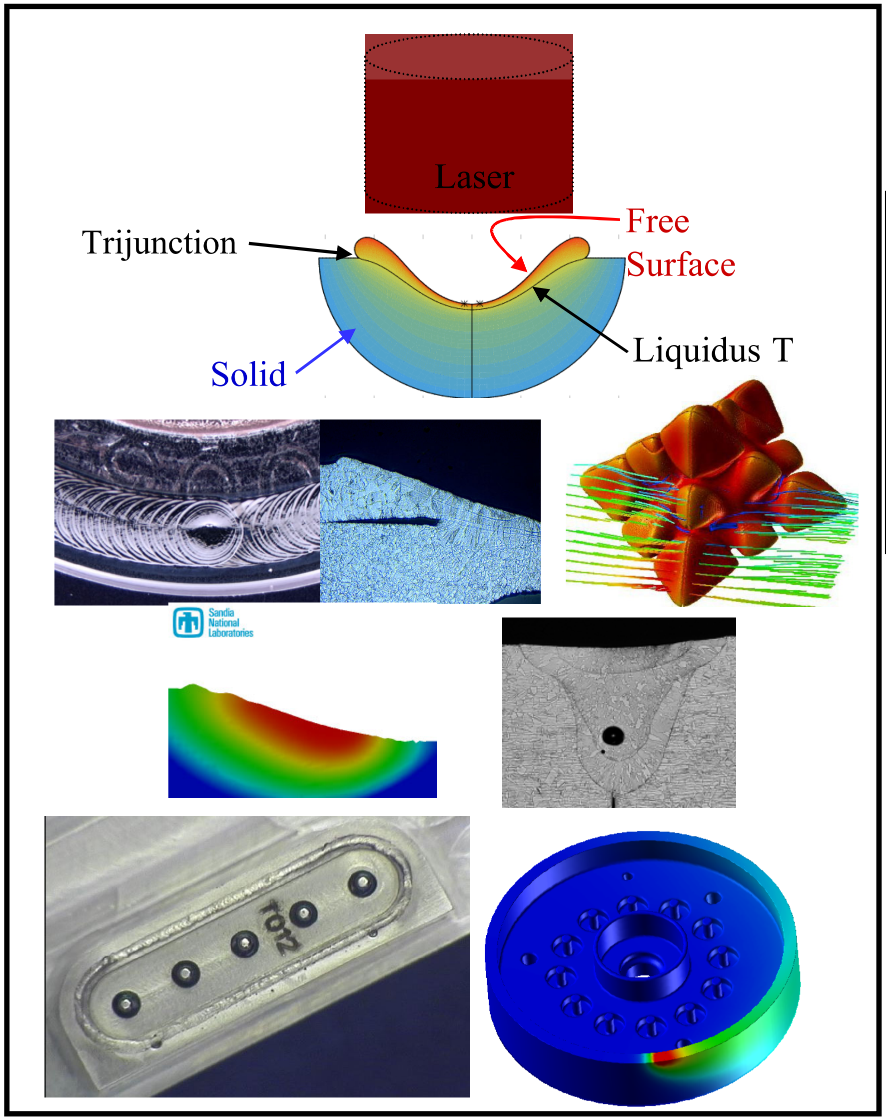

Welding, Brazing, and Soldering are used extensively in manufacturing

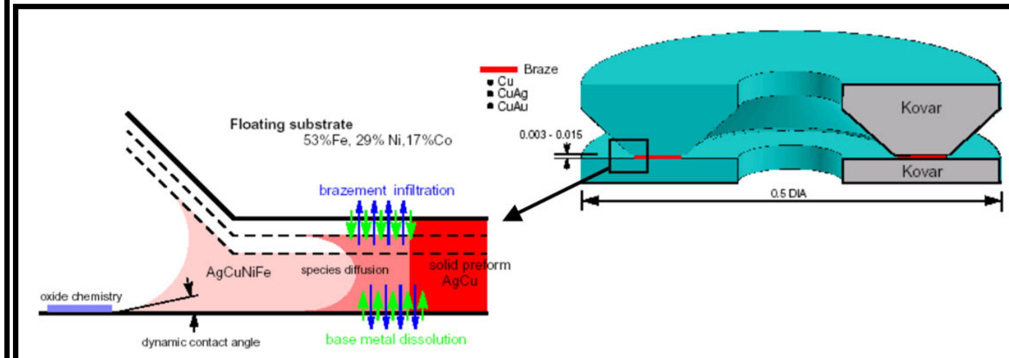

Keyhole welding models: Pore formation and Residual Stress

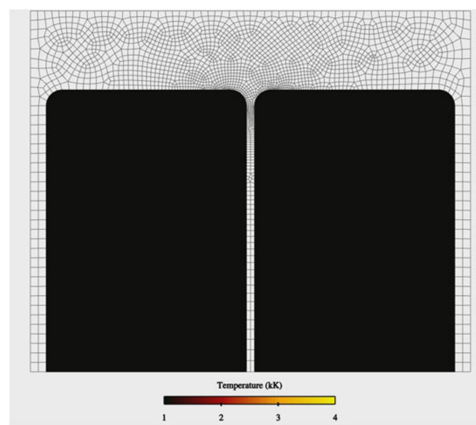

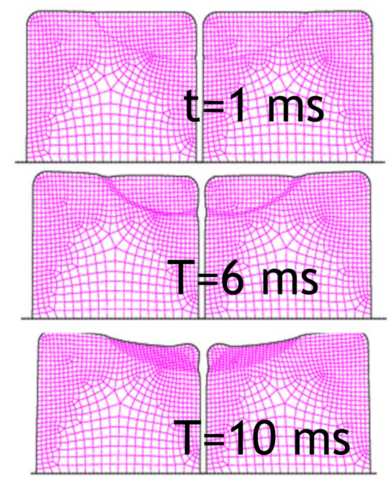

Proppant Modeling

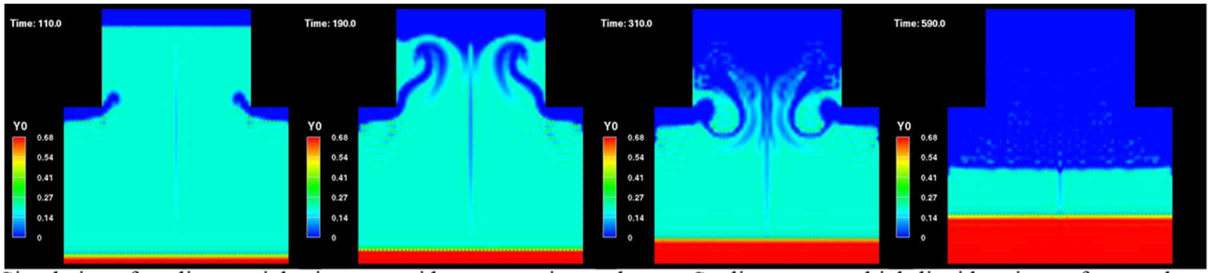

Simulation of settling particles in a cup with a contraction at the top. Settling causes a high-liquid region to form under ledges, which then leads to density-driven secondary flows.

Note V-shaped interface at suspension/clarified zone in second frames.

Recirculation causes slightly convex interface in final (rather than a "hill" in the middle that intuition would predict)

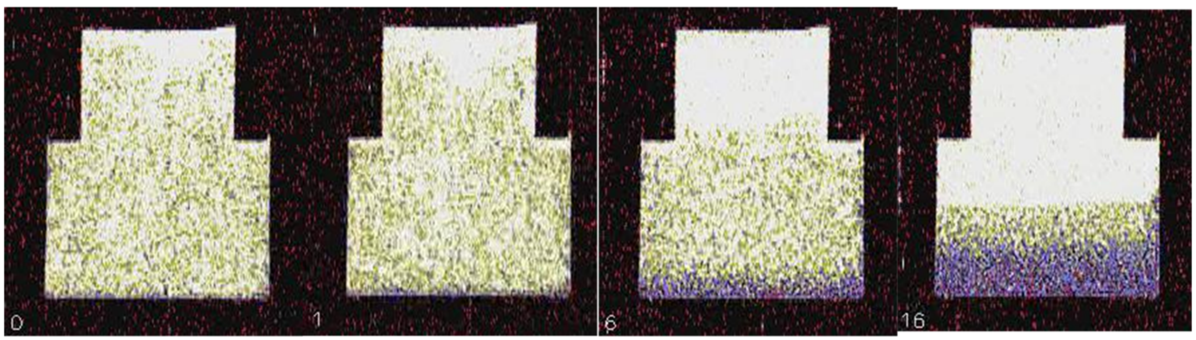

NMR imaging of same geometry

(Left) NMR images by Altobelli, New Mexico Resonance, Albuquerque

(Below) Photos in thin slit by Prof. Peter Clark, University of Alabama

Model of hydrofrac operation: gravity dominating

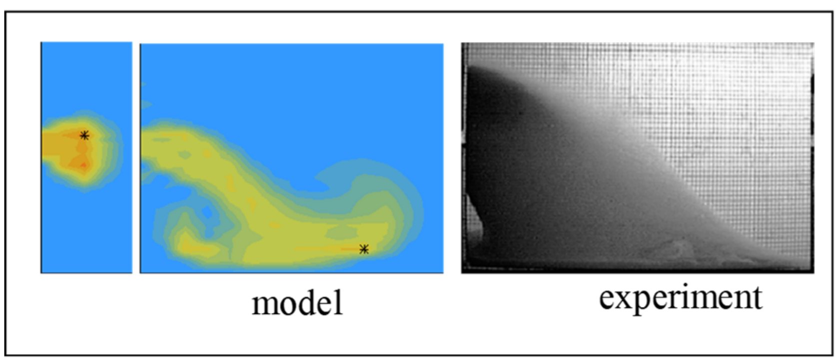

Model of hydrofrac operation: viscous resuspension dominating

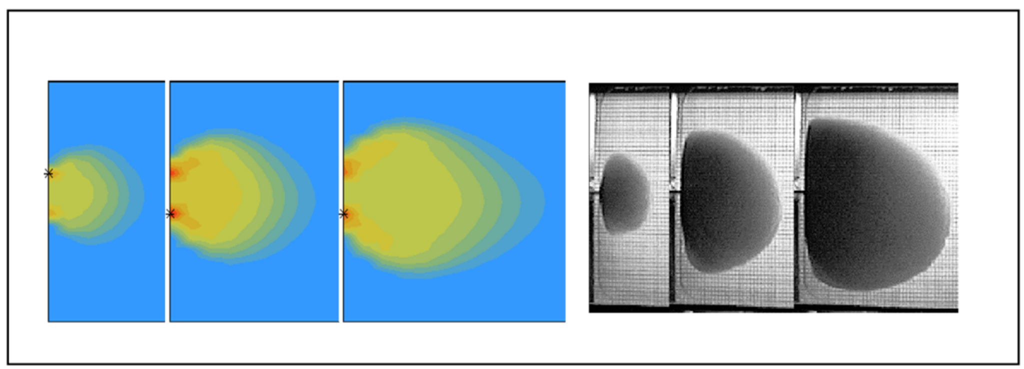

Milli-Fluidic Experiment to Understand Branching Flow for Proppant Transport

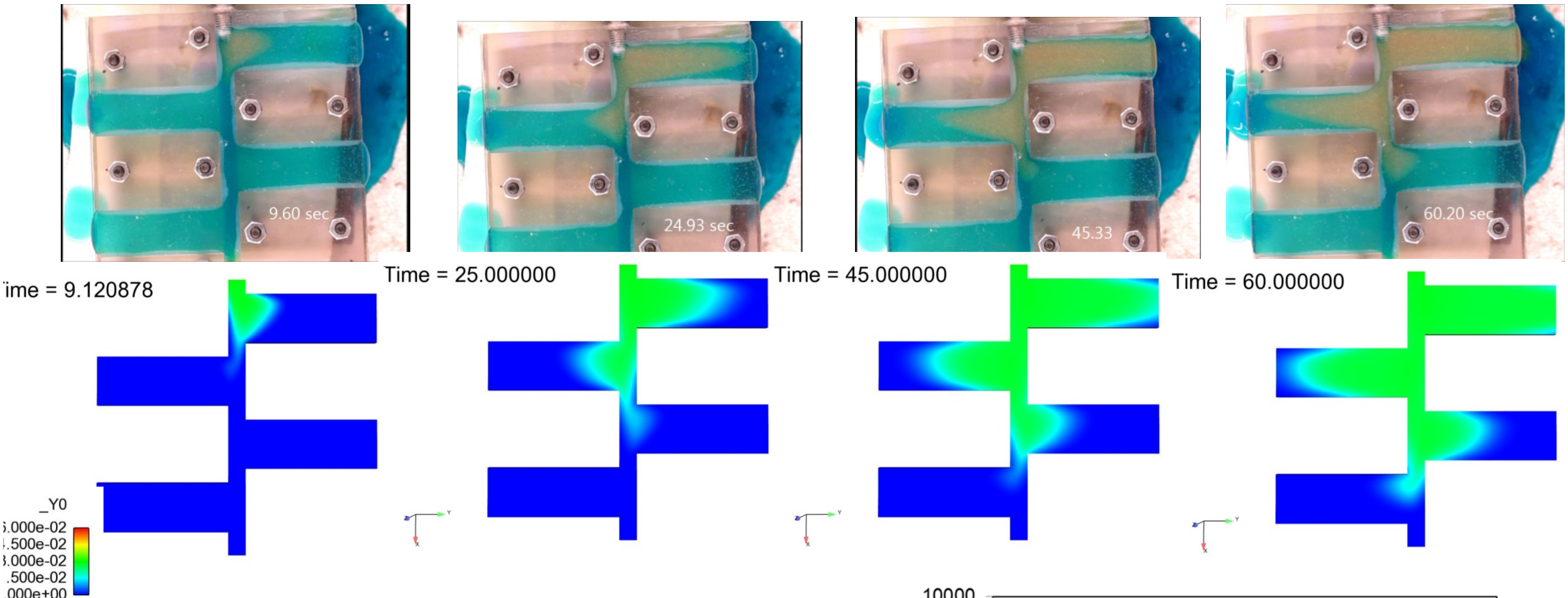

- First run of experiment uses dilute particle concentration of 0.03 volume fraction
- Material is alumina in guar
- Rheology is quite complex
- Fairly good agreement between the model and experiment, though model too fast at later times

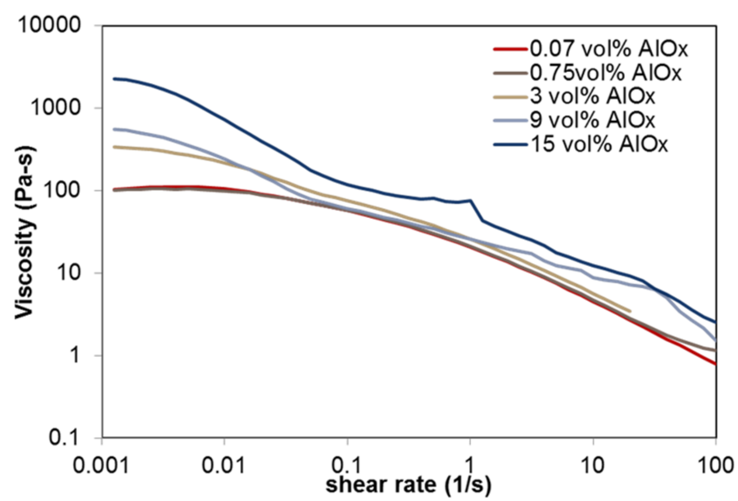

Millifluidic VE Suspension Flow: Decoupling Algorithm

3D mesh (Hex27) 47,416 Elements and 430,335 Nodes

- Timings are taken as representative from Newton iterations
- There is around a 5 times speedup when Newton iterations are compared
- Decoupled run was able to reach 900 time steps in the same time the fully coupled reached 100 time steps.

	Assembly (sec)	Solve (sec)	Total (sec)
Decoupled Mat 1	32	70	102
Decoupled Mat 2	7	1	8
Decoupled Mat 3	16	2	18
Decoupled Mat 4	11	2	13
Decoupled Total	66	75	141
Fully Coupled	300	400	700

Suspension Balance Model For Red Blood Cells

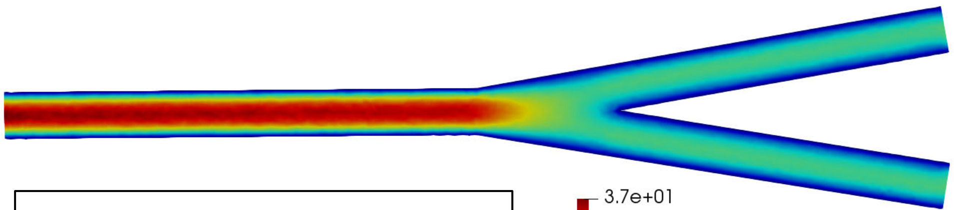

Max Velocity = 37 mm/s

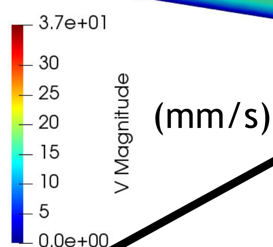

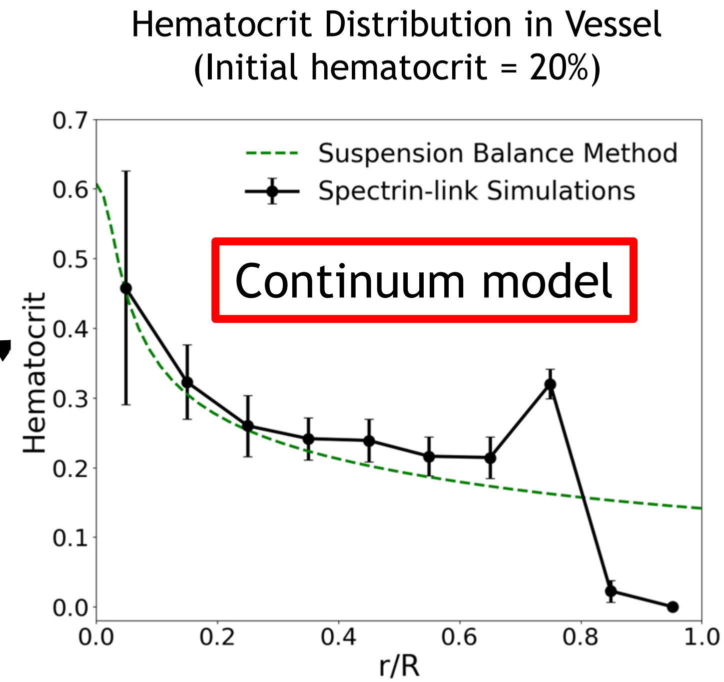

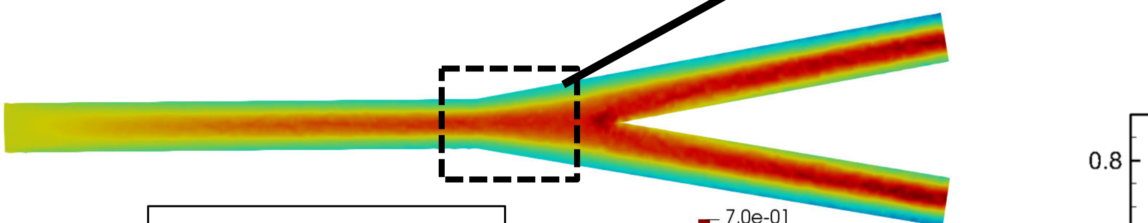

Red blood cell volume fraction (hematocrit distribution)

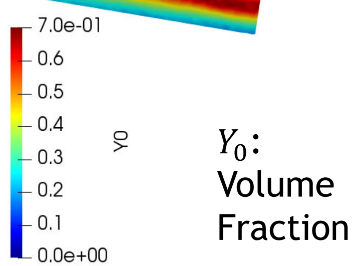

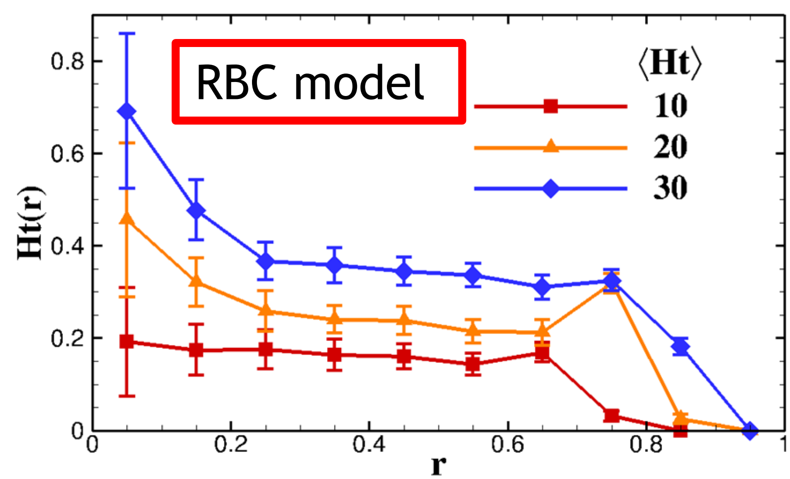

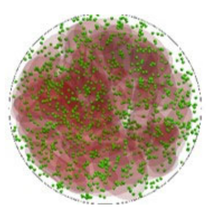

Red blood cell models from Georgia Tech (Leo Liu & Cyrus Aidun)

Thixotropic Model with Structure Factor to Capture Agglomeration/Breakup

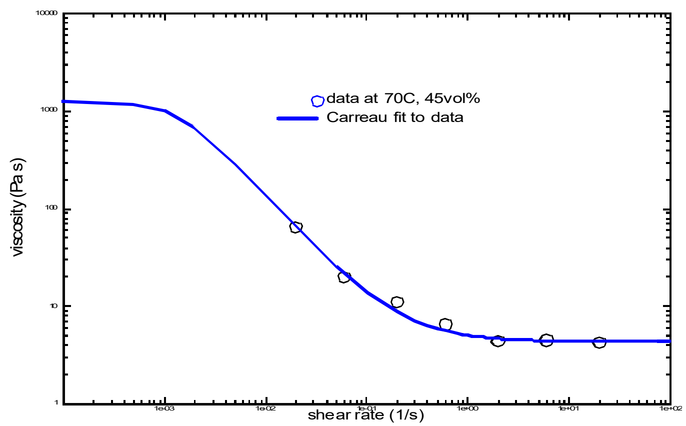

Steady State Viscosity Data of Alox suspension at 70°C (symbols) fit to a Carreau-Yasuda Model (line)

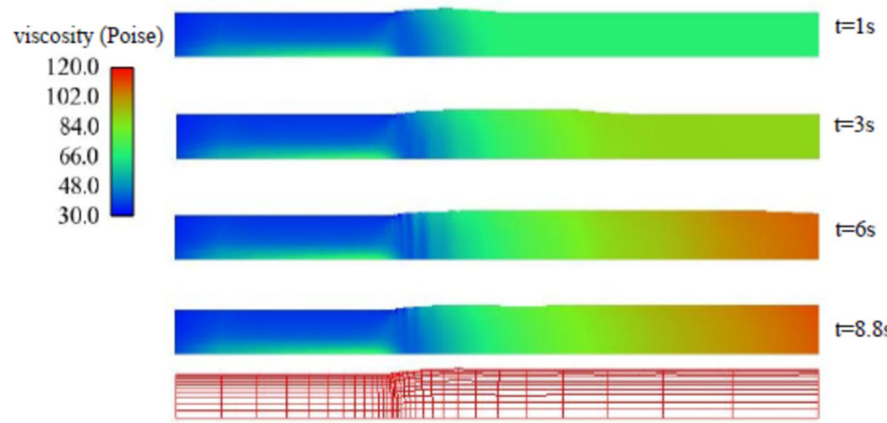

Simple aggregation network model

- Captures time-dependent response and steady-state viscosity

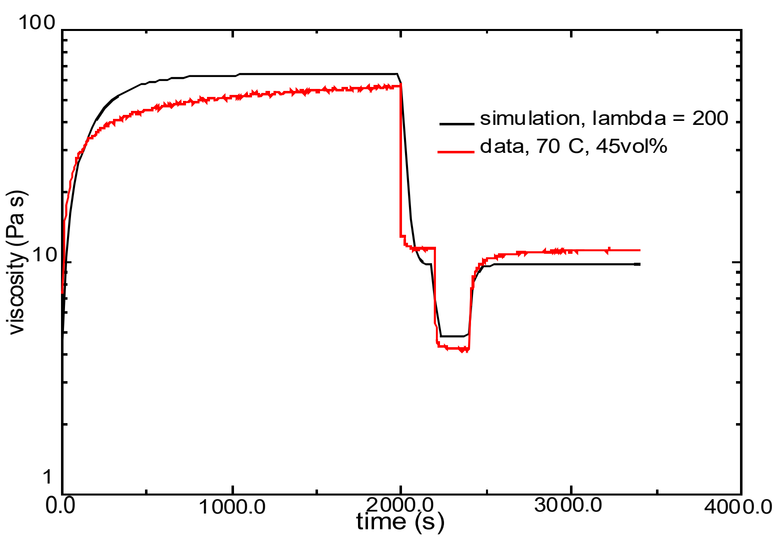

$$\frac{d\xi}{dt} = -k_r \dot{\gamma}^m \xi + k_f (1-\xi)$$

$$k_r = k_r^o e^{-\frac{E_b}{RT}}$$

$$k_f = k_f^o e^{-\frac{E_f}{RT}}$$

$$\xi = \frac{[b]}{[b_{\max}]}$$

$$\eta = \eta_\infty + (\eta_o - \eta_\infty)\xi^p$$

Barnes 1997

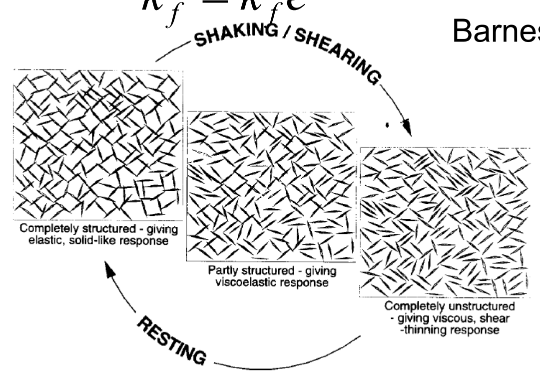

Injection Molding of Ceramic Pastes

- Our modeling has predicted non-isothermal injection molding of ceramic precursor pastes

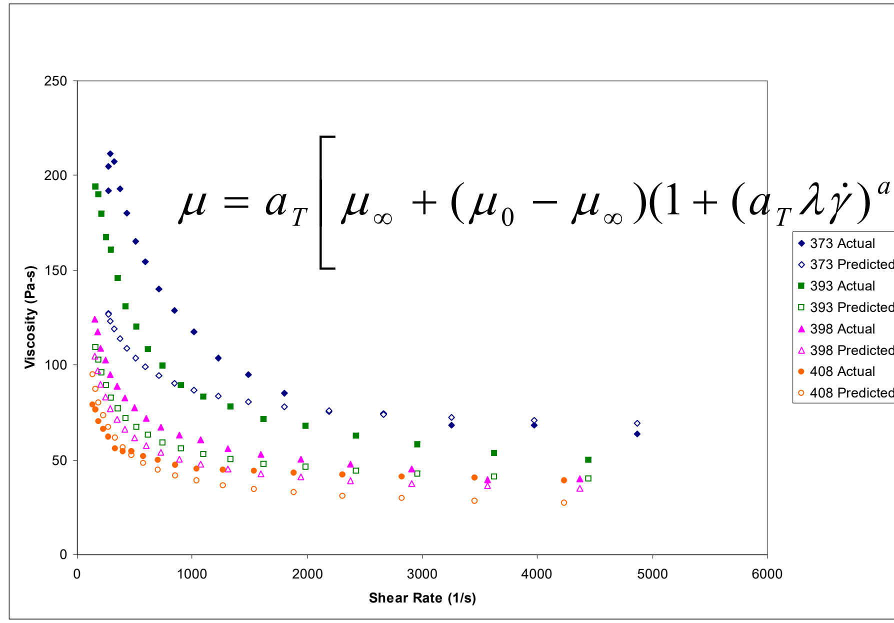

$$\mu = a_T \left[\mu_\infty + (\mu_0 - \mu_\infty)\left(1 + (a_T \lambda \dot{\gamma})^a\right)^{\frac{(n-1)}{a}} \right]$$

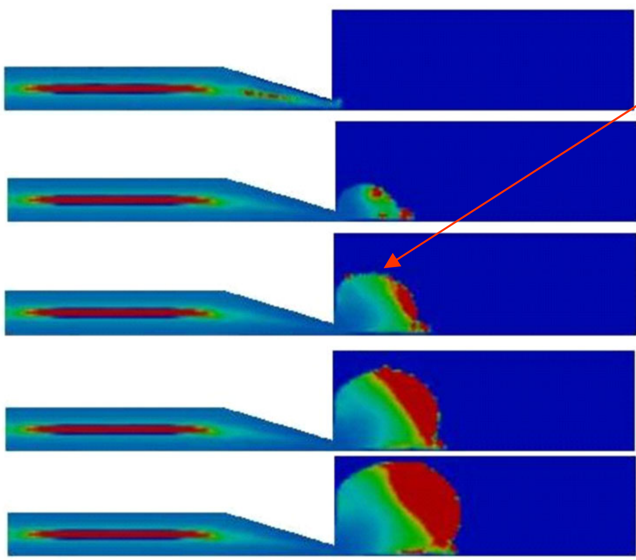

flow front

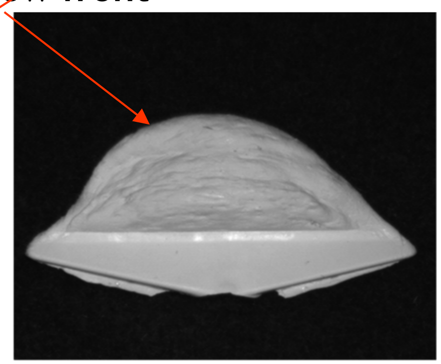

Temperature-dependent rheology and fit to a Carreau-Yasuda model (L. Mondy and L. Halbleib)

Model was validated with experiments in which partially filled mold was quickly cooled to capture intermediate state (R. Rao, P. Yang)

Improvements in Distributor Design Predicted with Modeling

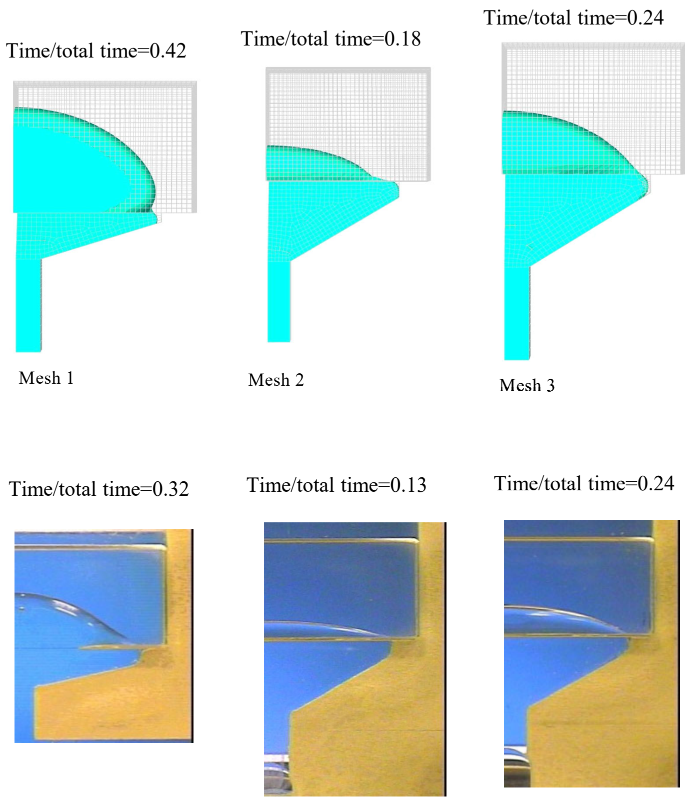

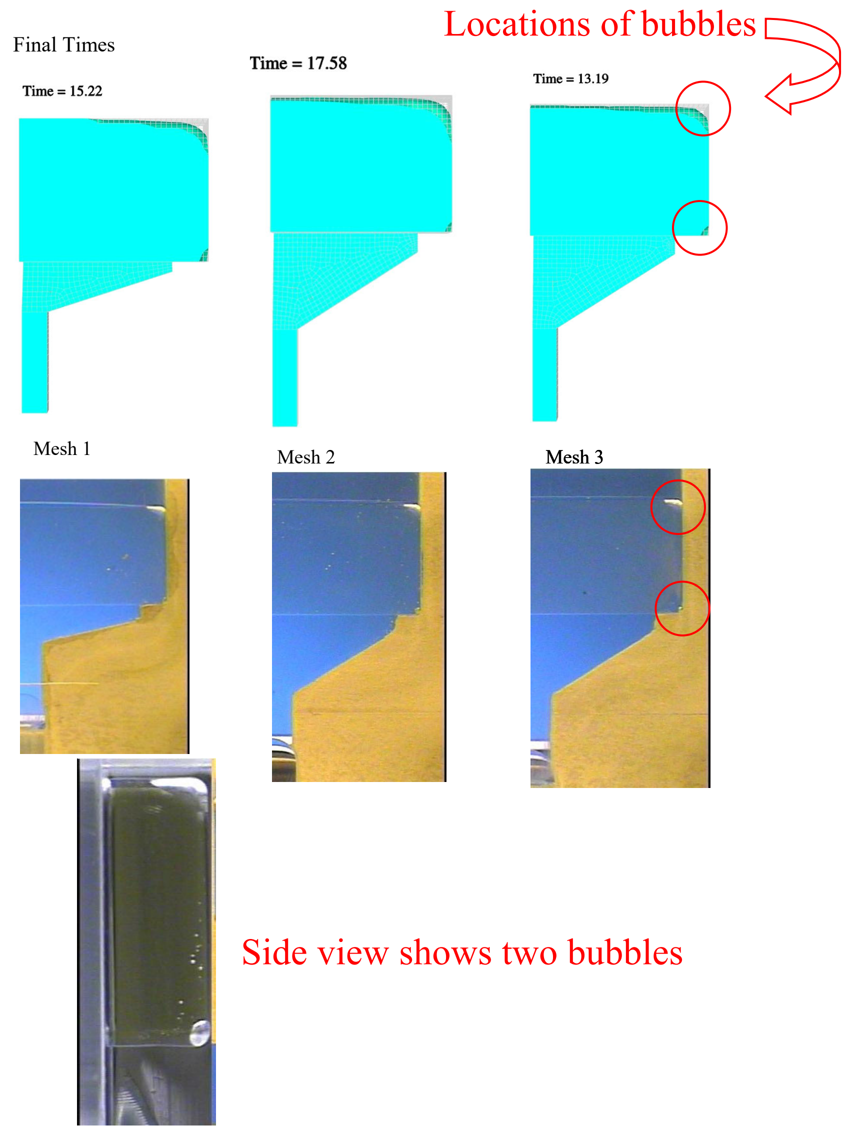

- Qualitative aspects captured – effect of distributor on “flatness” of front and number and location of bubbles
- Increasing wetting speed in model from that measured improves shape of front

Coextrusion Flow in the Splitter Using a Carreau Models

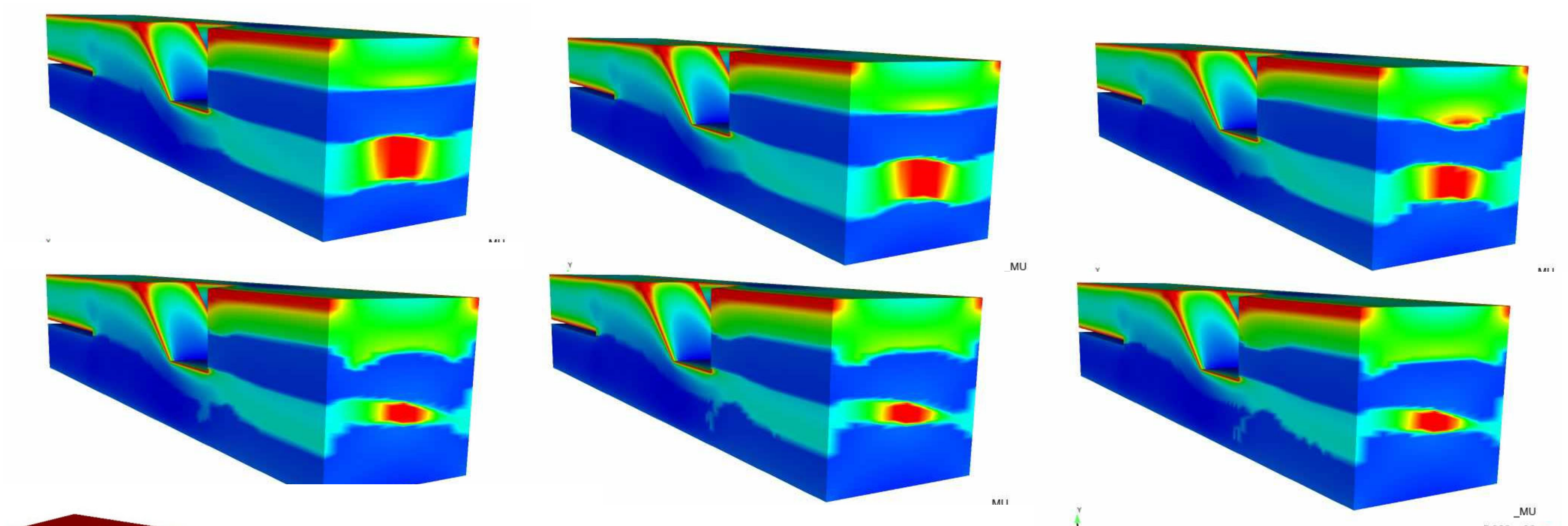

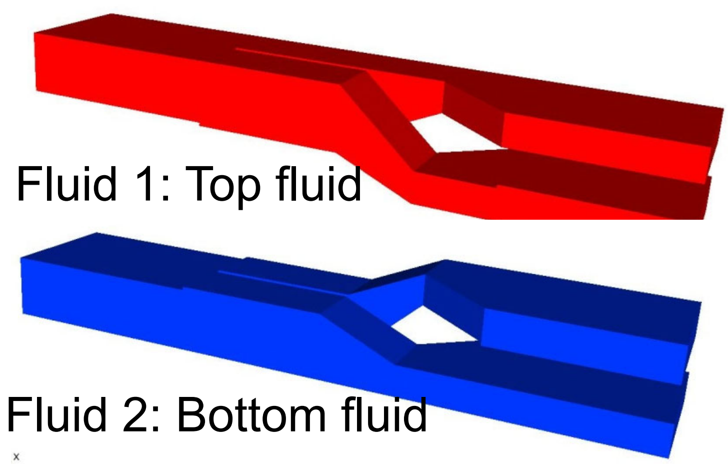

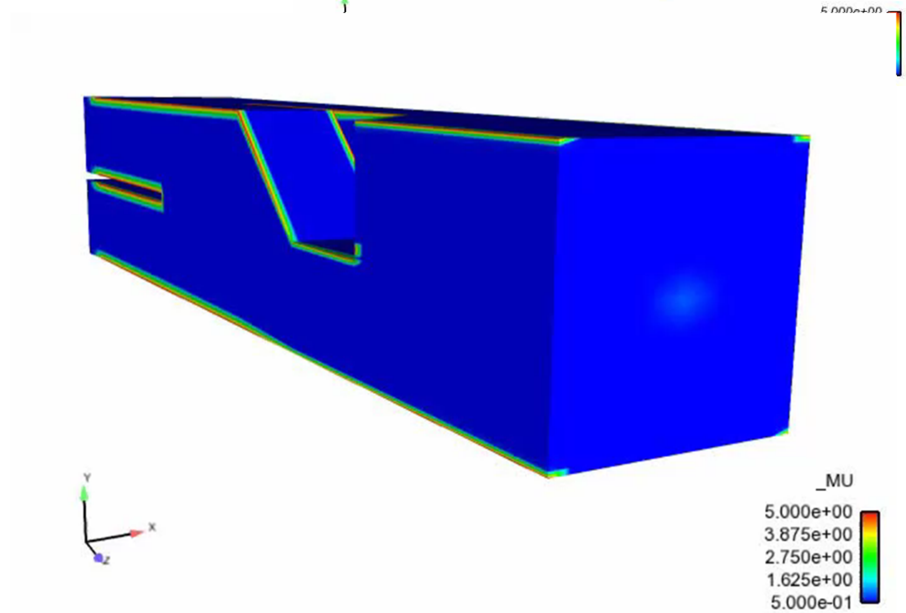

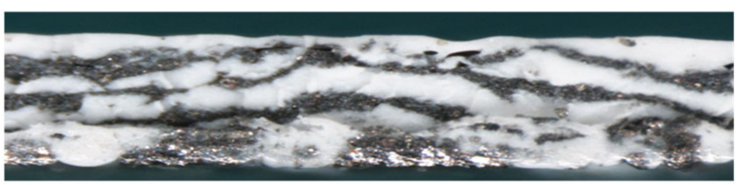

Viscoelastic Modeling of Blade Coating

GOMA 6.0 with log-conformation formulation to improve stability at high Weissenberg Number

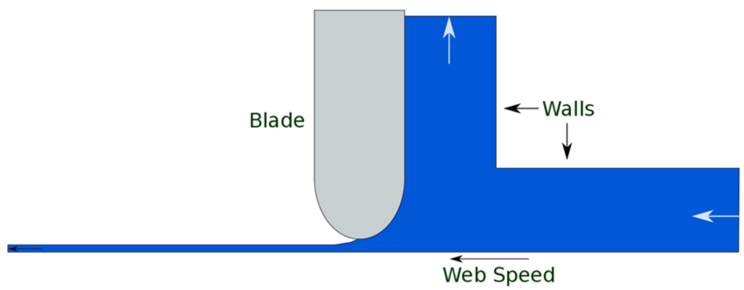

Maximum Web Speed

Giesekus
DEVSS-G: 18.2 cm/s
DEVSS-G Log Conf: 35.5 cm/s

Phan Thien Tanner
DEVSS-G: 4.6 cm/s
DEVSS-G Log Conf: 28.8 cm/s

- For Newtonian fluids, the film thins as the web speed increases.
- Viscoelastic film thickness is non-monotonic, thickens and then thins
- Log conformation greatly increased maximum web speed

Log-conformation tensor increases maximum web speed obtained for blade coating

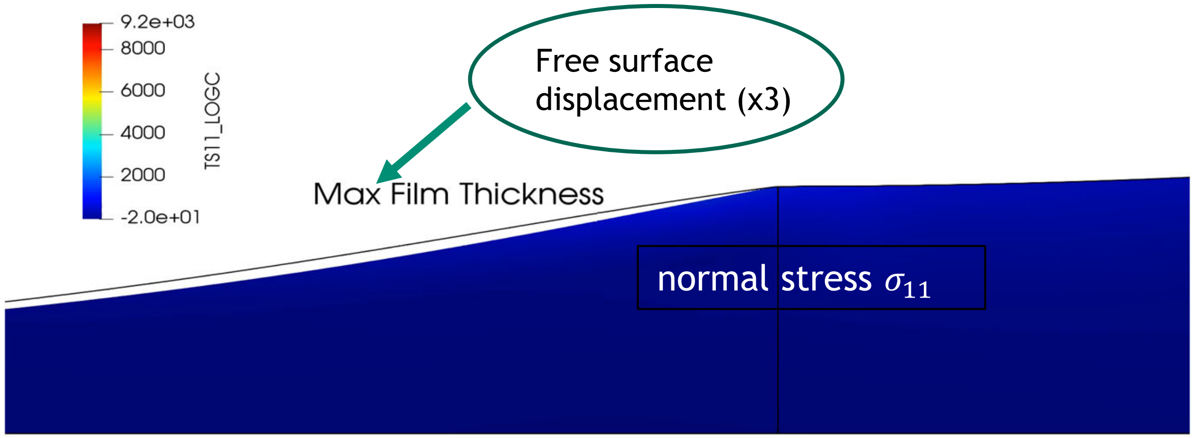

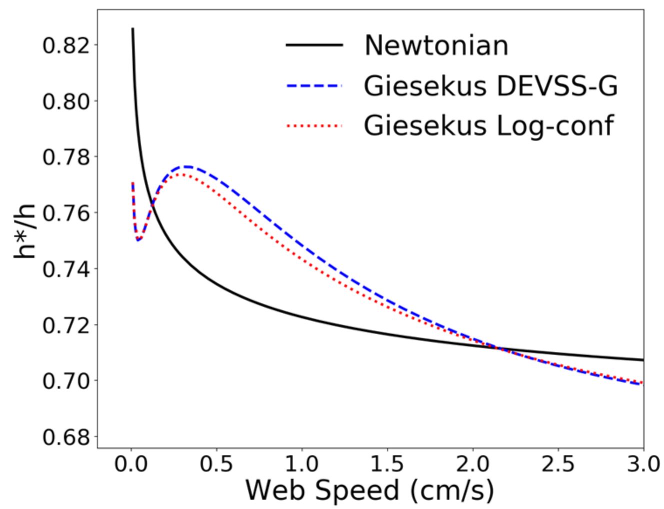

Reference: Fattal and Kupferman, *J. Non-Newtonian Fluid Mech.* **123** (2004)

Martin et al, Viscoelastic Blade Coating, C&F, 2019

3D Viscoelastic Mold Filling: Property Averaging Versus Stress Ghosting

- 3D Level Set with segregated approach:
  - Level Set Equation
  - Momentum and Continuity solve
  - Stress
  - velocity gradient in their own matrix
- 8-node hex stabilized with DEVSS and PSPP
- Mix of iterative and parallel direct solvers
- Property averaging goes unstable
- Ghost is much smoother

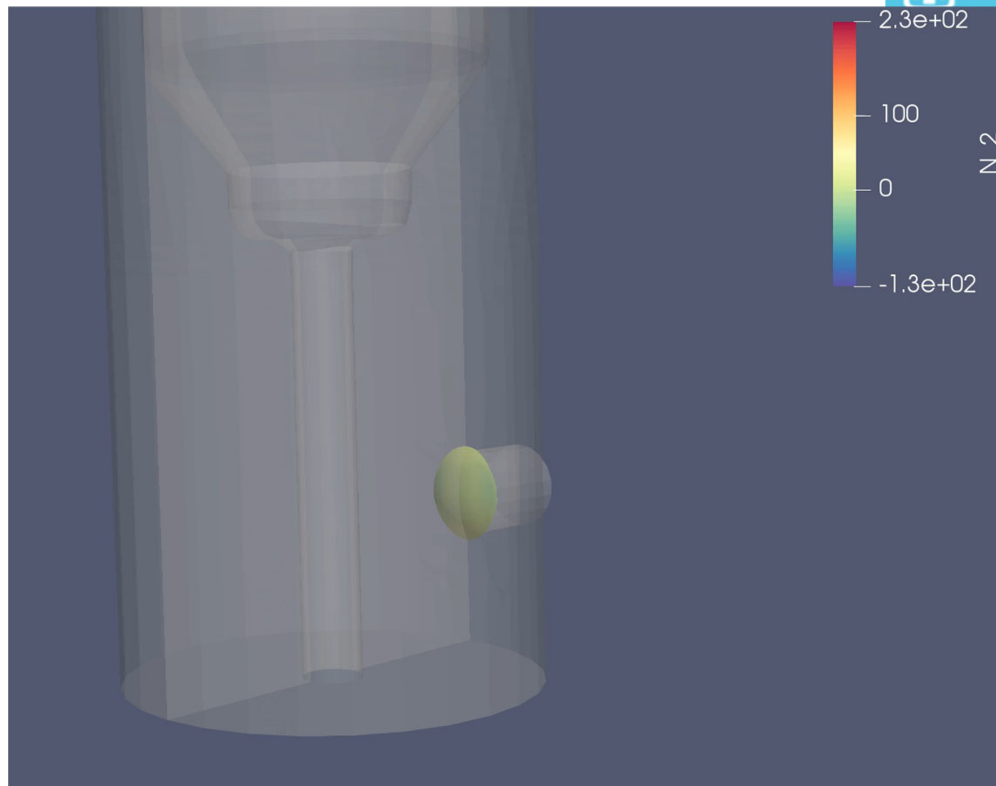

$$\int_\Omega \left[\rho(\phi)\left(\frac{\delta \boldsymbol{u}}{\delta t}\cdot \boldsymbol{v} + \boldsymbol{u}\cdot\nabla\boldsymbol{u}\right)\cdot\boldsymbol{v} - (\boldsymbol{T} - p\boldsymbol{I}) : \nabla\boldsymbol{v}\right] d\boldsymbol{x} = 0$$
$$\int_\Omega \nabla \boldsymbol{u} q \; d\boldsymbol{x} = 0 \tag{1}$$

$$\int_\Omega \left[\frac{\delta\phi}{\delta t} + \boldsymbol{u}\cdot\nabla\phi\right]\cdot\psi_{ls}\; d\boldsymbol{x} = 0 \tag{4}$$

$$\int_\Omega [\boldsymbol{G} - \nabla\boldsymbol{u}] : \boldsymbol{\psi_G}\; d\boldsymbol{x} = 0 \tag{2}$$

$$\int_\Omega \left[\lambda(\phi)\left(\frac{\delta\boldsymbol{\tau}}{\delta t} + \boldsymbol{u}\cdot\nabla\boldsymbol{\tau} - \left(1 - \frac{\xi}{2}\right)(G^T\cdot\boldsymbol{\tau} + \boldsymbol{\tau}\cdot G)\right.\right.$$
$$\left.\left. + \left(\frac{\xi}{2}\right)(\boldsymbol{\tau}\cdot G^T + G\cdot\boldsymbol{\tau})\right) + Z\boldsymbol{\tau} - \mu_p(\phi)(\nabla\boldsymbol{u} + \nabla\boldsymbol{u}^T)\right] : \boldsymbol{\psi_\tau}\; d\boldsymbol{x} = 0 \tag{3}$$

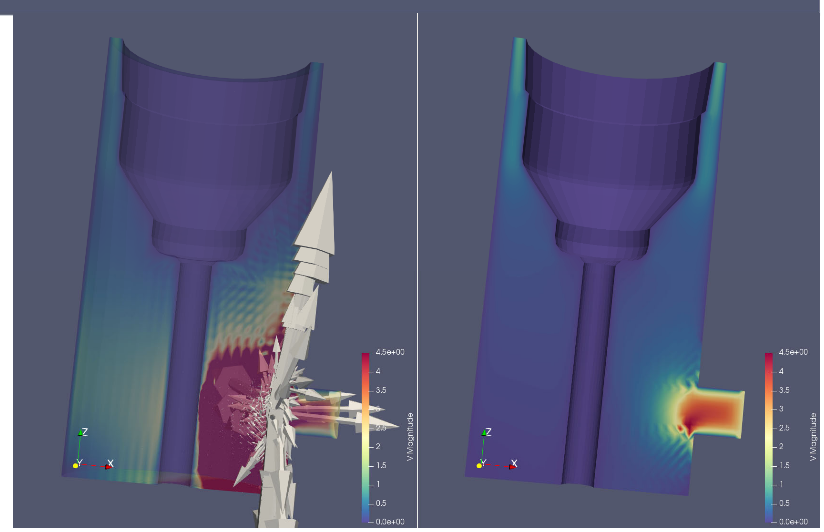

Level Set Surface Tension

Traditional Continuum Surface Stress (CSS) in Goma
Surface tension is added as an extra stress to the momentum equation

$$\nabla \cdot T = \nabla \cdot (\sigma(\boldsymbol{I} - \boldsymbol{nn})\delta(\phi))$$

Hysing (2006) introduced using Laplace-Beltrami operator on the identity mapping in order, which results in an artificial diffusion term

$$\Delta_s id_\Gamma = \kappa \boldsymbol{n}, \qquad (id_\Gamma)^{n+1} = (id_\Gamma)^n + \Delta t^{n+1} \boldsymbol{u}^{n+1}, \qquad \Delta \mathrm{t}^{\mathrm{n+1}} = \mathrm{t}^{\mathrm{n+1}} - \mathrm{t\hat{}n}$$

$$f_\sigma = \sigma \kappa \boldsymbol{n} \delta(\phi) \rightarrow f_\sigma^{n+1} = \sigma(\Delta_s (id_\Gamma)^n + \Delta t^{n+1} \Delta_s \boldsymbol{u}^{n+1})$$

This alternative formulation reduces spurious currents generated from the capillary force

$$\nabla_s = (I - nn)\nabla$$
$$\Delta_s = \nabla_s \cdot \nabla_s$$
$$\sigma = surface\ tension$$
$$\phi = level\ set$$
$$\delta(\phi) = smoothed\ Dirac\ delta$$

$\Delta_s \boldsymbol{u}$ term acts as artificial diffusion

- Tested on a static drop problem which is a drop placed in equilibrium with no forces acting on it other than surface tension.
- The results to the right show velocity vectors for the CSS and Hysing version of surface tension.
- We can see that spurious currents are improved in Hysing's formulation

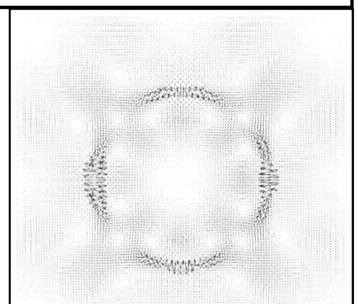

CSS 1X magnification

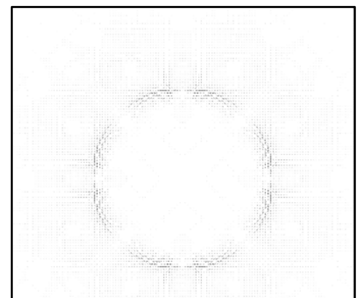

Hysing 10X magnification

Static drop example problem tests formulation

S. Hysing (2006) A new implicit surface tension implementation for interfacial flows

Newtonian Drop in a Viscoelastic Fluid: Constriction X~ 0.001 Ca~0.5 De~0.4

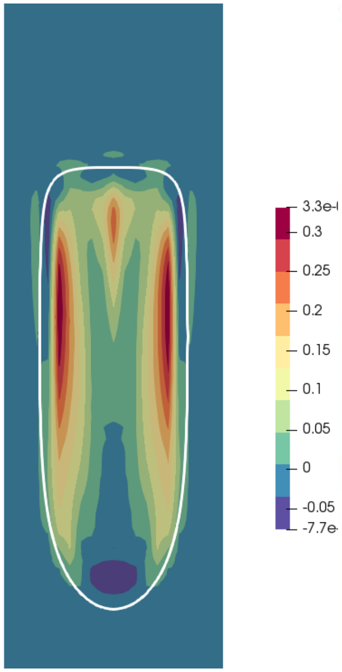

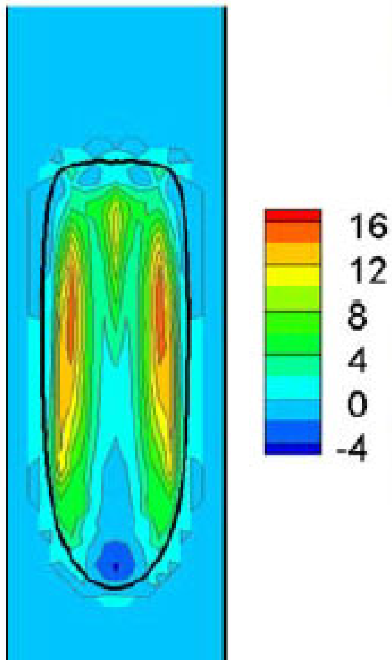

Verification test: 10a from Chung et al., 2009

Droplet Shapes and Stress Profiles for Various Scenarios

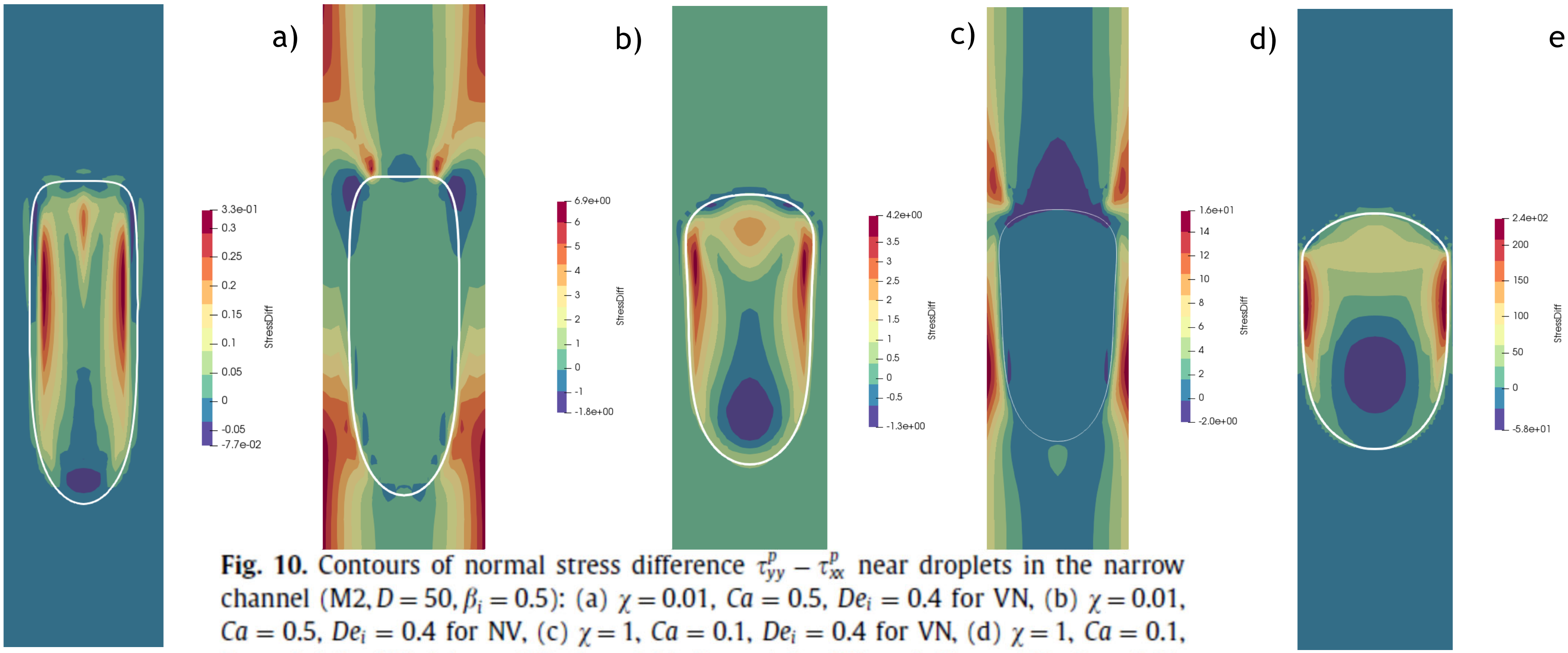

Fig. 10. Contours of normal stress difference $\tau^p_{yy} - \tau^p_{xx}$ near droplets in the narrow channel (M2, $D = 50$, $\beta_i = 0.5$): (a) $\chi = 0.01$, $Ca = 0.5$, $De_i = 0.4$ for VN, (b) $\chi = 0.01$, $Ca = 0.5$, $De_i = 0.4$ for NV, (c) $\chi = 1$, $Ca = 0.1$, $De_i = 0.4$ for VN, (d) $\chi = 1$, $Ca = 0.1$, $De_i = 0.4$ for NV, (e) $\chi = 100$, $Ca = 0.01$, $De_i = 1$ for VN, and (f) $\chi = 100$, $Ca = 0.01$, $De_i = 0.4$ for VN. (e) and (f) are reproduced from Chung et al. (2008).

Velocity-Pressure Splitting to Improve Iterative Solver Performance

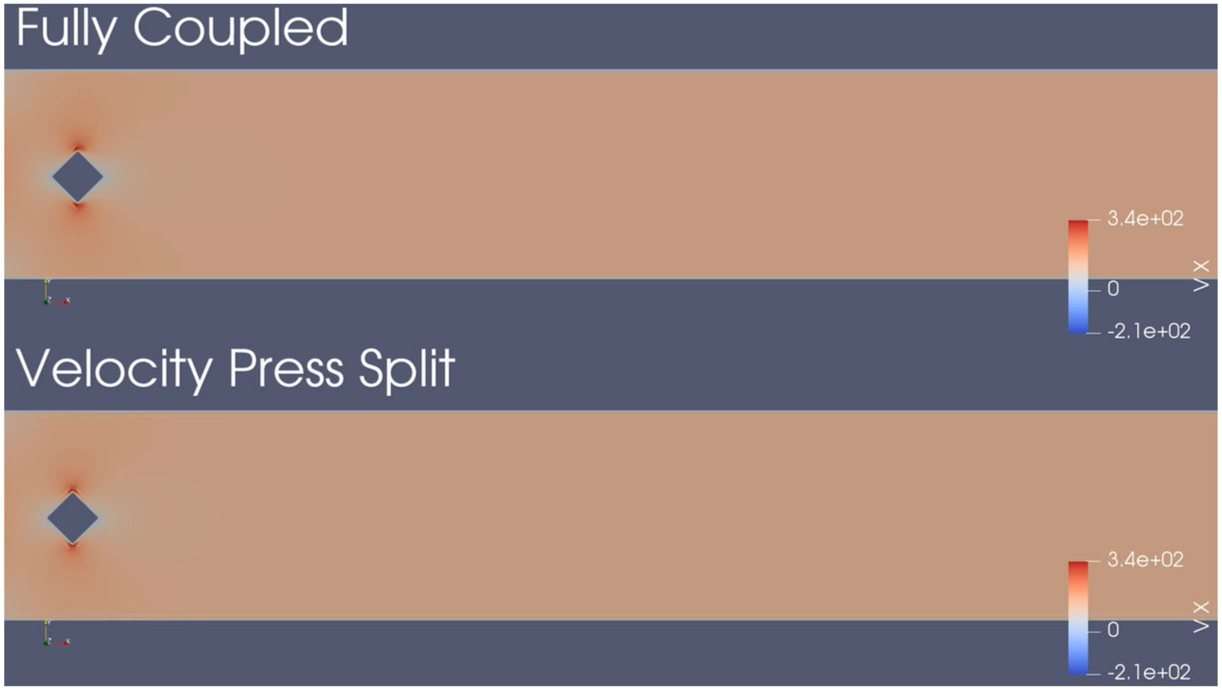

- Three-Step Projection with Pressure Poison
- Poiseuille flow past an obstruction

Zahedi et al., IJNMF, 2012
Guermond et al., JCP, 2000

1. Calculate intermediate velocity

$$\frac{1}{\Delta t}\left(\rho^{n+1}u_*^{n+1} - \rho^n u^n\right) - \rho^{n+1}u_*^n \cdot \nabla u_*^{n+1} = -\nabla p^n - \mu^{n+1}\nabla \cdot \nabla u_*^{n+1} + \rho^{n+1}\mathbf{g} \quad (1)$$

2. Find pressure, Pressure poisson comes from requirement of solenoidal velocity

$$\frac{\nabla \cdot \nabla \left(p^{n+1} - p^n\right)}{\rho^{n+1}} = \frac{-1}{\Delta t}\nabla \cdot u_*^{n+1} \quad (2)$$

3. Update velocity using pressure

$$\frac{u^{n+1} - u_*^{n+1}}{\Delta t} = -\frac{\nabla\left(p^{n+1} - p^n\right)}{\rho^{n+1}} \quad (3)$$

Elastoviscoplastic Flow Model: Saramito

Yield stress model developed by Saramito[1]

- Model is a viscoelastic liquid above the yield stress and an elastic solid below yield
- Implemented for Oldroyd-B, PTT, and Giesekus models.
- Regularized model also implemented

$$|\boldsymbol{\sigma}_d| = \sqrt{\mathrm{tr}(\boldsymbol{\sigma}_d \cdot \boldsymbol{\sigma}_d)/2}$$

$$\mathcal{S} = \max\left(0, \frac{|\boldsymbol{\sigma}_d| - \tau_{\text{yield}}}{|\boldsymbol{\sigma}_d|}\right)$$

Regularized model

$$\mathcal{S} = F \cdot \log\left(1 + e^{\frac{1}{F}\frac{|\boldsymbol{\sigma}_d| - \tau_{\text{yield}}}{|\boldsymbol{\sigma}_d|}}\right)$$

Model-dependent

$$\lambda\left[\frac{D\boldsymbol{\sigma}}{Dt} - \overset{\nabla}{\boldsymbol{\sigma}}\right] + \mathcal{S}\boldsymbol{g}(\boldsymbol{\sigma}) = -2\eta_p\dot{\gamma},$$

Flow past a cylindrical obstacle

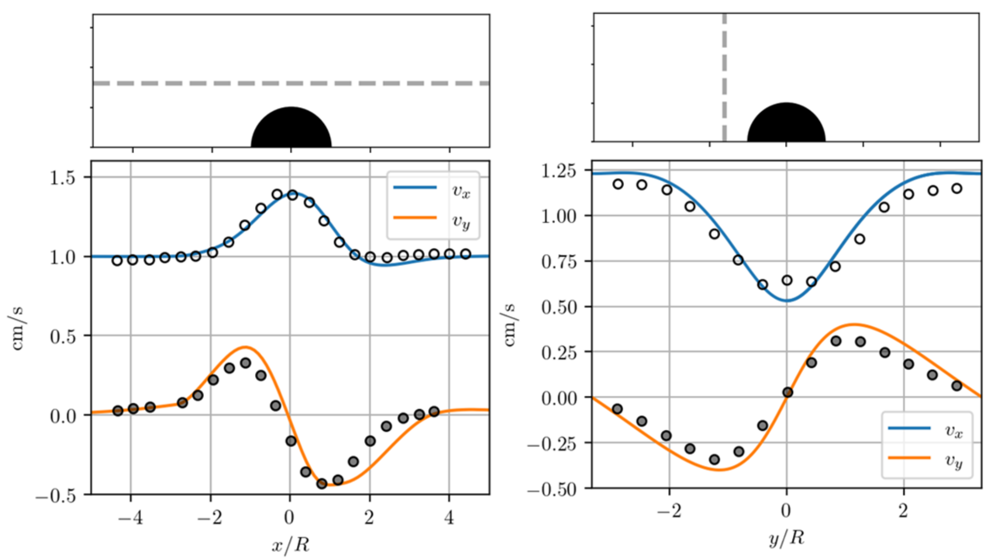

[1] Saramito, P. Journal of Non-Newtonian Fluid Mechanics. 145 (2007) 1-14
[2] Chedaddi, I. *et al*. *The European Physical E*. (2011) 34:1

"Award Winning" Documentation

- ❑ GOMA 6.0 USER'S MANUAL
  - Available on DOE/OSTI and GitHub website
- ❑ GOMA SUPPLEMENTAL MANUAL FOR ADVANCED TOOLS
  - Automated Continuation, Stability, Augmenting conditions
- ❑ TUTORIALS
  - Memos explaining how to run advances problems with the files to run the problems
- ❑ RELATED DOCUMENTATION
  - MEMOS, SAND Reports, and
- ❑ DEVELOPERS' MANUAL
- ❑ GOMA test suite
- ❑ Interactive training
  - Beginners, developers, git, parallel, shell equations, viscoelastic flow etc
- ❑ Coming soon – **Possible GOMA book**!

TRAINING, VERIFICATION, VALIDATION, ADVANCED USAGE

GOMA 6.0 Wrap-Up/Status

- Goma 6.0 - Open-source (https://goma.github.io/)
- User/developer/research base at 3M, Corning, P&G, Avery Dennison, UT, CU, UNM, UIUC, UM, UU (past history with >10 other institutions)
- Ready as a research tool in nanomanufacturing, reduced order modeling, complex rheology, shell technology, etc.
- Over 3000 pages of documentation (user-manual, developers manual, tutorials, etc.)
- Easy to add new equations and physics
- Excellent platform for research and proposals

GOMA 7.0 – Coming Soon!

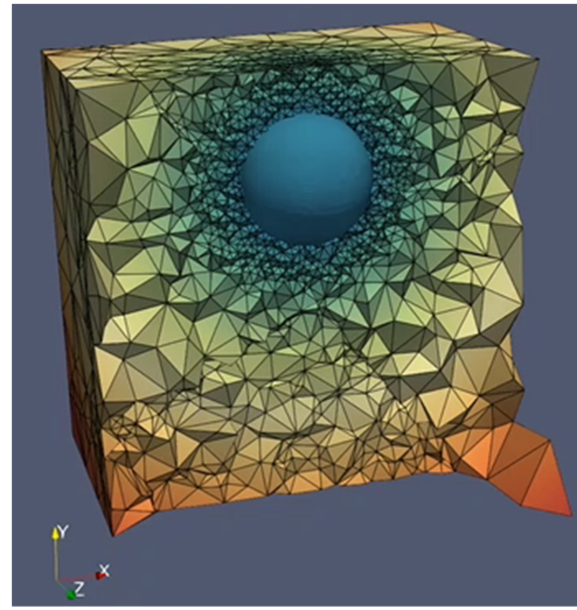

- Improved Material Models
  - Suspension balance model improvements
  - Viscoelastic level set and advanced boundary conditions
  - Polyurethane foam model
  - Population Balance Equations/Quadrature Method of Moments models for foams and emulsions
- Algorithmic Improvements
  - Segregated solution strategy
  - Improved SUPG for Species equations, tets, and tri
  - Quadratic Triangles
  - Hysing/Denner level set surface tension for reducing spurious
  - Pressure element variables output to exodus - use them as initial guesses
  - Automatic rotations in 3D
- Adaptive meshing of linear triangles and tetrahedra.
  - Implemented using Omega_h library
  - Supports an adaptive ALE mesh so automatic remeshing is performed
  - Adapts to level set interfaces in 2D in 3D to reduce level set problem size

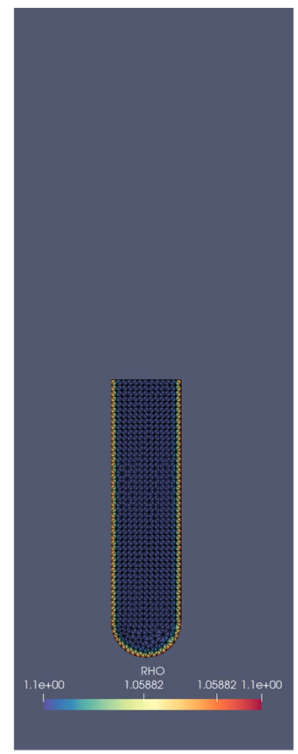

Thank You for Your Attention

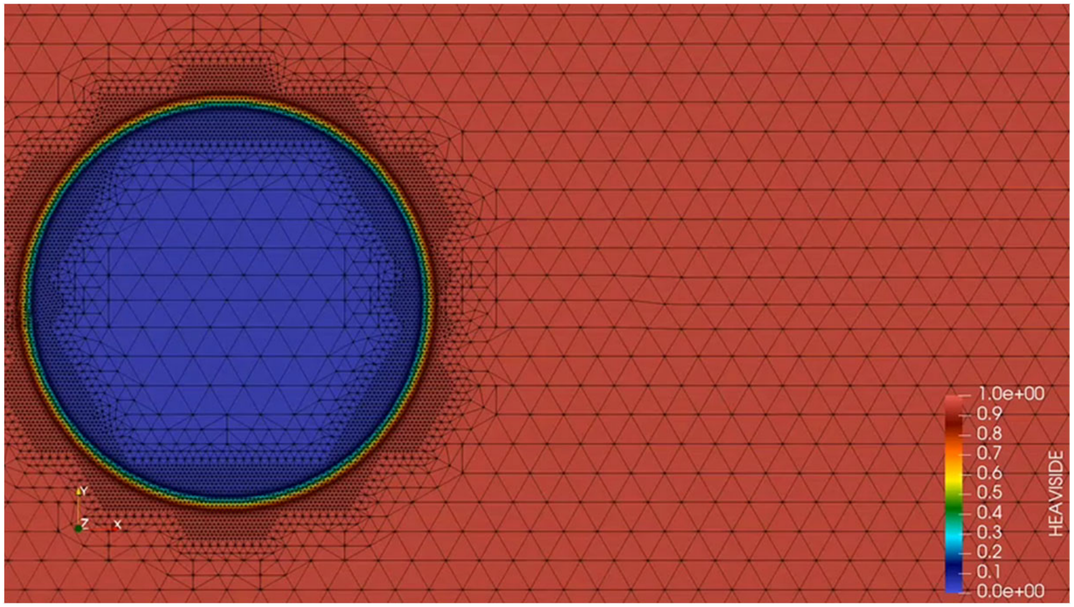

Questions or Comments?

Goma Publications

- Tjiptowidjojo, Kristianto, et al. "Mass Transfer Limited KOH Etching in Crystalline Silicon using a Confinement Mask." ECS Journal of Solid State Science and Technology 9.3 (2020): 034013.
- Cochrane, A. et al. (2019) Elastohydrodynamics of roll-to-roll UV-cure imprint lithography. Industrial & Engineering Chemistry Research 58(37)
- Cochrane, A., Tjiptowidjojo, K., Bonnecaze, R. T. and Schunk, P. R. 2018. "Multiphase model for nanoimprint lithography". International Journal of Multiphase Flow. DOI-Link
- Tjiptowidjojo, K.; Hariprasad D. S.; Schunk, P. R. 2018. "Effect of blade-tip shape on the doctoring step in gravure printing processes". Journal of Coatings Technology and Research. Volume 15. DOI-Link
- Hariprasad, D. S., Grau, G., Schunk, P. R., Tjiptowidjojo, K. 2018. "A computational model for doctoring fluid films in gravure printing". Journal of Applied Physics. Volume 119. DOI-Link
- Roberts, S. A. and P. R. Schunk. 2014. "A reduced-order model for porous flow through thin, structured materials". International Journal of Multiphase Flow. Volume 67. DOI-Link
- Roberts, S. A., Noble, D. R., Benner, E. M. & Schunk, P. R. 2013. "Multiphase hydrodynamic lubrication flow using a three-dimensional shell finite element model". Computers & Fluids. Volume 87. 25 October 2013, Pages 12–25
- Roberts, S. A.; Noble, D. R.; Benner, E. M. & Schunk, P. R. (2013), 'Multiphase hydrodynamic lubrication flow using a three-dimensional shell finite element model', Computers & Fluids. Volume 87, 25 October 2013, Pages 12–25
- Roberts, S. A., & Schunk, P. R. (2014). A reduced-order model for porous flow through thin, structured materials. *International journal of multiphase flow*, *67*, 25-36.

Goma Publications

- Mondy, L., Rao, R., Lindgren, E., Sun, A., Adolf, D., Retallack, C. and Thompson, K., 2011. Modeling coupled migration and settling of particulates in curing filled epoxies. Journal of Applied Polymer Science, 122(3), pp.1587-1598.
- Moore, N., Tjiptowidjojo, K., Schunk, P. R. 2011, "Comment on Hydrophilicity and the Viscosity of Interfacial Water", Langmuir, 27(6) pp 3211-3212.
- Roberts, S.A. and Rao, R.R., 2011. Numerical simulations of mounding and submerging flows of shear-thinning jets impinging in a container. Journal of Non-Newtonian Fluid Mechanics, 166(19-20), pp.1100-1115.
- Grillet, A.M., Rao, R.R., Adolf, D.B., Kawaguchi, S. and Mondy, L.A., 2009. Practical application of thixotropic suspension models. Journal of Rheology, 53(1), pp.169-189.
- H. D. Rowland, W. P. King, A. C. Sun, and P. R. Schunk Cross, GLW 2008. "Predicting polymer flow during high-temperature atomic force microscope nanoindentation" Macromolecules. Vol.40, iss.22, p.8096-8103
- Rao, R.R., Mondy, L.A. and Altobelli, S.A., 2007. Instabilities during batch sedimentation in geometries containing obstacles: A numerical and experimental study. International Journal for Numerical Methods in Fluids, 55(8), pp.723-735.
- S. Reddy, P. R. Schunk, and R. T. Bonnecaze, 2005. "Dynamics of low capillary number interfaces moving through sharp features", Physics of Fluids, 17, 122104.
- H. D. Rowland, W. P. King, A. C. Sun, and P. R. Schunk 2005. "Simulations of nonuniform embossing: The effect of asymmetric neighbor cavities on polymer flow during nanoimprint lithography", J. Vac. Sci. Technol. B 23(6), 2958-2962.
- H. D. Rowland, A. C. Sun, P. R. Schunk, W. P. King, 2005. "Impact of polymer film thickness and cavity size on polymer flow during embossing: toward process design rules for nanoimprint lithography". J. Micromech. Microeng. 15, 2414-2425.

Goma Publications

- Sun, A., Baer, T., Reddy, S., Mondy, L., Schunk, R., Sackinger, P., Rao, R., Noble, D., Bielenberg, J. and Graham, A., 2005. Wetting in pressure driven slot flow. WIT Transactions on The Built Environment, 84.
- Noble, D. R. ; Schunk, PR ; Wilkes, E. D. ; Rao, R. R. ; Baer, T. A. 2004. "Finite element simulations of fluid-structure interactions via overset meshes and sharp embedded interfacial conditions". Computational and Experimental Methods (2004) Vol.10, p.77-86
- Noble, D.R., Schunk, P.R., Wilkes, E.D., Baer, T., Rao, R.R. and Notz, P.K., 2003. Large deformation solid–fluid interaction via a level set approach. Sandia, Report, SAND2003-4649.
- Rao, R., Mondy, L., Sun, A. and Altobelli, S., 2002. A numerical and experimental study of batch sedimentation and viscous resuspension. International journal for numerical methods in fluids, 39(6), pp.465-483.
- H. Fan, Y. Lu, A Stump, S. T. Reed, T. Baer, P. R. Schunk, V. Luna, G. Lopez, and C. J. Brinker 2000. "Rapid prototyping of patterned functional nanostructures." Letter to Nature, 4 May 2000.
- R. A. Cairncross, P. R. Schunk, T. A. Baer, R. R. Rao, and P. A. Sackinger, 2000. "A finite element method for free surface flows of incompressible fluids in three dimensions. Part I. Boundary fitted mesh motion.". Int. J. Numer. Meth. Fluids., 33, 375-403.
- T. A. Baer, P. R. Schunk, R. A. Cairncross, R. R. Rao, and P. A. Sackinger, 2000. "A finite element method for free surface flows of incompressible fluids in three dimensions. Part II. Dynamic Wetting Lines". Int. J. Numer. Meth. Fluids., 33, 405-427.
- P. A. Sackinger, P. R. Schunk and R. R. Rao 1996. "A Newton-Raphson Pseudo-Solid domain Mapping Technique for Free and Moving Boundary Problems: A Finite Element Implementation", J. Comp. Phys., 125, p. 83-103.
- P. R. Schunk and R. R. Rao 1994. "Finite Element Analysis of Multicomponent Two-Phase flows with Inter-phase mass and Momentum Transport" Int. J. Numer. Meth. Fluids., 18, 821-842.